Joint transceiver design and power optimization for wireless sensor networks in underground mines

Mémoire

Md Zahangir Alam

Maîtrise en génie électrique - avec mémoire
Maître ès sciences (M. Sc.)

Québec, Canada

Joint Transceiver Design and Power Optimization for Wireless Sensor Networks in Underground Mines

Mémoire

Md Zahangir Alam

Sous la direction de:

Paul Fortier, directeur de recherche
Mohamed Lassaad Ammari, codirecteur de recherche

Résumé

Avec les grands développements des technologies de communication sans fil, les réseaux de capteurs sans fil (WSN) ont attiré beaucoup d'attention dans le monde entier au cours de la dernière décennie. Les réseaux de capteurs sans fil sont maintenant utilisés pour a surveillance sanitaire, la gestion des catastrophes, la défense, les télécommunications, etc. De tels réseaux sont utilisés dans de nombreuses applications industrielles et commerciales comme la surveillance des processus industriels et de l'environnement, etc. Un réseau WSN est une collection de transducteurs spécialisés connus sous le nom de nœuds de capteurs avec une liaison de communication distribuée de manière aléatoire dans tous les emplacements pour surveiller les paramètres. Chaque nœud de capteur est équipé d'un transducteur, d'un processeur de signal, d'une unité d'alimentation et d'un émetteur-récepteur. Les WSN sont maintenant largement utilisés dans l'industrie minière souterraine pour surveiller certains paramètres environnementaux, comme la quantité de gaz, d'eau, la température, l'humidité, le niveau d'oxygène, de poussière, etc. Dans le cas de la surveillance de l'environnement, un WSN peut être remplacé de manière équivalente par un réseau à relais à entrées et sorties multiples (MIMO). Les réseaux de relais multisauts ont attiré un intérêt de recherche important ces derniers temps grâce à leur capacité à augmenter la portée de la couverture. La liaison de communication réseau d'une source vers une destination est mise en œuvre en utilisant un schéma d'amplification/transmission (AF) ou de décodage/transfert (DF). Le relais AF reçoit des informations du relais précédent et amplifie simplement le signal reçu, puis il le transmet au relais suivant. D'autre part, le relais DF décode d'abord le signal reçu, puis il le transmet au relais suivant au deuxième étage s'il peut parfaitement décoder le signal entrant. En raison de la simplicité analytique, dans cette thèse, nous considérons le schéma de relais AF et les résultats de ce travail peuvent également être développés pour le relais DF.

La conception d'un émetteur/récepteur pour le relais MIMO multisauts est très difficile. Car à l'étape de relais L, il y a 2^L canaux possibles. Donc, pour un réseau à grande échelle, il n'est pas économique d'envoyer un signal par tous les liens possibles. Au lieu de cela, nous pouvons trouver le meilleur chemin de la source à la destination qui donne le rapport signal sur bruit (SNR) de bout en bout le plus élevé. Nous pouvons minimiser la fonction objectif d'erreur quadratique moyenne (MSE) ou de taux d'erreur binaire (BER) en envoyant le signal utilisant le chemin sélectionné. L'ensemble de relais dans le chemin reste actif et le reste des relais s'éteint, ce qui permet d'économiser de l'énergie afin d'améliorer la durée de vie du réseau. Le meilleur chemin de transmission de signal a été étudié dans la littérature pour un relais MIMO à deux bonds mais est plus complexe pour un

relais multiple. Dans la première partie de ce mémoire, nous proposons un algorithme de recherche de meilleur chemin avec une parfaite connaissance de l'état de canal (CSI). Nous considérons un système de relais AF multisauts MIMO avec un récepteur d'erreur quadratique moyenne minimale (MMSE) utilisé au niveau du récepteur. Nous avons simplifié le réseau parallèle en liaison relais MIMO multisauts en série équivalente en utilisant le meilleur relais.

La transmission de données d'un nœud vers les autres nœuds via une liaison sans fil dans les mines souterraines peut être affectée par le bruit gaussien, la réflexion et les interférences. L'un des défis du déploiement de WSN dans les mines souterraines est la faible consommation d'énergie requise, car les nœuds de capteurs transportent une banque de puissance irremplaçable et limitée. Par conséquent, l'allocation de puissance optimale est la caractéristique de conception la plus importante pour les réseaux de stockage dans l'environnement minier. Une fois que nous avons le réseau série, nous proposons une stratégie pour concevoir conjointement le précodeur source, les filtres relais, et les matrices de récepteurs linéaires en utilisant une technique d'optimisation convexe avec la connaissance parfaite du CSI et une contrainte de puissance totale. En s'appuyant sur les analyses théoriques, nous effectuerons des simulations Matlab pour vérifier l'investigation théorique.

Abstract

With the great developments in wireless communication technologies, Wireless Sensor Networks (WSNs) have gained attention worldwide in the past decade and are now being used in health monitoring, disaster management, defense, telecommunications, etc. Such networks are used in many industrial and consumer applications such as industrial process and environment monitoring, among others. A WSN network is a collection of specialized transducers known as sensor nodes with a communication link distributed randomly in any locations to monitor environmental parameters such as water level, and temperature. Each sensor node is equipped with a transducer, a signal processor, a power unit, and a transceiver. WSNs are now being widely used in the underground mining industry to monitor environmental parameters, including the amount of gas, water, temperature, humidity, oxygen level, dust, etc. The WSN for environment monitoring can be equivalently replaced by a multiple-input multiple-output (MIMO) relay network. Multi-hop relay networks have attracted significant research interest in recent years for their capability in increasing the coverage range. The network communication link from a source to a destination is implemented using the amplify-and-forward (AF) or decode-and-forward (DF) schemes. The AF relay receives information from the previous relay and simply amplifies the received signal and then forwards it to the next relay. On the other hand, the DF relay first decodes the received signal and then forwards it to the next relay in the second stage if it can perfectly decode the incoming signal. For analytical simplicity, in this thesis, we consider the AF relaying scheme and the results of this work can also be developed for the DF relay.

The transceiver design for multi-hop MIMO relay is very challenging. This is because at the L-th relay stage, there are 2^L possible channels. So, for a large scale network, it is not economical to send the signal through all possible links. Instead, we can find the best path from source-to-destination that gives the highest end-to-end signal-to-noise ratio (SNR). We can minimize the mean square error (MSE) or bit error rate (BER) objective function by sending the signal using the selected path. The set of relay in the path remains active and the rest of the relays are turned off which can save power to enhance network life-time. The best path signal transmission has been carried out in the literature for 2-hop MIMO relay and for multiple relaying it becomes very complex. In the first part of this thesis, we propose an optimal best path finding algorithm at perfect channel state information (CSI). We consider a parallel multi-hop multiple-input multiple-output (MIMO) AF relay system where a linear minimum mean-squared error (MMSE) receiver is used at the destination. We simplify the parallel network into equivalent series multi-hop MIMO relay link using best relaying, where the best relay

selects the maximum possible gain path.

The data transmission from one node to the other nodes through a wireless link in underground mines may be affected by Gaussian noise, reflections, and interferences, and this is due to multi-path propagation. One of the challenges of WSN deployment in underground mines is the lower power-consumption requirement as sensor nodes carry limited irreplaceable power banks. Therefore, optimum power allocation is the most important design characteristics for WSNs in the mining environment. Once we have the series network, we propose a strategy to jointly design the source precoder, relay filters, and linear receiver matrices using convex optimization with perfect CSI knowledge with total power constraint. Based on the theoretical analysis, we carry out Matlab simulations to verify the theoretical investigations.

Contents

List of Figures

List of Tables

List of abbreviations

ACK	Acknowledgment
AF	Amplify-and-Forward
AWGN	Additive White Gaussian Noise
BD	Block Diagonalization
BER	Bit Error Rate
BRS	Best Relay Selection
BS	Base Station
CDMA	Code Division Multiple Access
CEO	Chief Executive Officer
CF	Code-and-Forward
CR	Cognitive Radio
CSI	Channel State Information
DCN	Data Collecting Node
DF	Decode-and-Forward
DGN	Data Gathering Node
EM	Electromagnetic Wave
EVD	Eigen Value Decomposition
FC	Fusion Center
GEN	Generalized Nash Equilibrium
GENP	Generalized Nash Equilibrium Problem
GMD	Geometric Mean Decomposition
GPRS	General Packet Radio Services
GV-MAC	Gaussian Vector Multiple Access Channel
ITA	Intracluster
ITE	Intercluster
IWF	Iterative Water-Filling
KKT	Karush-Kuhn-Tucker
LAN	Local Area Network
LEACH	Low Energy Adaptive Clustering Hierarchy
LOS	Line Of Sight
LP	Linear Program
LQ	Lloyd Quantizer

MAC	Medium Access Control
MC	Monitoring Center
MIMO	Multiple-Input Multiple-Output
MISO	Multiple-Input Single-Output
ML	Maximum Likelihood
MMSE	Minimum Mean Square Error
M-QAM	M-ary Quadrature Amplitude Modulation
MSD	Mean Square Distortion
MSE	Mean Square Error
MSR	Maximum Sum Rate
NI	Noise-plus-Interference
NLOS	Non-Line Of Sight
PCM	Pulse Code Modulation
QPSK	Quadrature Phase Shift Keying
QoS	Quality of Services
RDS	Relay Diversity Ordering Selection
RIWF	Robust Iterative Water-Filling
SIMO	Single-Input Multiple-Output
SINR	Signal-to-Interference-Noise Ratio
SISO	Single-Input Single-Output
SNR	Signal-to-Noise Ratio
SR	Sum Rate
STBC	Space Time Block Code
SVD	Singular Value Decomposition
TDMA	Time Division Multiple Access
VBLAST	Vertical-Bell Laboratories Layered Space-Time
VMIMO	Virtual Multiple-Input Multiple-Output
VQ	Vector Quantizer
WF	Water-Filling
WSNs	Wireless Sensor Networks
WWW	World Wide-Web
ZF	Zero-Forcing

Acknowledgments

First of all I would like to express my sincere thanks to my thesis supervisor, Professor Paul Fortier, for all the guidance and encouragements he has offered me throughout the period of this research. I am extremely indebted to him for guiding this work and for his helpful input and discussions.

I am also grateful to my co-supervisor Dr. Mohamed Lassaad Ammari for his valuable advices and for mentoring me with techniques, developments, and codings. I would like to thank my colleague Marwa Chouk for assisting me with analytical developments in techniques related to wireless sensor networks.

Finally, I would also like to thank my parents and friends for their constant love and support throughout the course of my studies to pursue higher studies.

Chapter 1

Introduction

With the advanced developments in wireless communication technologies, wireless sensor networks (WSNs) have gained attention worldwide in the past decade and are now being used in health monitoring, disaster management, defense, telecommunications, etc. Such networks are also used in many industrial and consumer applications such as industrial processes and environment monitoring, and so on. The unprecedented success of WSN in those sectors has led to the emergence of this technology in the mining industry. The limitations of WSN in mining implementations will be discussed in this chapter.

1.1 Brief Introduction to WSNs

A WSN is a collection of specialized transducers known as sensor nodes with a communication link distributed randomly in any locations to monitor parameters such as temperature, humidity, pressure, chemical concentration, pollutant levels, etc. Each sensor node is equipped with a transducer, a signal processor, a power unit, and a transceiver. The transducer converts the physical quantity into an electrical signal, and after processing the electrical signal, the transceiver transmits data to the other nodes. The power of each sensor node is supplied from an energy source, usually a battery, which defines the life-time of the overall network. The components of a WSN enable wireless connectivity and refer to a group of dedicated sensor nodes. A sensor node may vary in size from millimeter-size custom silicon to large-size integrated units. The range of wireless connectivity depends on the environment in which it is deployed, and it can be extended by adding relay nodes between a gateway and a leaf node for a particular topology [1].

1.1.1 WSN Architecture

A WSN is a collection of sensor nodes that are grouped into clusters to exchange information among the connected nodes. A node after sensing and processing any physical or environmental data, communicates it with other nodes in the cluster to exchange information. They can cooperatively pass

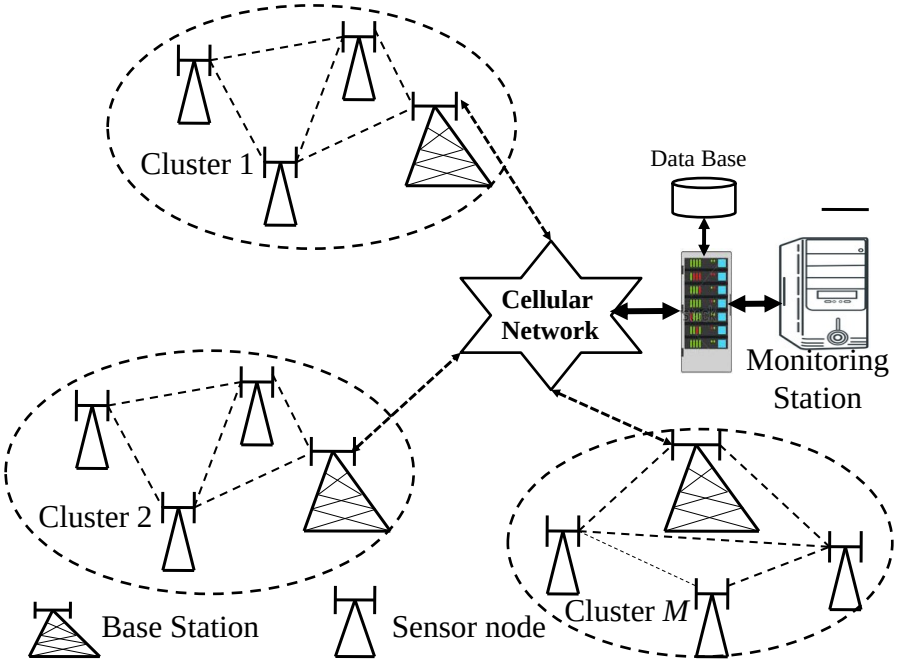

Figure 1.1 – WSN architecture for environmental monitoring.

their data via self-configuration and a multi-hop routing network to a sink to further analyze using different tools. Here, the cooperative communication refers to the process where the transmitting node sends not only its own data but also sends its neighbor nodes data. A base station acts as an interface between user nodes and the network by communicating in many ways such as Internet, satellite, and mobile communication networks. A typical WSN contains a large number of sensor nodes distributed randomly in a large area. A WSN node is equipped with sensing and computing devices, radio transceivers and a power source. Nodes can communicate among themselves using radio signals. A representation of a wireless sensor network is provided in Fig. 1.1 to monitor and measure data from a remote location. In this system, a sensor node sends the measurements to the network (GPRS in this case) via a base station. Nowadays, most of the research on WSNs is conducted on energy efficient algorithms which gives better system performance with less power and transceiver design to extend the life-time of the network.

1.2 WSNs in Underground Mines

Environmental monitoring in underground mine galleries, which are basically long and narrow (they can be several kilometers in length), is a crucial task to ensure safe working conditions. WSNs are now being widely used in the underground mining industry to monitor some environmental parameters, including the amount of gas, water, temperature, humidity, oxigen level, dust, etc. The transmitted

signal through the channel is attenuated and distorted by the absorption and reflection is taken into account in the medium due to rough surface structure through which the signal travels, and the transmitted power decreases with the distance by an inverse power law, $P_0 d^{-\nu}$, where P_0 is the transmitted power and ν is the attenuation constant which depends on the material of the floor, ceiling, and walls [2]. The mine areas can be divided into two major parts, a) the open areas that include rooms and pillars, and b) the tunnels that include the passageways. When the signal travels through multi-paths, the signal at any receiving node may be added constructively or destructively. The signals are added constructively when their frequency and phase are similar and the signal are added destructively when their frequency and phase are different. The random fluctuations of the electromagnetic (EM) waves may disconnect the node-to-node link due to fading, and a transmitter will try to enhance the power to continue the transmission over harsh fading channels [3]. The drawback of this method is the high energy consumption which may alternatively diminish the life-time of the network.

WSN nodes are deployed in underground mines for continuous monitoring of critical phenomena by employing multi-hop routing to provide more scalability for system construction. But the practical implementation of this technology is not easy because the sensors need to self-organize which means that they should be able to reconfigure themselves depending on the monitored environment [4]. The self-organization algorithm allows the sensor node to distribute power in such a way that they converge in a stable equilibrium state. We will discuss the self-organization technique in detail in the next chapter. Sensor nodes measure local physical quantities and forward them to the fusion center (FC) via a number of connected relay nodes. The data transmission from one node to the other nodes through a wireless link in underground mines may be affected by Gaussian noise, reflections, and interferences [5], [6]. The self-organizing algorithm enables multihop routing to provide higher quality of service (QoS) and bandwidth efficiency [3], [7]. The consumption of excess energy may rapidly turn off the battery power supply and it may decrease the network lifetime [8], so new life-time maximization mechanisms and protocols are required for the development of WSNs in underground environments [9]. In some other wireless network applications, extra energy can be inserted from external renewable sources to overcome the shortage of energy [10], but external energy feeding is not feasible in the underground environment.

1.3 General Overview and Objectives

1.3.1 Motivations

Multiple-input multiple-output (MIMO) relays are important techniques for WSN deployment in highly fading environment that can be used to reduce the path loss, increase the power efficiency, and network coverage. Due to the limited power supply, the optimization of the MIMO relay networks has gained much attention in recent years. In MIMO relaying, the source signal is amplified and forwarded to the destination through a number of relay nodes. Each relay terminal may be equipped

with a single antenna for single node or multiple antennas for multiple nodes. This can be done according to different protocols such as amplify-and-forward (AF), decode-and-forward (DF), and compressed-and-forward (CF) [11]. The analog AF is the simplest and most used protocol in which non-regenerative relays are used to linearly process the incoming signals. In non-regenerative relay, the relay only amplifies and re-transmits the received signal to the destination or next relay. Among the variety of AF relay structures, the simple two-hop one way model from source to destination using single antenna relays has been targeted in the major research works. In a few researches, multiple antenna multi-hop parallel relaying has been carried out in some special cases. The DF protocol uses a decision based receiver (MMSE or zero-forcing (ZF) receiver) to construct the source symbol before amplifying and forwarding. For the multiple relaying DF scheme in long source-destination communication, a processing delay due to signal decode and reconstruction is introduced during the decision action at each relay node for forwarding the exact input signal to the next node. The larger data size in some applications consumes more energy for decoding and reconstruction of original data in each relay stage. In this case, the CF protocol is used to forward compressed data to the destination. Depending on the relay strategy, some power allocation methods have been proposed for WSNs to obtain the best possible quality of service (QoS) based on the assumption of perfect synchronization and available channel state information (CSI). Sensor nodes are only able to communicate in a short range due to the inherent limitations in the size, power, and cost [12]. Several works about the power allocation in multi-hop transmission systems have been proposed to minimize total transmission power under a constraint on QoS at the destination. Usually, a QoS constraint is considered in the optimization but in [13], an outage probability constraint is considered for the optimal power allocation schemes for both regenerative and non-regenerative systems to design power allocation algorithm that minimizes system outage probability. In [14], a general multi-hop WSN power optimization is considered using AF relaying based on MMSE and mean sum-rate (MSR) constraint subject to individual, local, and global power constraints. Our goal is to find the optimal solution for the power assignment of parallel multiterminal multi-hop WSN relay with local and global power constraints. The power allocation algorithm should be in such a way that the receiver reconstructs the input data so that it can increase the input-output mutual information and decrease the mean-square-error (MSE) of the signal. The input-output mutual information is an indicator of how much coded information accurately passed to the receiver through the fading channel for the corresponding power solution. The small size sensor node are only able to communicate in a short range due to the shortage of power supply [12]; in the case of the mining environment, multihop communication can be recommended to cover the large area [15]. Again, the obstacles between the source and destination further affect the transmission and an alternative strategy is proposed to mitigate this effect to design multihop WSNs employing AF relaying [16]. The power allocation problem of WSNs employing the distributed AF protocol has been considered through noisy observation of a Gaussian random source based on the minimum mean-squared error (MMSE) estimation rule [17].

Authors in [13] studied the problem of both regenerative and non-regenerative multi-hop systems. For both systems, optimizing power allocation reduces outage probability. They concluded that a

non-regenerative system with optimum power solution outperforms a regenerative system with no optimization. A linear non-regenerative approach has been proposed in [18] for multiuser multi-hop MIMO relay systems using an MMSE receiver at the destination node. The work addresses the issue of multi access communication through non-regenerative AF relays, where terminals have multiple antennas. They solve the optimization problem for source precoder matrices and relay amplifying matrices with the assumption that MSE matrices at the destination can be decomposed into the sum of the MSE matrices at all relay nodes. They used water-filling power allocation in each of sub-channel so that the signal can be transmitted through the link with higher gain. It enables the power allocation at each relay node in a distributed manner at a high signal-to-noise ratio (SNR) environment which requires local CSI knowledge. In some other environments, where direct link between the source and the destination is sufficiently strong, general optimization is not sufficient in the joint design process, so extensive research efforts need to be devoted to solve the power optimization for such a problem. Also, AF relaying becomes the effective means to improve performance and coverage of wireless system when direct link is present along with the relay. In [19], a simple joint optimization algorithm has been introduced which iteratively finds a local optimal solution for the precoder and relay matrices in the presence of a direct link using AF relaying systems. The minimization of QoS objective function based on the MMSE criteria for MIMO AF relaying system is non-convex due to non-linear matrix operation, and thus finding the optimal solution is intractable. For a single stream transmission, the problem is convex even if the direct link is available. The DF relay forwards noiseless data to the destination, thus in contrast it provides better performance for reliable source-relay-destination link. For DF relaying without a direct link, the joint precoder designing problem at source and relay can be easily obtained by singular value decomposition (SVD) by splitting the problem into two independent sub-problems. In the case of DF relaying with a direct link, [20] developed a distributed precoder designing method for source and relay with less computational complexity using SVD and water-filling. The design of the precoder matrix at the source, and at all relays require proper CSI knowledge but in practical communications, CSI is obtained through channel training/estimation. There is a CSI estimation error due to channel noise, quantization errors, and outdated channel estimates, which may substantially degrades system performance [21]. A limited work has been carried out for optimal solution for multi-hop relaying based on imperfect CSI information [21], [22]. We propose to design a multi-hop parallel multiterminal MIMO AF relaying system based on a powerful convex optimization technique with perfect CSI knowledge at all source, relay, and destination terminals. The channel in underground mines is harsh and time-varying in nature [5].

1.3.2 Our Approach

The classical multi-terminal multi-relay or multiple source/destination systems have been investigated in recent works. Parallel relay network, which is a special case of multiple relay network was first introduced by Schein in [23]. Based on the work in [23], two-hop AF parallel relay networks have been investigated in [24], [25] where each relay terminal is equipped with multiple antennas. In

many applications, multi-hop parallel relay networks are being used. In regenerative DF relaying, the relay decodes the incoming signal and after perfect reconstruction, transmits it to the destination. [13] studies the non-regenerative and regenerative relay networks and shows that optimum power allocation in regenerative relaying achieves the best QoS performance. To the best of our knowledge, no work has been done in the literature to design and analyze multi-hop parallel relay networks, and it is the main contribution of this thesis. In the case of parallel multi-hop relaying, each terminal can be considered as a source for the next relay, and equivalently we can consider that each relay terminal has more than one user. For multi-user MIMO systems, the major design problem is the elimination of interference from other users in the same or other networks. At the present time, to handle this problem, block diagonalization (BD) is used which divides the multi-user channel into several single user channels without interference. To handle the error propagation problem, detection is used with the BD scheme in [26] which attains single-symbol decodability. Authors in [27] proposed a selection relaying scheme where the relay decodes the signal provided that the channel has higher signal-to-noise ratio (SNR) or gain. The selection relaying based carrier-noncooperative scheme is less general and provides worse performance in deep fading [28]. Our first approach to simplify the complex parallel multi-hop relaying is to use the block diagonal property to reduce the interference from other users in the selection relaying. Then, we design an optimum precoder for source and all relay terminals to minimize the bit error rate (BER) at the detection terminal for a known receiver matrix by using convex optimization solvers.

1.4 Contributions

Our contributions are the following:

1. Simplification of parallel multi-hop relay networks using block-diagonalization with the help of selection relaying.
2. Optimum precoder design to solve the power optimization problem with AF relaying using standard convex solvers subject to local and global power constraints under perfect CSI knowledge.

1.5 Outline of the Thesis

In Chapter 2, a literature review of the problem of power allocation for cooperative sensor networks to provide the maximum system performance with power constraint is presented. In particular, the water-filling power allocation published in recent works is discussed to explain the fundamental technique of power allocation. We present the model of a WSN network that can be used to measure some environmental parameters in underground mines in Chapter 3. In this chapter, we will also present the network simplification method. Then, we also provide the joint transceiver design of the simplified network using a powerful convex optimization technique. In Chapter 4, we present the optimum proposed precoder design for source, and relay terminals for the perfect CSI case. In this chapter,

we also present simulation results based on the theoretical investigations. Finally, in Chapter 5, we present conclusions for this work.

Chapter 2

Communications and Wireless Sensor Networks

This chapter discusses the problem associated with the deployment of WSNs in fading environments such as in underground mines. Our focus will be on the energy optimization of sensor networks depending on the operational environment.

2.1 Communications

The energy efficient communication between the source and destination through the wireless medium requires less interference from other sources. For this reason, the WSN transceiver must allow medium access control (MAC) protocols that are developed for communicating with neighbor nodes via a shared radio channel.

2.1.1 Space-Time Block Code (STBC) MIMO Technique

Exploiting multiple antennas at transmitter and receiver provides substantial benefits in both increasing system capacity and immunity to deep fading in wireless channels by using space-time coding [29]. On the other hand, space-time coding techniques are used in modern MIMO wireless communication to achieve antenna diversity gain. The concept of space-time coding is based on the idea that the probability of multi-symbols through multiple statistically independent fading channels simultaneously experienced deep fading is low due to the use of a code matrix for each source. A space-time coded MIMO system with M transmit antennas and N receive antennas is illustrated in Fig. 2.1 according to [29], [30]. The binary bit stream is mapped into symbols $\{S_i\}_{i=1}^{L}$ by quadrature phase shift keying (QPSK) modulation and then the symbol stream of size L is space-time encoded into $\left\{x_i^{(t)}\right\}_{i=1}^{M}$ $M \times T$ space-time code words, where i is the antenna index, and $t \in [1, \cdots, T]$ is the time index. Here, the M symbols are transmitted by a codeword over T symbol periods with the symbol rate, $R = M/T$ (symbols/channel). Let $h_{j,i}^{(t)}$ denotes a Rayleigh-distributed channel gain from the ith transmitting an-

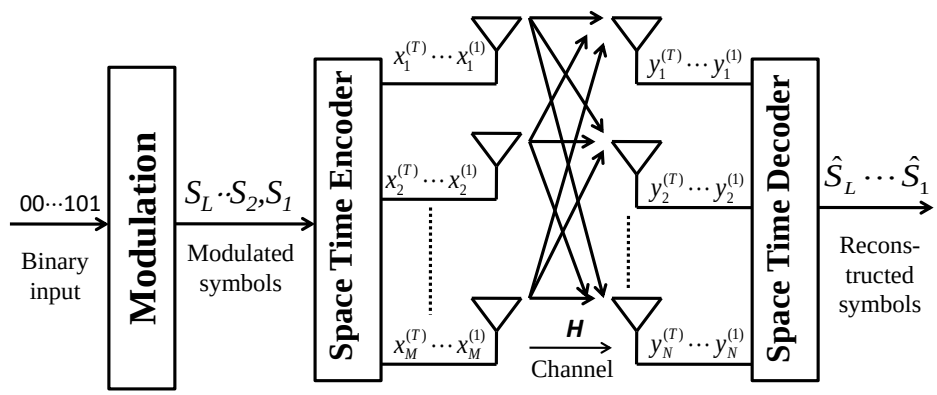

Figure 2.1 – Space-time coded MIMO systems.

tenna to the jth receiving antenna over the tth symbol period. Then we can express the MIMO channel as $\mathbf{H}(t) = [\mathbf{h}_1^{(t)}, \cdots, \mathbf{h}_M^{(t)}] \in \mathcal{C}^{N\times M}$, where, $\mathcal{C}^{N\times M}$ is the set of complex matrices of dimension $N \times M$ and $\mathbf{h}_i^{(t)} = [h_{1i}^{(t)}, h_{2i}^{(t)}, \cdots, h_{Ni}^{(t)}] \in \mathcal{C}^{N\times 1}$. The input-output relationship for the flat fading MIMO channel $\mathbf{H}$ can be expressed as:

$$\mathbf{y}(t) = \mathbf{H}(t)\mathbf{x}(t) + \mathbf{z}(t) \tag{2.1}$$

where $\mathbf{H}(t)$ is the $M \times N$ complex channel matrix and

$$\mathbf{y}(t) = [y_1^{(t)}, \cdots, y_N^{(t)}] \tag{2.2}$$

$$\mathbf{x}(t) = [x_1^{(t)}, \cdots, x_M^{(t)}] \tag{2.3}$$

$$\mathbf{z}(t) = [z_1^{(t)}, \cdots, z_N^{(t)}] \tag{2.4}$$

are complex row vectors of the received signal, transmitted signal, and noise, respectively at time index t. If the channel $\mathbf{H}(t)$ does not change within a block, then (2.1) can be expressed as:

$$\mathbf{Y} = \mathbf{H}\mathbf{X} + \mathbf{Z} \tag{2.5}$$

where $\mathbf{X} = [\mathbf{x}^T(1), \cdots, \mathbf{x}^T(T)]$, $\mathbf{Y} = [\mathbf{y}^T(1), \cdots, \mathbf{y}^T(T)]$, and $\mathbf{Z} = [\mathbf{z}^T(1), \cdots, \mathbf{z}^T(T)]$. The space-time encoder generates the $M \times T$ complex transmitted matrix $\mathbf{X}$ from the input symbol vector $\mathbf{S} = [S_1, S_2, \cdots, S_L]$ by the operation as

$$\mathcal{G}_c(\mathbf{S}) : \mathcal{C}^{L\times 1} \longmapsto \mathcal{C}^{M\times T} \tag{2.6}$$

under the condition that the row vectors of matrix $\mathbf{X}$ are orthogonal to each other. The matrix operator $\mathcal{G}_c(\mathbf{S})$ is called space-time block code (STBC) operator which was first introduced by Alamouti for 2 transmitting antennas and multiple receiving antennas [31]. If the channel matrix $\mathbf{H}$ is known at the receiver then the decoding step uses a maximum likelihood (ML) coherent detector to find the input symbols.

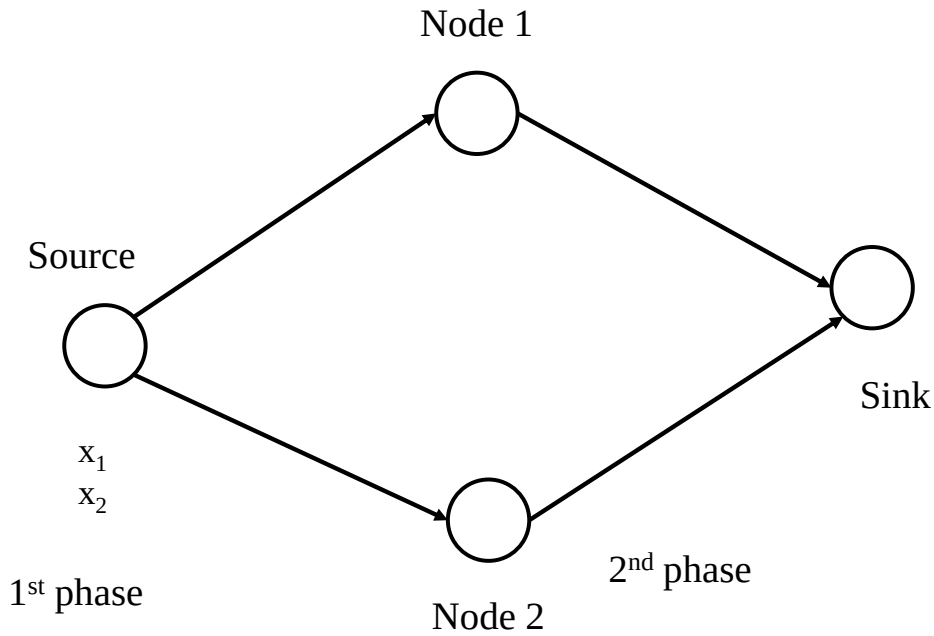

Figure 2.2 – Transmission with STBC combining scheme.

2.1.2 Cooperative Diversity and Cluster Formation

The cooperation of multiple users using a collection of distributed antennas in a cell form a partnership for transmitting not only their own information, but also the information of their neighbors. This form of space diversity is known as cooperation diversity where terminals share their antenna and other resources to create a virtual array. In this case, a user requires more power in order to send both its own signal and the signal of its neighbors. The users in cooperation diversity estimate the realized SNR between them to start a message exchange action through cooperative communication. A user simply forwards the received signal after amplification subject to its power constraint known as AF relaying protocol or fully decode, re-encode and re-transmit the message known as DF relaying protocol. Some researchers suggest to employ a threshold test on the estimated SNR between cooperating radios for the best expected performance, as measured in terms of outage probability for a given rate R. This method provides better performance in terms of outage probability. For a large rate normalized SNR (ρ_{norm}), [32] summarized the high average SNR approximations to the outage probability for AF and DF schemes as a function of the rate normalized SNR, $\rho_{norm} = 2\rho/(2^{2R} - 1)$. The repetition-based cooperative diversity alternatively decreases the bandwidth efficiency with the number of relaying terminals, because each relay requires full use of its own sub-channels for repeating transmission. An alternative STBC cooperative diversity scheme has been proposed in [33] to improve bandwidth efficiency of the repeating cooperation that allows all relays to transmit using the same sub-channel. The STBC cooperation diversity provides an efficient way for relaying signal even in deep fade in order to exploit full spatial diversity, and it may be readily deployed in WSN node cooperation in highly fading environments. In STBC cooperation, the signal is transmitted in the form of a code

matrix, the code matrix for 2×2 MIMO system can be represented as

$$\mathbf{X} = \begin{bmatrix} x_1 & -x_2 \\ x_2 & x_1 \end{bmatrix}$$

When each terminal transmits a message from its distributing columns from the code matrix, other terminals receive, and decode and transmit in the second phase using its distribution column from the code matrix. This can be explained with the help of node to sink communication using intermediate relays as in Fig. 2.2. The source node like to send source information $\mathbf{X} = [x_1, x_2]^T$ in the first time slot to the two intermediate relay node 1 and node 2. The two intermediate relays receive the code depending on the channel gain. The node having the highest channel gain decodes the code word and forward it to the sink node using its own code matrix. The sink node reconstructs the source node signal using the relay code matrix.

The MIMO communication in WSN requires sensor cooperation known as cooperative MIMO communication. In cooperative MIMO communication, a group of sensors cooperate to transmit and receive data based on the assumption of node cooperation where a set of low-end transmit nodes are connected with receiving nodes through a wireless link. The communication is divided into two time slot, intracluster slot (ITA) t_ε, and intercluster slot (ITE) $1 - t_\varepsilon$. The typical value of t_ε is very small, in the range from 0.005 sec up to 0.03 sec. During the ITA slot, local communications are assumed at the transmitter cluster using a time-division multiple-access (TDMA) scheme. In the ITA slot, each node has data symbols from other nodes and performs STBC operations as if each active node acted as a distinct antenna element in a centralized antenna array. Once STBC is done, during the ITE relay period $1 - t_\varepsilon$, M nodes (number of active nodes in the transmit cluster) transmit through an $M \times N$ MIMO channel or over N parallel MISO channels based on the Alamouti diversity approach [31]. Usually, virtual MIMO is formed by all active sensors in a cluster, and router nodes relay messages to nearby clusters using the AF or DF protocols via cooperative transmission in conjunction with the STBC scheme. The Low Energy Adaptive Clustering Hierarchy (LEACH) scheme designates potential sensor nodes as cluster heads. The cluster heads are selected from the nodes distributed in a region through an iterative process. The cluster head can select other neighbor nodes to form a group within a cooperative network. A dynamic cooperation clustering formation has been proposed in [34] where the cluster head selects M nodes from any number N_{total} sensor nodes $(M \leq N_{total})$. Any cluster with M nodes may send information to the destination via another cluster by using repetitive cooperative relay or STBC cooperative relay.

2.1.3 Medium-Access Control

As in many current wireless networks, terminals transmit on orthogonal channels, such as cellular and wireless local area networks (LANs). In wireless networks, we divide the available bandwidth into orthogonal channels and allocate these channels to the terminals which transmit on essentially orthogonal channels. The channel orthogonality means that all sub-carrier signals in the channel have a phase difference of 90 degrees. The designed algorithm needs to be flexible so that any new proto-

cols can be readily integrated into the existing networks. In all cooperative protocols, the transmitting terminals need to process their received signal to remove interferences from other sources. Severe attenuation over the wireless channel, insufficient electrical isolation between the transmit and receive circuitry, and current limitations in radio implementations preclude the terminals from full-duplex operation. To ensure half-duplex operations, each channel is divided into othogonal subchannels, and the synchronization between the terminals is required for effective cooperative diversity. In cooperative diversity transmission, the medium-access control protocol manages orthogonal relaying at the terminal with half-duplex constraint and do not transmit and receive simultaneously at the same time in the same frequency band. [33] illustrates an example of channel and subchannel allocations for repetition-based cooperative diversity, in which relays either amplify or fully decode and repeat the received signals. The repetitions must occur on orthogonal subchannels for the destination to combine these signals and achieve full diversity gains. For N terminals in noncooperative transmission, transmission between source and destination uses a fraction $1/N$ of the total degrees of freedom because each source-destination pair share the channel by $1/N$ times of the total available time period. Here, for the STBC cooperative diversity, relays use a suitable space-time code during the relaying period to transmit simultaneously on the same subchannel using half of the total degrees of freedom in the channel because each terminal uses half of the total available time.

2.1.4 Cooperative Relaying

The cooperative diversity protocol uses a variety of protocols including fixed and selection relaying. For fixed relaying, relays allow either amplification, or decoding, re-encoding and transmitting the signals to the next relay or destination with individual and total power constraints in both cases. Selection relaying performs transmission between terminals through fixed relaying based on the measured instantaneous SNR between the links. Let us consider a source transmitting a signal x_s to the relay terminal and the destination terminal at half of the time through channels $h_{s,r}$ and $h_{s,d}$, respectively for $t = 1, \cdots, T/2$. For cooperative diversity, we have

$$y_r[t] = h_{s,r} x_s[t] + z_r[t] \tag{2.7}$$

$$y_d[t] = h_{s,d} x_s[t] + z_d[t] \tag{2.8}$$

for $t = 1, \cdots, T/2$, where $y_r[t]$ and $y_d[t]$ are the relay and direct destination received signals from the source, respectively, and $z_i[t], i \in \{r,d\}$ is the noise effect. For the next half of the time, $t = T/2+1, \cdots, T$, the source does not transmit. Only the relay is transmitting the received signal to the destination through channel $h_{r,d}$. Thus we have

$$y_d[t] = h_{r,d} x_r[t] + z_d[t] \tag{2.9}$$

where $y_d[t]$ is the destination signal from the relay terminal only.

Fixed Relaying

Amplify-and-Forward: The relay during $t = T/2+1, \cdots, T$ processes $y_r[t]$ and forwards the received signal by transmitting [35]

$$x_r[t] = \beta y_r[t - T/2] \tag{2.10}$$

where the amplifying factor β is given by

$$\beta \leq \sqrt{\frac{P}{|h_{s,r}|^2 P + N_0}} \tag{2.11}$$

where N_0 is the noise variance and P is the power constraint. The destination can estimate the input signal from its received signal $y_d[t]$ by combining the two received signals using any suitable combining technique.

Decode-and-Forward: The relay processes $y_r[t]$ during $t = 1, \cdots, T/2$ by decoding an estimate of the source signal $\hat{x}_s[t]$, and transmits the signal

$$x_r[t] = \hat{x}_s[t - T/2] \tag{2.12}$$

Decoding at the relay can be done by employing either ZF or an MMSE receiver matrix.

Selection Relaying

If the measured channel gain $|h_{s,r}|$ falls below a certain threshold, the source may discard the source-relay link and continues the transmission through the source-destination direct link. On the other hand, if the measured channel gain $|h_{s,r}|$ lies above the threshold, the relay forwards the received signal to the destination using either AF or DF to achieve the diversity gain. If the relays have multi-input signal from different sources, the relay forwards the signal having the highest channel gain $|h_{i,r}|, i \in [1, \cdots, M]$, where M is the number of incoming signals having gain $|h_{i,r}|$ greater than a certain threshold.

2.1.5 Underground Channel Modeling

Signal propagation through underground tunnel depends mainly on three factors [36]: i) free space path loss; as a result the signal to noise ratio (SNR) decreases with the node distance, ii) multi-path fading; the EM waves reflected from the surfaces arrive with different time delays and produce fading; the impulse response of the channel represents the fading effect, and iii) noise; additive white Gaussian noise (AWGN) due to the presence of power lines, internal sources (electronic equipment), and electric motor, etc. The success of symbol transmission can be achieved by the proper selection of signal power and node-to-node distance, and the distortion of symbols can be mitigated by the estimation of the channel impulse response. The wireless channel in an underground mine can be described using different statistical distribution functions, and authors in [37] have selected probability distribution functions (pdf) for statistical characterization of the wireless channel to represent the

information about the multipath behaviors of the channel. They used two types of pdf functions, i) the Rayleigh fading distribution function that represents non-line of sight (NLOS), and ii) the Rician fading distribution function in the case of line of sight (LOS) transmission. This is because the LOS consists of both direct signal and reflected signals. To demonstrate the theory in underground mines, Alouini and colleagues [38] provided the solution of power allocation for a WSN network by considering the propagation through NLOS transmission while considering a Rayleigh fading channel. Here, they considered only the effects of all reflected signals from the obstacles and walls instead of direct LOS communication.

Usually, all nodes in the designed network remain fixed, hence we can say that the wireless link is stationary. In underground communications, the channel between two transceivers is relatively stable with respect to time. As a result, channel randomness is due to the position of the nodes rather than time. The received signal levels at different locations obeys a Rayleigh probability distribution with respect to distance instead of time. Each path in the underground channel $h_{i,j}, i \in [1, \cdots, N], j \in [1, \cdots, M]$ is in fact circular symmetric $\mathcal{CN}(0, \sigma_{i,j}^2)$ because each component $h_{i,j}$ is a complex circularly symmetric Gaussian random variable with mean 0 and covariance $\sigma_{i,j}^2$. The magnitude $|h_{i,j}|$ of the channel response is a Rayleigh random variable with density [39]:

$$f(h) = \frac{h}{\sigma^2} \exp\left\{-\frac{h^2}{2\sigma^2}\right\}, h \geq 0 \tag{2.13}$$

The channel coefficient $h_{i,j}$ from any transmitting antenna i to receiving antenna j is modeled as follows [40]

$$h_{i,j} = \sqrt{d_{i,j}^{-\nu_{i,j}}} \bar{h}_{i,j} \tag{2.14}$$

where $\bar{h}_{i,j}$ is a complex Gaussian random variable with zero-mean and variance $\sigma_{i,j}^2$, $\nu_{i,j}$ is the path loss exponent, and $d_{i,j}$ is the distance.

2.1.6 Water-filling Technique

Water-filling is one of the techniques in wireless communication for the optimum power allocation of sub-channels to obtain better system performance under individual power constraint or total power constraint. To enhance the data rate while maintaining a constant power in a sensor network, the traditional water-filling technique cannot be applied directly because the power allocation in WSN applications is not independent with respect to equilibrium state.

Water-filling Concept

For multiple channels, a subset of channels can be allowed to allocate power based on channel gains according to the water-filling algorithm. Basically, the process of water-filling is similar to pouring water in a tank in which the level of water is filled periodically to perform a particular task. In an ad-hoc network, the power of a channel is filled iteratively to maximize the total data rate through any fading environment. The unshaded portion in Fig. 2.3 represents the noise level of the corresponding

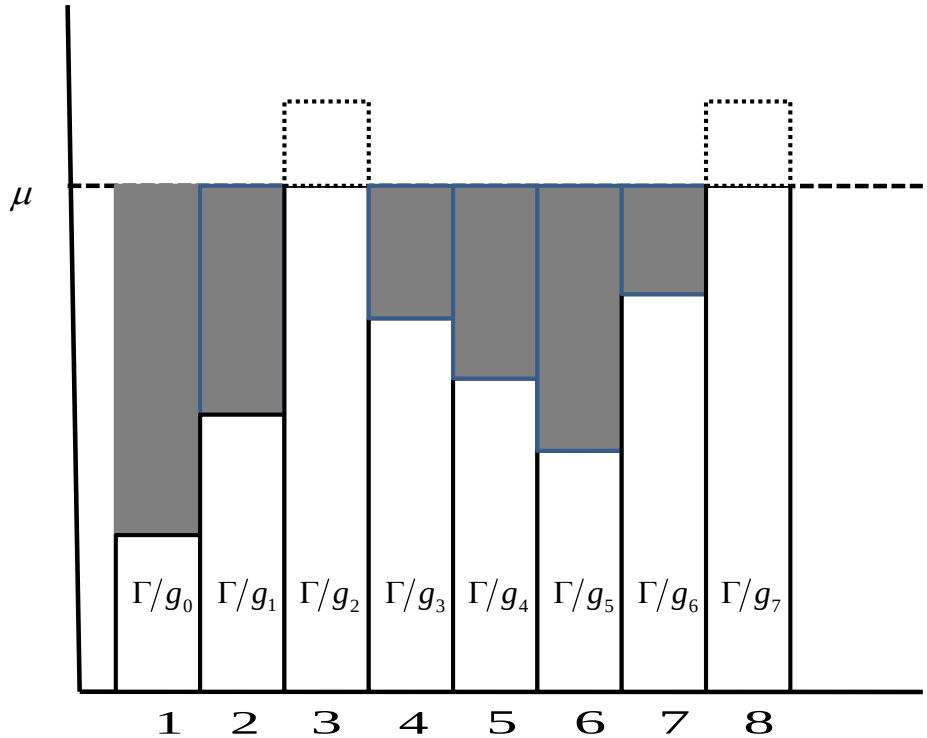

Figure 2.3 – Water-filling concept. The ratio between SNR gap (Γ) and channel gain $g_i, i = 1, \cdots, N$ gives the relative noise level.

channel and the shaded portion represents the power level or water level (μ). The amount of water or power allocated is proportional to the noise and interference in the channel. The allocated power (p_i) to the ith channel $h_i, i = [1, \cdots, N]$ can be expressed [41]

$$p_i^* = \left[\mu - \frac{1}{g_i^2}\right]^+ = \max\left[\mu - \frac{1}{g_i^2}, 0\right] \tag{2.15}$$

where $(x)^+ = \max(x,0)$, $g_i = |h_i|^2$, the water level μ is chosen so that $\sum_{i=1}^{N} p_i(\mu) = P$ because the sum of individual terminal powers is equal to P, P is the total power budget in the link, and N is the total number of orthogonal channels. The ultimate goal of water-filling is to maximize the capacity C:

$$C = \frac{1}{2}\sum_{i=1}^{N} \log_2\left(1 + \frac{p_i}{N_i}\right) \tag{2.16}$$

where N_i is the noise variance. The optimal solution that maximizes throughput based on Shanon's capacity equation can be found by water-filling with the condition that the quality of the radio channel is known at the transmitter. We perform water-filling through the following water-filling steps [42]:
step-1: Sort g_k from largest to smallest, i.e., $g_1 > g_2 > \cdots > g_N$
step-2: Find the constant K for $\Gamma \leq 1$ (where $\Gamma \leq 1$ is the SNR gap) using

$$K = \frac{1}{N}\left[\bar{\varepsilon}_x + \Gamma \sum_{k=1}^{N} \frac{1}{g_k}\right] \tag{2.17}$$

step-3: Calculate another energy level, $\bar{\varepsilon}_k$

$$\bar{\varepsilon}_k = K - \frac{1}{g_k};\ k \in [1, \cdots, N] \tag{2.18}$$

step-4: Omit the channel g_k having $\bar{\varepsilon}_k < 0$, and allocate the energy $\bar{\varepsilon}_k$ to the rest of the sub-channels, $g_k = g_k + \bar{\varepsilon}_k$, where $k \in [1, \cdots, N]$ with $N = N - n$, n is the number of iterations required to make $\bar{\varepsilon}_k > 0, \forall k$.

step-5: Continue step 1 to step 4 until all sub-channels have $\bar{\varepsilon}_k > 0$.

step-6: Calculate the bit rate of each sub-channel that satisfies $\bar{\varepsilon}_k > 0$, according to $R_k = \frac{1}{2}\log_2(1 + \bar{\varepsilon}_k g_k); \forall k$. The total sum-rate of the link can be written as:

$$R = \sum_{k=1}^{N-n} R_k \tag{2.19}$$

The challenge of deploying water-filling in WSNs is the convergence, especially in fading environments [43], and the convergence analysis will be carried out in the following sub-section.

Challenges of Implementation in WSNs

The water-filling technique transmits signal through the channel having a gain greater than a threshold level and discards transmission on a given channel if the SNR is lower than a threshold value. In WSN cluster networks, if one node assign more power over other neighbors, then its transmission may cause interference to other neighbor users. So, the arbitrary power assignment technique cannot be used directly in sensor networks due to the generation of interferences when clusters are formed. The power increment of any node follows an equilibrium state in which any node is not able to enhance the transmission power independently over a fading channel when the SNR is lower than a threshold value, i.e., the sensor node operation is related to other neighbor nodes in the network. The network designers are looking for how rapidly it converges to the equilibrium state that can be defined as the phase in which a node cannot allocate power independently without concern about its neighbors, and the water-filling parameters calculation by the Lagrangian becomes more complex. The noise-plus-interference (NI) level from the receiver may be further corrupted by additional channel noise and interferences which may misleads the water-filling technique to determine the channel status. Also, the NI level plays an important role during power allocation in the convergence for finding the uniform energy level of each node. If the NI level is corrupted by random channel noise, then it takes more time to fill the noisy channel and more energy through the iterative process [43].

The goal of power allocation in each channel of the network is to enhance the life-time of the network. This concept can be explained by considering a network in which cost functions $J_i(u_i, u_{-i})$ are continuously differentiable and convex on agents action space u_i, then there exists a local point u^* under the following condition [44]:

$$[\nabla J_1(u^*)^T, \cdots, \nabla J_{N_L}(u^*)^T]^T = 0 \tag{2.20}$$

where $\nabla J_i(u^*), i \in [1, \cdots, N_L]$ is the gradient of the local cost function $J_i(u^*)$. In cooperative WSNs, node equipped with a single antenna communicate with the receiver through a distributed MIMO

channel [45], [46] where the transmission strategy of any node depends on the other nodes. The cost function between node i and node j for a transmission between them corresponding to the local decision variable u_i refers only to the transmission power as: $J(u_{ij}) = f(e_{ij}/E_i)$, where E_i is the remaining energy at node i and e_{ij} is the minimum required energy from node i to node j to make a successful transmission over the fading channel. Let us consider that a node remains active if its remaining energy satisfy $E_i \geq E_0$, where E_0 is a minimum threshold level. The life-time of the network is the time until the remaining energy E_i of any nodes in the network goes down to E_0, i.e., $E_i < E_0$. A game theory approach for power allocation of sensor nodes in the equilibrium state requires the CSI knowledge and the CSI of each link can be obtained via a feed-back channel from the receiver. The availability of CSI at the transmitter achieves the highest capacity and it can be achieved by adapting the signal power to the particular channel realization. With the CSI information, the transmitter allocates power based on water-filling solutions corresponding to maximizing the channel mutual information by transmitting at the maximum available power. In Game Theory based water-filling solutions, each link tries to reach a high data rate without transmitting more power by shuting off power from a link which cannot support a minimum data rate, and this operation saves energy by discarding transmission through a fading channel having less data rate. Hence, the utility function of the game needs to be well-designed to coordinate among sensor nodes to determine the strategy of resource allocation.

2.1.7 Performance Evaluation

The network designer ultimate goal is to propose a good networking strategy that meets the required upper and lower bounds in the capacity region by finding the cut-set upper bounds [47]. In water-filling, power allocation maximizes the information capacity. The wireless link can be modeled as a group of parallel Gaussian channels (for channel orthogonality) that can be partitioned into discrete narrowband sub-channels with channel bandwidth of δf Hz. In single carrier communications, capacity calculation follows Shanon's information capacity theorem, but in practical broadcast communications, the SNR gap (Γ) is used to determine the efficiency [48]. The SNR gap is the ratio of ideal SNR at which the system can transmit at most C bits/transmission to a practical SNR at which the system can transmit R bits/transmission, and it compares the practical system with the ideal modulation system. The capacity of a single channel in bits/transmission is given by [41]

$$C = \frac{m}{2}\log_2(1 + SNR) \tag{2.21}$$

where m is the modulation order. The SNR gap (Γ), can be calculated by a similar expression for the SNR of practical systems: $\Gamma = \frac{SNR}{2^{2R/m}-1}$. For the STBC encoding scheme and modulation order $m = 2$, the SNR gap is used to determine the data rate for the n-th sub-channel, h_n, $n = [1, \cdots, N]$, in multi-carrier communications [48]

$$R_n = \log_2\left(1 + \frac{|\, h_n \,|^2\, \varepsilon_n}{2\Gamma_n \sigma_n^2}\right) = \log_2\left(1 + \frac{G_n \varepsilon_n}{\Gamma_n}\right) \tag{2.22}$$

where, $G_n = \frac{|h_n|^2}{2\sigma_n^2}$, σ_n^2 is the noise variance, and $\varepsilon_n = \frac{\Gamma_n}{G_n}(2^{R_n} - 1)$.

As we will see in section 2.2, nodes in a wireless sensor network receive data from neighbor nodes and forward it to the final destination through multi-hop relay communication, and in some cases the signal is distorted in the medium due to long transmission distances. As a result, the network designers used bit error rate (BER), minimum mean square error (MMSE), capacity, and outage probability as performance measuring terms to explain how efficiently the network can transmit the signal through a fading channel over long distances during the study of the efficiency of power allocation techniques.

2.2 Wireless Sensor Networks (WSNs)

In a typical WSN, information collected by multiple sensor nodes need to be transmitted to the fusion center (FC) via relay nodes. Each node sends the measurements to the receiver node which acts as a relay node to forward the messages from previous nodes to the FC. Depending on the transmission distance and wireless channel characteristics, a local node sends measurements first to a connected neighbor node (which forwards the data to another node as relay node), then the data will be transmitted to the final destination through multihop-based routing. The multihop-based routing assumes that each node is connected cooperatively with each other. One of the main objective of WSN protocols is the maximization of the network life-time subject to efficient node to node or node to destination data transmission at total power constraint. The efficient way of life-time enhancement is the energy saving protocol design at the MAC layer.

2.2.1 WSN Communication Protocol

WSNs are a kind of ad hoc network consisting of thousands of sensor nodes that communicate with each other using international standards such as ZigBee PRO, Wireless HART, and ISA100.11a. Details of the discussion of the standards have been investigated in [49] for the energy efficient developments of WSN components. The rapid development of high-speed integrated electronic devices and wireless technology enables sensors with characteristics of low power consumption, self-organizing, multi-parameter sensing, higher life-time, and faster wireless communication ability to connect different sensors to monitor multiple types of environmental parameters. Researchers are now concentrating on the deployment of WSNs in the mining industry. Recently, strategies for the energy efficient deployment of WSNs in underground coal mines have been presented in [50], [51]. The structure of WSN systems [52] for coal mine monitoring is composed of a data processing and control module (processor), a communication module, and a power supply module.

Sensor nodes are placed at a certain distance (from 50 m up to 500 m) randomly and forward data to a sink node which works as a gateway or web server to connect the sensor network and an external network. An air pollution monitoring system deployed in coal mines using a network of nodes (Waspmotes) to obtain surroundings air quality is described in [53]. The data from Waspmotes nodes are transmitted to a router or gateway (Meshlium) through a WSN. The communication architecture between gateways is basically to form multi connected WSNs under the same environment or various

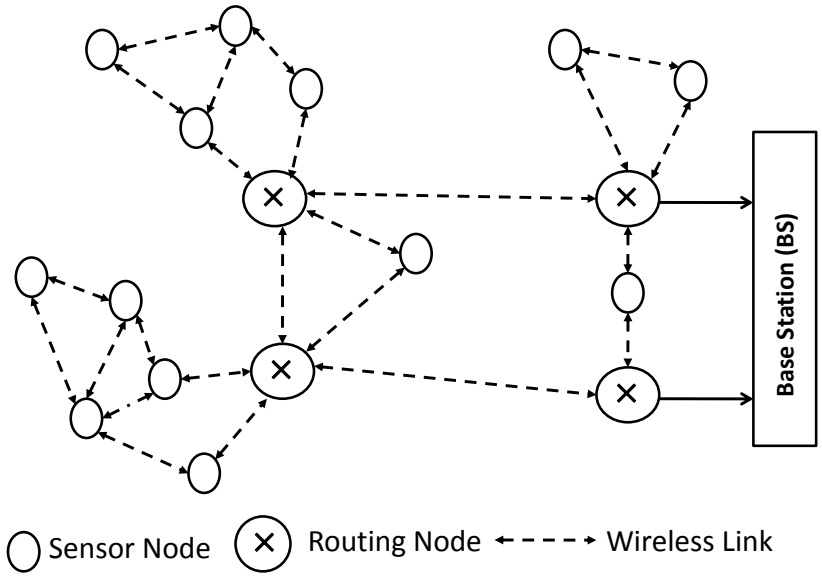

Figure 2.4 – Structure of a WSN for environment monitoring.

environments. An integrated WSN architecture for environment monitoring system is presented in Fig. 2.4 based on the work of [54]. In this architecture, the routing node act as a sink node which joins the sensor nodes to a WSN cloud. The environmental informations are collected by the sensor nodes and are sent to the routing node to forward the information to other routing nodes in the same environment or other environments to exchange data among all sensors. The sink node supports a number of protocols and standards such as ZigBee, Bluetooth, and related IEEE-802.15.4 communication specifications to access the World Wide-Web (WWW) services. The sink node transmits information to the Base Station (BS) via an optical fiber backbone network monitored by a remote manager. Due to the harsh environment and complex conditions of wireless links in underground environments, energy efficient reliable data transmission is the main concern of the design of the WSN topology.

2.2.2 Signal Analysis

For WSN cluster networks, the authors in [45] have considered that the theory of cooperative communications in cluster formation is closely related to MIMO technology, and explored the use of cooperative virtual MIMO (VMIMO) communications in WSNs. Alamouti diversity based MIMO for WSNs is carried out in [46] where individual single antenna array nodes cooperate with each other to form virtual MIMO systems. The authors in [55] considered a distributed detection system with interference channels for MIMO communication in WSNs where multiple transmitting nodes communicates with multiple receiving nodes through a virtual MIMO channel. Again, the energy cost

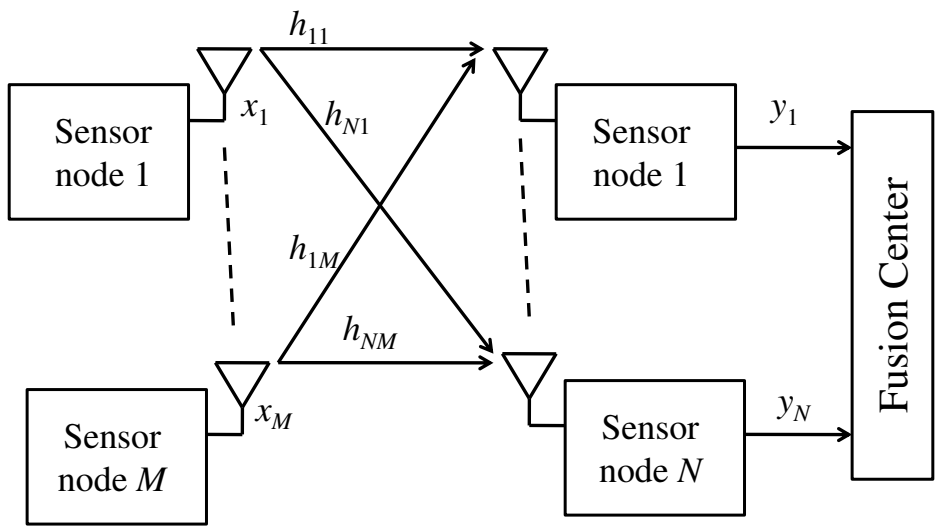

Figure 2.5 – Block diagram of MIMO interference channel, M transmitting nodes, and N receiving nodes.

for intracluster and intercluster transmission is not the same [56], but we will emphasize the energy consumption for transmission from one cluster to another cluster through a MIMO channel.

The distributed cooperative MIMO structure, we simply call it cooperative MIMO communication, requires less transmission energy than the noncooperative approach [57], [58]. The cooperative transmission among multiple nodes can be treated as multiple antenna MIMO, and the energy consumption of the MIMO approach and the noncooperative approach is presented in [46] over the transmission distance d where MIMO becomes more energy-efficient. In the same work, the Alamouti scheme for more than two antennas based MIMO systems can achieve lower error probability over a single-input single-output (SISO) system for Rayleigh fading channels under the same energy constraint. We can represent a general cooperative WSN model by a MIMO interference channel system [59] with M transmitting nodes and N receiving nodes equipped with a single antenna, as shown in Fig. 2.5. The input signal vector $\mathbf{x} = [x_1, \cdots, x_M]^T$ is transmitted to the FC through the MIMO channel $\mathbf{H} = \mathcal{C}^{N\times M}$ that can be modeled by the following baseband representation as:

$$\mathbf{y} = \mathbf{HFx} + \mathbf{z} \tag{2.23}$$

where, $\mathbf{y} = [y_1, y_2, \cdots, y_N]^T$ are the received signals at the FC, $\mathbf{F} = \text{diag}\{p_1, p_2, \cdots, p_M\}$ is a diagonal matrix where the diagonal elements are the associated power of each transmitter nodes, and $\mathbf{z} = [z_1, z_2, \cdots, z_N]^T$ is an additive Gaussian noise vector with zero mean and covariance matrix $\mathbf{R}$. The cooperative WSN in Fig. 1.1 can be treated as a MIMO multiple access communication system ([41], ch. 9), where each sender wishes to communicate through the Gaussian vector multiple access channel (GV-MAC). The Gaussian vector channel reduces to the Gaussian product channel when $M = N$, as depicted in Fig. 2.6, and consists of a set of parallel Gaussian channels ([41], ch. 3)

$$y_j = h_{j,j}x_j + z_j;\ \forall j \in [1:N] \tag{2.24}$$

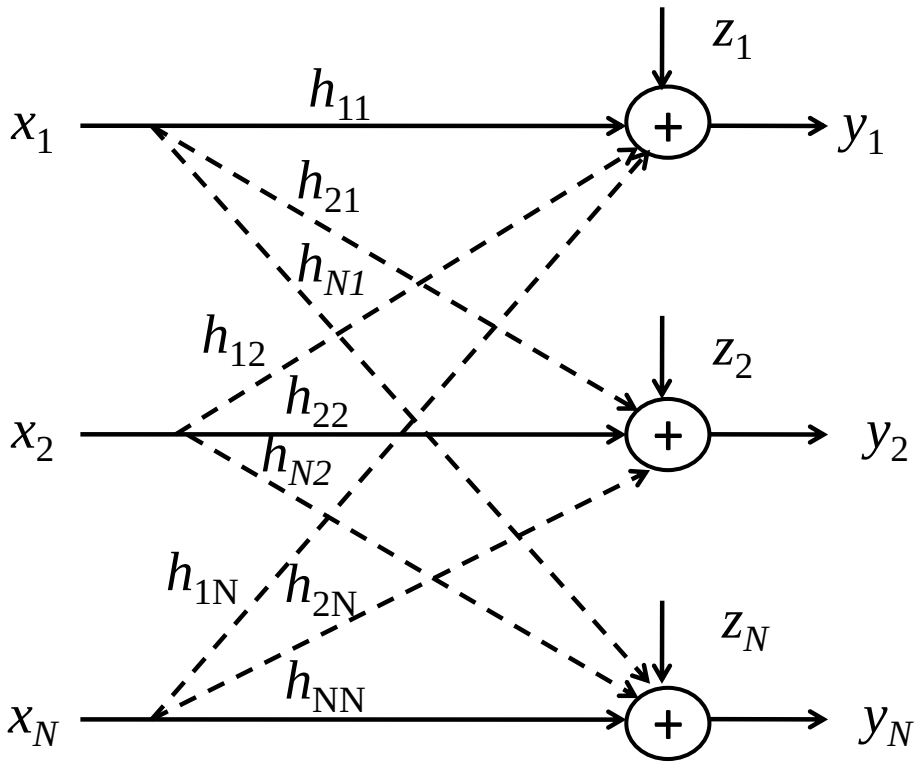

Figure 2.6 – N parallel Gaussian channels with interferences.

where $h_{i,j} = 0, i \neq j$ when the channel are orthogonal, and this is because there is no cross linkage between sub-channels. The SVD transformation decomposes the MIMO channel into multiple parallel sub-channels. The non-zero singular values of the diagonal matrix represent the number of sub-channels formed by SVD. The concept of formation of orthogonal parallel independent sub-channels has been discussed in [60]. The parallel product channel allows node j to communicate with only the corresponding receiver node j at different frequency bands or time slots, i.e., the parallel channels represent orthogonal dimensions. The channel is not a broadcast channel, nor a multiple access channel because each receiver is only interested in the corresponding transmitter. The authors in ([47], ch. 15) defined the channel as a Gaussian interference channel where each channel interferes with the others as shown by the dotted lines in Fig. 2.6. In this Gaussian interference channel (each interference term can be represented by Gaussian random variable), the transmission from the other $i \neq j$ nodes to the jth node is treated as noise. For non-orthogonal channel (channel where there is a cross linkage between sub-channels) with symmetric interference, the input-output relation can be expressed as:

$$y_j = h_{j,j}x_j + \sum_{i=1, i\neq j}^{N} h_{i,j}x_i + z_j;\ \forall j \in [1:N] \tag{2.25}$$

where the second part and last part in the right side of (2.25) represents the noise-plus-interference (NI) level associated with link j.

2.2.3 Receiver Design with Power Constraint

One of the main challenges for the energy solution of WSN receiver design in underground mines is the dual optimization of capacity or sum-rate maximization, and how effectively it can estimate the transmitted symbol which is defined by the MMSE estimation. We discuss the joint MMSE and MSR constraint receiver by considering a single hop MIMO WSN channel with M transmit and N receive antennas. A zero-mean uncorrelated transmit signal vector $\mathbf{x} \in \mathbf{C}^{M\times 1}$ of unit variance is transmitted through the MIMO $\mathbf{H} \in \mathbf{C}^{N\times M}$ channels with $\mathsf{E}\left\{\mathbf{x}\mathbf{x}^T\right\} = \mathbf{I}$, where $\mathsf{E}\{\cdot\}$ is the mathematical expectation, and $(\cdot)^T$ represents matrix transpose. The received signal vector $\mathbf{z} \in \mathbf{C}^{N\times 1}$ can be expressed using (2.23) without considering the precoder matrix $\mathbf{F}$ as $\mathbf{z} = \mathbf{H}\mathbf{x} + \mathbf{v}$, where, $\mathbf{x} = [x_1, \cdots, x_M]^T$ is the $M \times 1$ spatial transmitted vector, $\mathbf{H}$ is the $N \times M$ channel matrix of entries $h_{j,i}, j \in [1, \cdots, N], i \in [1, \cdots, M]$, where the fading coefficients $h_{j,i}$ is a complex Gaussian random variable with zero-mean and unit variance. The noise vector $\mathbf{v} = [v_1, \cdots, v_N]^T$ is additive complex white Gaussian with zero-mean and unit variance. In actual scenarios, any link k is corrupted by interference signals from the other $M-1$ links, and the received signal z_k for link k is expressed according to the Gaussian interference channel model in (2.25) as:

$$z_j = h_{j,j}a_jx_j + \sum_{i=1, i\neq j}^{M} h_{j,i}a_ix_i + v_j \tag{2.26}$$

where $h_{j,j}a_jx_j$ is the desired signal for link j and $\sum_{i=1,i\neq j}^{M} h_{j,i}a_ix_i$ is the cochannel interference from the other $M-1$ links, and v_j is the zero mean additive noise. The signal to interference-plus-noise ratio (SINR) of link j, γ_j, is given by

$$\gamma_j = \frac{\mid h_{j,j}a_j \mid^2}{\mid \sum_{i=1,i\neq j}^{M} h_{j,i}a_i \mid^2 + v_j} \tag{2.27}$$

This model can be easily extended to multi-hop frequency selective channels according to [14]. The amplifying factor, a_j, captures the effect of path-loss, shadowing and frequency non-selective fading of the jth link by using the AF or the DF cooperative protocol [61], [62]. The generalized feedback allows the sources to act as relay when it forwards the signal from the previous sender. The fading channel $\left\{h_{j,i}\right\}$ between relay nodes and FC are Rayleigh distributed with gain factors $g_{j,i} = \mid h_{j,i} \mid^2$. The optimal estimator seeks to estimate source signals, $\hat{x} = \sum_{i=1}^{N} w_iz_i = \mathbf{w}^T\mathbf{z}$, where $\mathbf{w} = [w_1, \cdots, w_N]^T$ represents the weighting vector of the estimator filter with equal number of transmitting and receiving antennas, i.e., $M = N$. The input $\mathbf{x}$ and output $\mathbf{z}$ are related by the Gaussian conditional probability density [63]

$$P_{\mathbf{z}|\mathbf{x};\gamma}(\mathbf{z}|\mathbf{x};\gamma) = (2\pi)^{-N/2}\exp\left[-\frac{1}{2} \parallel \mathbf{z} - \gamma\mathbf{H}\mathbf{x} \parallel^2\right] \tag{2.28}$$

where $\parallel \cdot \parallel$ represents the Euclidean norm, and γ is the channel SNR. The conditional probability expresses the reconstruction of input $\mathbf{x}$ through the output observation $\mathbf{z}$ in the presence of fading channel $\mathbf{H}$, and the accuracy of the reconstruction is expressed by the estimation error that can be calculated by solving $\parallel \mathbf{z} - \gamma\mathbf{H}\mathbf{x} \parallel^2$. The estimation error based on the observation $\mathbf{z}$ is defined by the MMSE which is a function of γ [64]

$$\mathrm{MMSE}(\gamma) = \mathsf{E}[(\mathbf{x} - \mathsf{E}\{\mathbf{x}|\mathbf{z}(\gamma)\})^2] \tag{2.29}$$

We would like to estimate $\mathbf{x}$ by a function $f(\mathbf{z}(\gamma)) = \mathbf{w}^T\mathbf{z}$ using the following minimization

$$\min_{f(\cdot)} \mathsf{E}[(\mathbf{x} - f(\mathbf{z}(\gamma)))^2] \tag{2.30}$$

$$\text{subject to: } f(\mathbf{z}(\gamma)) = \mathbf{w}^T\mathbf{z}$$

The input-output mutual information of channel and MMSE are functions of γ, denoted by $\mathrm{I}(\gamma)$ and $\mathrm{MMSE}(\gamma)$, respectively, and satisfying the following relationships [64]

$$\frac{\mathrm{d}}{\mathrm{d}\gamma}\mathrm{I}(\gamma) = \frac{1}{2}\mathrm{MMSE}(\gamma) \tag{2.31}$$

$$\mathrm{I}(\gamma) = \frac{1}{2}\int_0^{\gamma} \mathrm{MMSE}(\gamma)\mathrm{d}\gamma \tag{2.32}$$

The mutual information between two random variables $\mathbf{x}$ and $\mathbf{z}$ can be expressed as

$$I(\mathbf{x};\mathbf{z}) = \mathsf{E}\left[\log_2 \frac{P_{\mathbf{z};\gamma|\mathbf{x}}(\mathbf{z};\gamma|\mathbf{x})}{P_{\mathbf{z};\gamma}(\mathbf{z};\gamma)}\right] \tag{2.33}$$

where $P_{\mathbf{z};\gamma}(\mathbf{z};\gamma)$ is the marginal pdf of $\mathbf{z}$. Combining (2.32) and (2.33), we have the joint equivalent representation of $\mathrm{I}(\gamma) - \mathrm{MMSE}(\gamma)$ [64]

$$\mathsf{E}\left[\log_2 \frac{\mathrm{d}P_{\mathbf{z};\gamma|\mathbf{x}}}{\mathrm{d}P_{\mathbf{z};\gamma}}\right] = \frac{1}{2}\mathsf{E}\left[\int_0^{\gamma} (\mathbf{x} - f(\mathbf{z};\gamma))^2 \mathrm{d}\gamma\right] \tag{2.34}$$

The joint formula in (2.34) connects the input-output mutual information and MMSE by estimating the input as a function of γ. We are looking for the γ_k value of link k such that it always satisfies $\gamma_k > \gamma_\beta$, where γ_β is the minimum threshold value, otherwise the link k will be shutdown from transmission due to excess noise and interference. This can be confirmed by an optimal water-filling power allocation to all nodes such that the interference from the other $N-1$ links is minimized. The goal of the power allocation is to solve the following optimization problem for joint I-MMSE

$$\min_{\gamma} \mathsf{E}[(\mathbf{x} - f(\mathbf{z};\gamma))^2] \tag{2.35}$$

$$\text{and } \max_{\gamma} \mathrm{I}(\mathbf{x};\mathbf{z},\gamma) \tag{2.36}$$

$$\text{subject to: } N\mathbf{a}\mathbf{a}^T = P$$

$$\gamma \geq \gamma_\beta$$

If the CSI is unknown, then the MIMO channel $\mathbf{H}$ can be estimated [65] as

$$\bar{\mathbf{H}} = \mathbf{H} + \mathbf{H}_e \tag{2.37}$$

where $\bar{\mathbf{H}}$ and $\mathbf{H}_e$ denote the mean estimation and estimation error of $\mathbf{H}$. The detection procedure assumes that $\bar{\mathbf{H}}$ is a perfect estimation corresponding to the true channel, and in closed-loop feedback solution the channel estimation $\bar{\mathbf{H}}$ is available in both transmitter and receiver which makes perfect power allocation via water-filling. Here, we use the estimation mean $\bar{\mathbf{H}}$ instead of the real channel $\mathbf{H}$

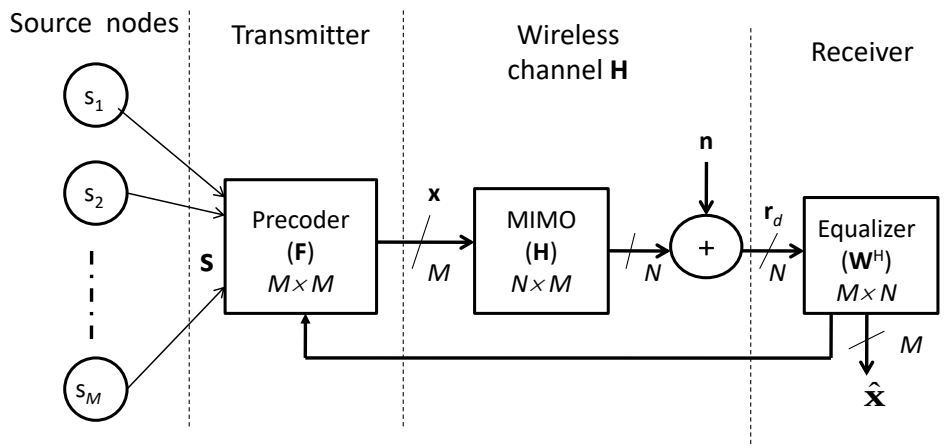

Figure 2.7 – MIMO channel with precoder matrix.

in further analysis. The estimation error and mutual information have the following form considering the quantized feedback channel $\bar{\mathbf{H}}$ [64], [65]

$$\mathsf{E}[\| (\mathbf{x}-\hat{\mathbf{x}}) \|^2] = \mathrm{tr}[(\Sigma^{-1}+\gamma\bar{\mathbf{H}}\bar{\mathbf{H}}^T)^{-1}\bar{\mathbf{H}}] \tag{2.38}$$

$$\mathrm{I}(\mathbf{x};\mathbf{z}) = \frac{1}{2}\log_2\det\left(\mathrm{I}_N + \hat{\mathbf{J}}\hat{\mathbf{J}}^T(\mathbf{F}_W)^{-1}\right) \tag{2.39}$$

Using the SVD transform, we have $\bar{\mathbf{H}} = \mathbf{U}\Sigma\mathbf{V}^T$, where Σ is a square matrix, whose diagonal elements are composed of non-negative real eigenvalues $\lambda_{i,i}$, $i = 1,\cdots,N$, $\hat{\mathbf{J}} = \bar{\mathbf{H}}\mathbf{V}\mathbf{Z}$, $\mathbf{F}_W = \mathbf{I}_N + \mathsf{E}_{\mathbf{J}_e}[\mathbf{J}_e\mathbf{J}_e^T|\hat{\mathbf{J}}]$, $\mathbf{J}_e = \mathbf{H}_e\mathbf{V}\mathbf{Z}$, and the elements of diagonal matrix $\mathbf{Z} = \mathrm{diag}\{p_1,\cdots,p_{N_t}\}$ are given by

$$p_i = \left(\omega - \frac{1}{\lambda_{i,i}^2}\right)^+ \tag{2.40}$$

$$\text{subject to: } \sum_{i=1}^{N_t} p_i = P$$

2.2.4 Single-hop Transceiver Design

We present here the precoder design for a single hop transmission through a MIMO system employing M transmitters and N receivers for simplicity, and extend the analysis for multi-hop transmission in the next chapter. The input-output relationship can be expressed as

$$\mathbf{r}_d = \mathbf{H}\mathbf{s} + \mathbf{n} \tag{2.41}$$

where $\mathbf{s} \in \mathcal{C}^{M\times 1}$ is the complex transmit vector, $\mathbf{H} \in \mathcal{C}^{N\times M}$ is the complex channel between the source and destination, $\mathbf{r} \in \mathcal{C}^{N\times 1}$ is received signal vector, and $\mathbf{n} \in \mathcal{C}^{N\times 1}$ is the independent and identically distributed (i.i.d.) zero-mean complex Gaussian random vector with variance σ_n^2. The point-to-point communication through the MIMO channel in (2.41) can be modeled as a Gaussian vector channel [41], and the channel reduces to the Gaussian product channel consisting of a set of parallel Gaussian

single-input single-output (SISO) channels. The formation and convex optimization of the Gaussian product channel has been analyzed in Chapter 3 of [41] by considering the product channel as different frequency bands, or time slots, forming an orthogonal signal dimension.

The Geometric Mean Decomposition (GMD)-based linear transform is used to decompose the MIMO channel into parallel SISO sub-channels. GMD is basically another form of SVD where the gain of each sub-channels can be expressed by the geometric mean of channel gains obtained by SVD. For the channel matrix $\mathbf{H}$, the linear transform of $\mathbf{H}$ by SVD is given as $\mathbf{H} = \mathbf{U}\Lambda\mathbf{V}^H$, where $\mathbf{U}$ and $\mathbf{V}$ are unitary matrix and Λ is a diagonal matrix with singular values $\lambda_{H,1} \geq \lambda_{H,2} \geq \cdots \geq \lambda_{H,K}$, $K = \text{rank}(\mathbf{H})$ or $K = \min\{M, N\}$. For GMD, there exists an upper triangular matrix $\mathbf{R} \in \mathcal{R}^{K\times K}$ having identical diagonal elements derived from the SVD by

$$r_{ii} = \left(\prod_{k=1}^{K} \lambda_{H,k}\right)^{1/K};\ 1 \leq i \leq K \tag{2.42}$$

The non-zero singular values formed by the SVD represent the unequal SNRs of the parallel sub-channels while the GMD gives uniform SNRs on all sub-channels due to the equal gains of all the sub-channels. In this section, we will present an SVD technique to design a precoder at the transmitter and an equalizer at the receiver for the formation of independent parallel SISO sub-channels over the MIMO channel. In most cases, the theory and analysis of the MIMO channel decomposition in the literature is carried out according to the fundamental work of [66] on SVD or on the GMD-based MMSE-VBLAST design scheme.

With the precoder scheme in Fig. 2.7, the baseband signal in (2.41) can be written as

$$\mathbf{r}_d = \mathbf{HFs} + \mathbf{n} = \mathbf{Hx} + \mathbf{n} \tag{2.43}$$

where $\mathbf{F} \in \mathcal{C}^{M\times M}$ is the source precoder matrix, $\mathbf{x} \in \mathcal{C}^{M\times 1} = \mathbf{Fs}$ is the transmit signal vector after precoding, and other symbols having the usual meaning of (2.41). The solution of the precoder is given by SVD as $\mathbf{F} = \mathbf{V}\Phi^{1/2}$ where $\Phi \in \mathcal{R}^{K\times K}$ denotes a diagonal matrix as $\Phi = \text{diag}\{\phi_1, \phi_2, \cdots, \phi_K\}$ whose element ϕ_i determines the assigned power to the i-th sub-channels, $1 \leq i \leq K$, and ϕ_i is found via the water-filling process

$$\phi_i(\mu) = \left(\mu - \frac{\alpha}{\lambda_{H,i}^2}\right)^+,\ 1 \leq i \leq K \tag{2.44}$$

where μ is the water-level, and is chosen such that $\sum_{i=1}^{K} \phi_i(\mu) = \rho\alpha$, $a^+ = \max(a, 0)$. We define $\alpha = \sigma_n^2/\sigma_x^2$, where $\rho = \text{tr}\left\{\mathbf{FF}^H\right\}/\alpha$ is the SNR, $\text{E}[\mathbf{xx}^H] = \sigma_x^2\mathbf{I}$, $\mathbf{I}$ is the identity matrix with dimension K, and $\text{tr}\left\{\mathbf{FF}^H\right\} \leq P$, P is the total power constraint. For the nulling matrix of MMSE-VBLAST, consider the following augmented matrix

$$\mathbf{H}_a = \begin{bmatrix} \mathbf{H} \\ \sqrt{\alpha}\mathbf{I}_K \end{bmatrix}_{(K+K)\times K}$$

Now, the nulling vector of the i-th layer (Lemma III.2, [66]) is

$$\mathbf{w}_i = r_{H_a,ii}^{-1}\mathbf{q}_{H_a,i};\ i = 1, 2, \cdots, K \tag{2.45}$$

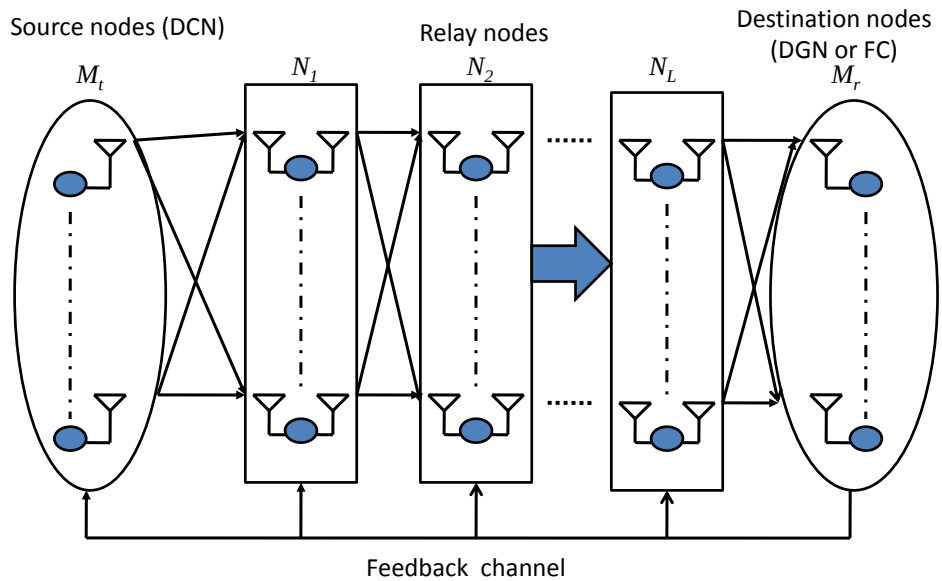

Figure 2.8 – L-hop WSN relay network with M_t source nodes, N_L relay nodes and M_r destination nodes.

where $\left\{\mathbf{q}_{H_a,i}\right\}_{i=1}^{K}$ denote the columns of $\mathbf{Q}_{H_a}^{u}$ and $\{r_{H_a,ii}\}_{i=1}^{K}$ the diagonal elements of matrix $\mathbf{R}_{H_a}$. We obtain $\mathbf{Q}_{H_a}^{u}$ and $\mathbf{R}_{H_a}$ through the QR-decomposition of $\mathbf{H}_a$.

2.2.5 Multi-hop WSN Algorithm

WSNs are usually composed of a large number of sensing devices deployed randomly in a certain areas that can transmit their data to the destination through multi-hop intermediate relays. In traditional wireless networks such as cellular systems, the system design aims to provide high QoS and bandwidth efficiency. The power constraint for all the electronic devices in such a network is an issue but they have easy access to a power supply and exhausted batteries in the handset can be replace or recharge. On the other hand, power conservation in WSNs is an important issue because the recharging or replacing of batteries is not a convenient process, especially when WSNs carry non-replaceable power source and are placed in some remote locations like underground mines. So, the designer needs to focus on this most important of constraints for WSNs which is the low power consumption requirements.

The group of nodes in a cluster sends information to the group of sensors in the next cluster like a multi-hop MIMO relay using repetitive cooperative diversity or STBC cooperative diversity. Nodes in each cluster relay signals to each other using a MIMO channel either with the AF or DF relay protocol. A joint linear receiver design and power allocation of a general multi-hop WSN MIMO AF relaying scheme has been employed in [14] to obtain the best possible QoS at the destination. The proposed strategy is to jointly design the receivers and power allocation parameters that contain the optimal complex amplification coefficients for each relay node via an alternating optimization approach. By

appropriately adjusting the power levels at each terminal between the source, the relays, and the destinations, significant performance gains can be obtained. Most of the power allocation techniques for WSN in research is based on the assumption that perfect CSI is available at each terminals. But a limited research has been carried out recently based on imperfect CSI knowledge due to high channel fading. The optimum design can improve the system efficiency (i.e., BER or outage probability) at full CSI information. In the work, two kinds of linear receivers are designed, namely, the MMSE receiver and the maximum sum-rate (MSR) receiver at individual, local, and global power constraints.

A general L-hop WSN with multiple relay nodes is shown in Fig. 2.8, based on [14]. The WSN consists of M_t source nodes, M_r destination nodes, and N_l relay nodes, $l \in [1, \cdots, L]$. The source first broadcasts the $M_t \times 1$ signal vector $\mathbf{s}$ to the first N_1 relay node, and the first relay node forwards the received signal to the second relay node N_2 using the AF protocol. Each group of relay nodes receives the noisy signals, and after amplification broadcasts them to the next relay terminal. The source signal $\mathbf{s}$, after amplification in each relay, reaches the fusion center. The fusion center estimates the source signal $\hat{s}_d$ and it also calculates the amplification coefficient of each relaying stage. The proposed design is formulated for the following MMSE optimization problem with global power constraint

$$U(\mathbf{W}_d, \mathbf{a}_1, \cdots, \mathbf{a}_L) \triangleq \arg \min_{\mathbf{W}_d, (\mathbf{a}_l)_{l=1}^{L}} \mathrm{E}[||\mathbf{s} - \hat{s}_d||^2] \tag{2.46}$$

$$P_s + \sum_{i=1}^{L} P_i \leq P$$

where $(.)^H$ denotes the complex-conjugate transpose, P_s and P_i are the source and i-th node transmitted powers, P is the total power constraint, $\mathbf{a}_i$ is the optimal amplification coefficients of the i-th relay node, and $\mathbf{W}_d$ is the optimum receiver matrix at destination.

2.2.6 Self-organizing Method

Self-organization is used to determine the shortest routing path to minimize processing time and energy consumption. During the operational period of a network, if any resource changes its action pattern, then self-organization reallocates resources (such as power, frequency, etc.,) according to the requirements. Self-organization in wireless sensor networks is a protocol that provides a variety of functions: sharing processing and communication capacity, forming and maintaining structure, conserving power, etc., and it may re-configure its function to cope with the environmental changes without human intervention [67]. The self-organization technique assigns different frequency bands to each node to avoid interference, and different time-slots for message transmission between nodes to prevent collision of data packets in the medium of transmission. In the self-organizing protocol, a node will re-transmit the same message if it has not heard the acknowledgment message from the receiver. The self-organizing protocol must be designed to provide the solution of the requirements for a given hardware and software limitations, robust algorithm mechanism and energy-efficient communication techniques. At the equilibrium state, any node rejects a forwarding rate beyond its maximum rate or the network shuts down a node if the node forwards more packets than the global maximum

in the same time. In the forwarding routing scheme, self-organization maintains uniform probability of transmission among all nodes. In equilibrium power assignment, no user can attain a higher rate by changing its power allocation strategy and the communication rates do not depend on initial power allocation [68]. Hence, the resource allocation in any node by the self-organizing protocol should follow the Nash equilibrium.

The channel characteristics in underground mines is harsh and the transmission is not the same as in free space propagation. The self-organizing method allows the transmitter to be active when communication is needed and turned off in case of deep fading to make the WSN as energy efficient as possible [69]. Communication is possible if the signal-to-noise (SNR) ratio of the corresponding channel is higher than a threshold SNR, i.e., $SNR_{jk} \geq SNR_{\beta}$, else the channel is turned off and no symbol transmission takes place through the channel. The self-organizing technique increases transmission power by $n_1 \Delta p_0$ to make the channel active by satisfying $SNR_{jk} \geq SNR_{\beta}$, where Δp_0 is the step of power increment and n_1 is the number of iterated enhancement. The transmitted power enhancement by a factor $n_1 \Delta p_0$ consumes more energy stored in batteries of the WSN, and this decreases the life-time of the WSN.

2.2.7 Functional Implementation

When two or more nodes transmit data through the same channel, some part of their signals may overlap which can increase the probability of collisions, and decrease the reliability of data transmission. Therefore, the transmitter must resend the same message until it securely reaches the receiver. This may increase the power budget and time consumption. The radio transmission from other nodes in another sub-group or other radio technology that use the same frequency band may cause interferences, and the signal may be lost. The transmitted signal can be lost in the medium due to fading which prevents a transmitted packet to reach a receiver or the signal may be reflected from a close object which causes interferences. As a result, no message is transmitted from a transmitter node to a receiver node. The echo of the signal from any close obstacle causes distortion of the received signal. The multipath fading on the sensor network signal transmission greatly depends on the position and the nature of the objects in the operational environment [70]. So, in terms of noise and interference, one of the challenges of sensor network deployment is the choice of the location of nodes such that nodes are less affected by noise and interferences.

On the other hand, the operational environmental characteristics vary in time, known as time-varying channel, and after adjusting the transmission parameters, the sensor nodes may also lose data symbols at any time due to the time-varying nature of the channel. As a result, the sensor network requires a large amount of power to make a successful data transmission. Therefore, the self-organization technique needs to adapt to the instantaneous change of fading characteristics to continue the packet transmission over a time-varying channel. Hardware failure is one of the other challenges, because if a node fails to forward a message from the other nodes, then the topology of the network is required to change, which may cause a delay in operation and signal processing consumes extra energy. Hence,

the challenge of the self-organization protocol is to implement and design the self-configuration topology mechanism to change the routing algorithm of the network. Sensor networks need to maintain adequate quality of service (QoS) which is another challenging issue for the deployment of sensor nodes in fading environment due to resource constraints such as data processing, channel assignment, and power allocation in the channel. Frequency selection is an important factor for the QoS enhancement to protect the transmitter node from any form of interferences [71]. From the above discussion, the operation of a sensor network requires consumption of energy, but the energy source of the sensor node is limited, and the minimization of the power consumption is the main concern in all recent researches.

2.2.8 Routing Issue

A WSN consumes energy for local measurements and a major part of the energy is consumed for the reliable transmission through a number of relay nodes in multihop communication. WSN designers have to address the issue for suitable energy efficient routing techniques. Also, there is a constraint of the routing which is the capability of changing the topology during communication link failures. WSN designers have to face various routing challenges such as energy efficient routing, topology changing capability with the environment, and processing capability for each routing path. The routing problem in WSNs is represented by a graph $G = (V, E)$, where V is the set of all nodes, and E is the set of uni-directional or bi-directional communication channels connecting the nodes in the graph [72]. Here, the challenge in the routing problem is finding the minimum cost path from the starting source vertex to all destination vertices. The minimum cost function can be found by using optimization for the available graph edges which is actually a spanning tree $T = (V, E)$ that includes the source (i.e., a root node) and destinations (i.e., leaf nodes). The traditional energy optimized routing is shown in Fig. 2.9(a) where the spanning tree routing exchanges the same information through all connected nodes [73]. In this case, information from node A is transmitted to the destination through two branches. As a result, it takes more energy to forward a message to the destination. The total cost of the routing is associated with the cost of individual routing nodes. On the other hand, machine learning based routing in Fig. 2.9(b) requires only neighboring nodes information that is used to predict the full path quality of service [74]. This optimization is based on the fact that each node independently performs optimal routing with lower computational complexity. Let us consider a WSN having M nodes, the searched path j^* having lowest energy cost $J(i)$ with weight vector $w(t)$, is defined as [74]:

$$j^* = \arg\min_j \mid x_j(t) - w_j(t) \mid^2, j \in [1, \cdots, M] \tag{2.47}$$

where $x(t)$ is the input signal. The neighbor nodes updating weight vector to find their optimized path is given by

$$w_j(t+1) = w_j(t) + g(t)(x_j(t) - w_j(t)) \tag{2.48}$$

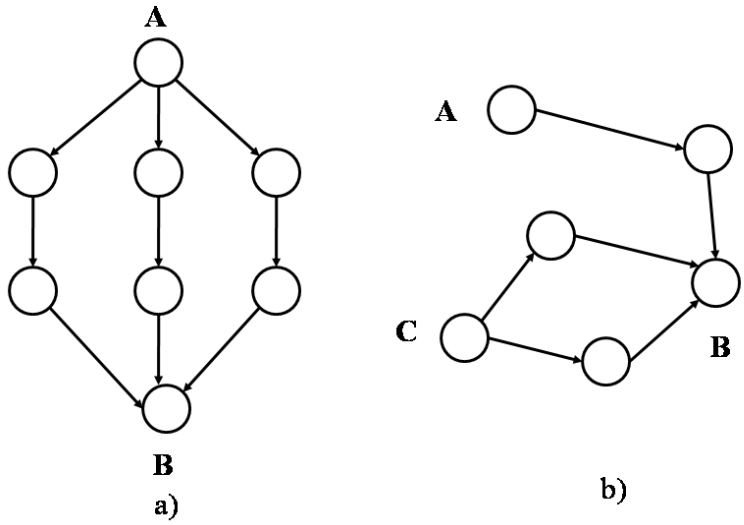

Figure 2.9 – Routing algorithm; a) Traditional routing, b) Optimum routing using single-hop communication.

where $w_j(t)$ is the value of the weight vector of the jth node at time index t, and $g(t)$ is a Gaussian neighborhood function of the form

$$g(t) = \frac{1}{\sqrt{2\pi\sigma}} \exp\left(-\frac{||j^* - j||^2}{2\sigma^2(t)} \right) \tag{2.49}$$

The network searching algorithm saves energy by reducing network traffic. In the case of dense geographical areas where each node sends messages to the neighbor nodes with the highest probability of success, the network first sends a local signal to all connected neighbor relay nodes and estimate the shortest energy path. If the shortest path is affected by large additive Gaussian noise or interferences, then the protocol searches for the alternative path having less noise or interferences. In contrast to point to point communication, sensor networks need to forward the received data from multiple neighbor nodes along with its own sensed signal to the central processor and for this, they require careful resource management in terms of energy, processing, and storage capacities. Before the design of the routing protocol, one must overcome many challenging factors such as node deployment, energy consumption, scalability, and network dynamics. Hierarchical or cluster-based routing are used to perform energy-efficient routing for WSNs in which higher energy nodes can be used to process information by clustering geographical areas. This routing is basically a two-layer routing where first a single layer is used to select clusterheads and the other is used for routing, information processing, and channel allocating. A self-organizing protocol can be used to support heterogeneous sensors to forward the data through a set of nodes that also act as routers for the communication backbone.

This protocol also uses multiple path capabilities to enhance the network performance by assigning alternative available channels. The protocol periodically sends a message to the receiver to predict the best path for calculating the link that gives the highest signal strength. The switching from one path to the highest energy one is selected according to an algorithm that allows the primary path until its energy falls below a prescribed level. In traditional mobile network communication systems, the transmitter sends a test message to the receiver through different paths, and examine the route having lowest energy cost. In [75], a multipath routing algorithm is used to increase the network capability for delivering data through unreliable environments.

The optimal path in best routing algorithm are chosen by finding a path requiring less energy to send a message from source to destination compared to other available paths. In cluster based routing where nodes are grouped under a cluster, routing is implemented by defining a cost function between any two users in terms of energy consumption, delay optimization, and other related parameters.

2.2.9 Energy Conserving Technique

A WSN node has to perform three main tasks: sensing, data processing, and communication. Among them, communication consumes the major portion of the total energy, and it may also depend on the type of sensing. The recharging of the battery may be impossible in some cases because nodes are deployed usually in a hostile or remote location. So, the life-time of the network is directly associated with the energy consumption of the network nodes. In some cases, energy is added from the external sources by using solar cells but external sources may exhibit discontinuous behavior which can affect the system performance. Energy consumption is taken into account by using efficient protocols during network activities based on the concept of switching off the components that are not needed in transmission [76]. A power management software is used to disconnect inactive components from the network when they are in sleeping mode. A node wakes up only when another node sends a network connection request; an alternative solution is that each node may remain active for a short time interval to accept connection requests from the neighbor nodes.

Collision avoidance schemes have been used recently to implement energy efficient transmission for Medium Access Control (MAC) protocols. MAC is an important technique that has been developed for wireless voice and data communication to enable the successful operation of the network. In the MAC protocol, the transmitter repeats the same message until it receive an acknowledgment (ACK) message from the receiver. The repetition of the same message consumes more energy in the network. The MAC protocol avoids collisions by allocating different time slot for each transmitter so that they can transmit at different time known as time division multiple access (TDMA) or it may assign different orthogonal codes to each source signals known as code division multiple access (CDMA). Alternatively, interference and additive Gaussian noise in the channel may corrupt the message, and the transmitter needs to resend the same signal until receiving an ACK confirmation from the receiver. In recent researches, MAC protocols are designed to reduce energy consumption by supporting scalability and collision avoidance. For example, the authors in [76] have developed a MAC protocol for

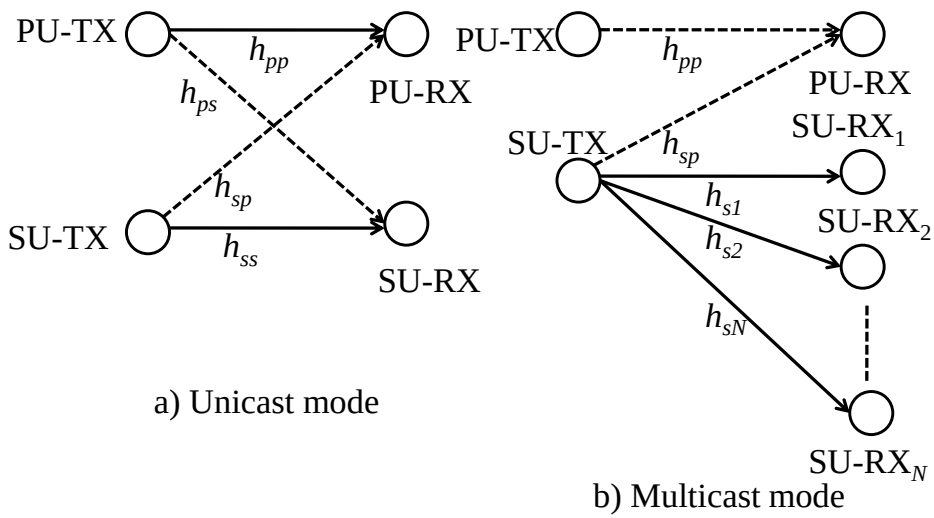

Figure 2.10 – Sensor node spectrum sharing configuration in two modes of operation.

energy reduction by using three novel techniques depending on the free space energy cost calculation given in [56], [57], [58] for sending information between nodes based on the instantaneous channel gain.

2.3 Power Control Policy

The water-filling energy minimization problem of wireless transmission is addressed in this section for a single transmitter and multiple receiver sensor network in a fading environment under total transmit power constraint.

2.3.1 Single Sensor Node Transmission

In this section, we discuss the optimum power calculation procedure of each transmitting node by considering a simplified network that consists of one primary link and one secondary link as shown in Fig. 2.10(a). The secondary link transmitter (SU-TX) communicates with the secondary link receiver (SU-RX) with interferences only to the primary link receiver (PU-RX). The channel power gains for the primary link, secondary link, and the link from SU-TX to PU-RX are denoted by $h_{p,p}$, $h_{s,s}$, and $h_{s,p}$, respectively. We denote SU-TX to PU-RX and SU-TX to SU-RX channel gains as $\gamma_p = \mid h_{s,p} \mid^2$ and $\gamma_s = \mid h_{s,s} \mid^2$, respectively. All the channel gains are assumed to be independent and identically distributed (i.i.d.) random variables (RVs) with probability density functions (pdf) denoted by $f(\gamma_p)$ and $f(\gamma_s)$. The additive noise at each receiver is assumed to be a Gaussian RV with zero mean and variance N_0. We consider that each secondary and primary link gains follow a Rayleigh distribution, i.e., $f(\gamma_s) = e^{-\gamma_s}$ or $f(\gamma_p) = e^{-\gamma_p}$, for $\gamma_p, \gamma_s \geq 0$ according to [III-B, [38]]. Our goal is to limit the transmission power P by an average power constraint $\mathsf{E}[P(\gamma_s)] \leq P_{avg}$ or a peak power constraint $P(\gamma_s) \leq P_{peak}$, where P_{avg} and P_{peak} are the average power and peak power budget. The

optimization of the power solution with channel gain γ_s is denoted with interference limit P_{avg} at the primary receiver as follows [38]:

$$\min_{P(\gamma_s)} \mathsf{E}\left[P(\gamma_s)\right] \leq P_{avg} \tag{2.50}$$
$$\text{subject to: } R(\gamma_s) \geq R_{min}$$

where R_{min} is the minimum transmission rate requirement for the fading gain γ_s. The transmission rate for the allocated power $P(\gamma_s)$ over the channel with gain γ_s, can expressed by [77]

$$R(\gamma_s) = \log_2\left(1 + P(\gamma_s)\gamma_s\right) \text{ bps/Hz} \tag{2.51}$$

The minimum power requirement for the instantaneous transmission rate, $R(\gamma_s)$ is given by [77]

$$P(\gamma_s) = \frac{1}{\gamma_s}\left[e^{1+W(\frac{\gamma_s P_c - 1}{e})} - 1\right] \tag{2.52}$$

where $W(.)$ is the main branch of the Lambert W function over the $[-1/e, \infty]$ region. The Lambert W function $W(x)$ is the solution of the equation $x = W(x)e^{W(x)}$ [78]. Equation (2.52) is a function of the channel gain γ_s, and we assume that all the instantaneous channel gains in the primary link and secondary link are known to the receiver. The Lagrangian solution of (2.50) is obtained by defining [79]

$$\mathcal{L}(P(\gamma_s), \lambda, \mu) = \mathsf{E}\left\{\log_2(1 + \gamma_s P(\gamma_s))\right\} - \lambda(\mathsf{E}\left\{P(\gamma_s)\right\} - P_{avg}) + \mu P_{out} \tag{2.53}$$

where P_{out} is the tolerable transmission outage probability of the fading channel, λ is the Lagrange multiplier, and μ is the water level. The outage probability is the probability that the instantaneous rate $R(\gamma_s)$ is less than a given rate R, i.e., $P_{out} = P_r\left\{R(\gamma_s) < R\right\}$, and we have the following outage probability for the secondary fading channel [80]

$$P_{out}(R, \gamma_s) = P_r\left\{\log_2(1 + P(\gamma_s) \mid h_{s,s} \mid^2) < R\right\} \tag{2.54}$$

The outage probability defines the outage event when a missed detection has happened in the presence of the target, and in this case none of the message can be detected at the FC with the total allocated power $P(\gamma_s)$ [81]. Hence, the power allocation solution should be formulated for minimizing both outage probability and sum power requirement while satisfying $R(\gamma_s) \geq R_{min}$. The closed-form outage probability solution is difficult for the MIMO case, so we show the system design for the single-input multiple-output (SIMO) case. The sub-problem in (2.53) has the following solution for a particular fading state

$$\min_{P(\gamma_s) \geq 0} \log_2(1 + \gamma_s P(\gamma_s)) - \lambda P(\gamma_s) \tag{2.55}$$

The solution of (2.55) is a concave function, and it can be expressed by the following definition as

$$f(P(\gamma_s)) = \log_2(1 + \gamma_s P(\gamma_s)) - \lambda P(\gamma_s) \tag{2.56}$$

The concave function $f(P(\gamma_s))$ attains its maximum value when the solution has a global minimum. Now, differentiating the Lagrangian with respect to $P(\gamma_s)$ to obtain the solution for $P(\gamma_s)$ [77]

$$P(\gamma_s) = \left[\frac{1}{\lambda \ln 2} - \frac{1}{\gamma_s}\right]^+ = \begin{cases} \acute{\lambda} - \frac{1}{\gamma_s}, & \text{if } \acute{\lambda} > \frac{1}{\gamma_s} \\ 0, & \text{otherwise} \end{cases} \tag{2.57}$$

where $\acute{\lambda} = \frac{1}{\lambda \ln 2}$. It is shown that transmission occurs through a channel only when $\frac{1}{\lambda} > \frac{1}{\gamma_s}$, which is known as the water-filling solution. We can write the closed-form solution by considering $\mu = \frac{1}{\lambda \ln 2}$, and (2.57) having the form

$$P(\gamma_s) = \left[\frac{1}{G^{-1}(R_{min})} - \frac{1}{\gamma_s}\right]^+ \tag{2.58}$$

where, $G(x) = E_1(x) = \int_1^\infty \frac{e^{-xt}}{t} dt$ is a first order monotonic exponential decreasing function. The secondary link transmitter SU-TX produces interference for the primary receiver PU-RX and the interference constraint is given by [79] $\Pr\{P(\gamma_s)\gamma_p \geq Q_{peak}\} \leq \varepsilon$, if $P(\gamma_s) \leq P(\gamma_p)$, where Q_{peak} is the interference limit and $P(\gamma_p) = \frac{Q_{peak}}{F_{\gamma_p}^{-1}(1-\varepsilon)}$ and $F_{\gamma_p}^{-1}$ is the inverse of the cumulative distribution function of γ_p. Our goal is for the secondary power $P(\gamma_s) \leq P(\gamma_p)$ with $R_{min} > G(P(\gamma_p))^{-1}$ and in this case the optimization power profile can be expressed in the following form

$$P(\gamma_s) = \max\left(\left[\frac{1}{G^{-1}(R_{min})} - \frac{1}{\gamma_s}\right]^+, P(\gamma_p)\right) \tag{2.59}$$

2.3.2 Multiple Receiver Power Allocation

We consider a secondary transmitter, SU-TX, communicating with multiple secondary receivers SU-RX (SU-RX$_1, \cdots$, SU-RX$_N$) by broadcasting a message through channel $\mathbf{h} = [h_{s,1}, \cdots, h_{s,N}]^T$, as in Fig. 2.10(b). It is also assumed that the transmitter SU-TX is aware of the NI ($\mathbf{I} = [I_{s,1}, \cdots, I_{s,N}]$) level of each SU-RX$_N$ terminal that is caused by the interference from neighbor SU-TX transmitters. The self-organizing method assigns a frequency to each receiver node to mitigate the interference caused by the nearby transmitter. In a time-varying fading environment, each channel is corrupted by noise and interferences, and in this case $\gamma_{s,i} = 0$ if $SNR_i \leq \beta_i; i \in [1, \cdots, N]$, where β_i is the threshold level of the ith channel. The signal received by each secondary receiver (SU-RX) from the secondary transmitter (SU-TX) is given by $y_{s,i} = h_{s,i}x + z_{s,i}$ where x is the input signal to channel $h_{s,i}$, and $z_{s,i}$ is the zero-mean additive white Gaussian noise with spectral density N_0. The goal of the solution is to minimize the power $P(\gamma_{s,i}) = P_{avg}, \forall i \in \{1, \cdots, N\}, \gamma_{s,i} \in \{\gamma_{s,1}, \cdots, \gamma_{s,N}\}$, where $\gamma_{s,i} = \mid h_{s,i} \mid^2$, by the following optimization

$$\min_{P(\gamma_s)} \mathsf{E}\left[P(\gamma_{s,i})\right] \leq P_{avg} \tag{2.60}$$

$$\text{subject to: } \sum_{i=1}^{N} \log_2(1 + \gamma_{s,i} P(\gamma_{s,i})) \geq R_{min}$$

$$\sum_{i=1}^{N} P(\gamma_{s,i}) \leq P_T$$

where $P(\gamma_{s,i}) > P(\gamma_p)$ and $R_{min} > G(P(\gamma_p))^{-1}$. The optimized solution for reallocating power to each channel $i \in \{1, \cdots, N\}$ can be solved by the following Lagrangian [38]

$$P(\gamma_{s,i}) = \max_{i \in \{1, \cdots, N\}} \left(\left[\frac{1}{G^{-1}(R_{min})} - \frac{1}{\gamma_{s,i}} \right]^{+}, P(\gamma_p) \right) \tag{2.61}$$

where $P(\gamma_p) = Q_{peak}/F_{\gamma_p}^{-1}(1-\varepsilon)$ over the $(-\infty, x)$ region.

2.3.3 Performance Comparison

We consider the $1 \times N$ SIMO sensor network as in Fig. 2.10. The outage probability $P_{out,\, i}$ of the ith message from the SU-TX node through the channel $h_{s,i}$ is given by [81]

$$P_{out,\, i} = 1 - \exp\left(-\frac{1}{P_i G_i} \right) \tag{2.62}$$

$$P_{out,\, total} = \prod_{i=1}^{N} P_{out,i} \tag{2.63}$$

where $G_i = \frac{g_i}{2^{R_i}-1}$, $g_i = \mid h_{s,i} \mid^2$ and $P_{out,\, total}$ is the system-level outage event. The goal of the power allocation $P_i \leq P$ is to minimize the outage probability $(P_{out,\, i})$ for the ith link through the following optimization

$$\min_{P_i} \sum_{i=1}^{N} \mathcal{F}(P_{out,\, i}) \tag{2.64}$$

$$\text{subject to}: \sum_{i=1}^{N} P_i \leq P$$

$$\mathcal{F}(P_{out,\, i}) = \ln\left[1 - \exp\left(-\frac{1}{P_i G_i} \right) \right]$$

$$P_i = \frac{\frac{P_T}{G_i}}{\sum_{j=1}^{k_0} \frac{1}{G_j}}, \; 1 \leq j \leq k_0$$

where $k_0 \in \{1, \cdots, N\}$ is the number of non-zero power channels, i.e., $P_i = A$, for $1 \leq i \leq k_0$, and $P_i = 0$ for $k_0 \leq i \leq N$. The optimization for the minimum outage probability in (2.62) can be solved by the following Lagrangian

$$\mathcal{L}(\lambda, P_1, \cdots, P_{k_0}) = \sum_{i \in k_0} \ln\left[1 - exp\left(-\frac{1}{P_i G_i} \right) \right] + \lambda \left(\sum_{i \in k_0} P_i - P_t \right) \tag{2.65}$$

Differentiating the Lagrangian with respect to P_k gives the power solution as

$$P_i^* = \left(\frac{1}{\lambda G_i^2} \right)^{1/3} \tag{2.66}$$

where, P_i^* is the power-allocation for i^{th} channel by water-filling with the minimization of the outage probability $(P_{out,\ total})$ for all link. Similarly, for the target outage probability, we formulate the following power budget

$$\min_{P_i} \sum_{i=1}^{N} P_i \leq P \tag{2.67}$$

$$\text{subject to}: \ \ln(P_{out,\ total}) = \sum_{i=1}^{N} \ln(P_{out,\ i})$$

Chapter 3

Power Optimization Techniques for WSNs in Underground Mines

Authors in [36] considered that the transmission loss should take into account the EM wave penetration through soil and rock, but in this work we focus on the loss calculations based on fading in the wireless medium. Power conservation is one of the main design objective of WSN implementation to increase the network life-time which can be achieved by designing power-efficient devices and communication protocols. Attenuation is proportional to the distance of transmission and more power is required to transmit higher data rates over long distances. On the other hand, extreme path-loss, reflection/refraction, multi-path fading, and noise are the main factors for the EM propagation in the underground environment. Comprehensive energy efficient communication protocols are required for data transmission among sensor nodes with minimum transmission rate and energy constraint. We will focus on the cost optimization based on the free space model [56], [57], [58] where the optimization solution is found under the assumption of finding a path that will be affected by less noise and interferences, and we like to find the path using the best relaying scheme. Based on the analytical problem investigated in Chapter 2, we will develop convex mathematical tools to achieve the solutions for the MMSE receiver design.

3.1 System Model

As shown in Figure 3.1 based on [54], the architecture of a WSN for monitoring the environment in underground mines consists of three type of nodes: sensor nodes, routing nodes, and sink nodes. The multiple sensor nodes (Waspmotes) communicate with the routing node or gateway (Meshlium) through a WSN network platform mainly to gather and forward data among different sensor nodes [53]. The sink node is deployed usually near the earth surface and is connected with multiple routing nodes to transmit data to a BS through an optical fiber backbone network. The sensor node uses the short range XBee-802.15.4 communication standard to communicate between other sensor nodes and the router depending on the transmit power and distance. In this figure, sensor node S1 is connected

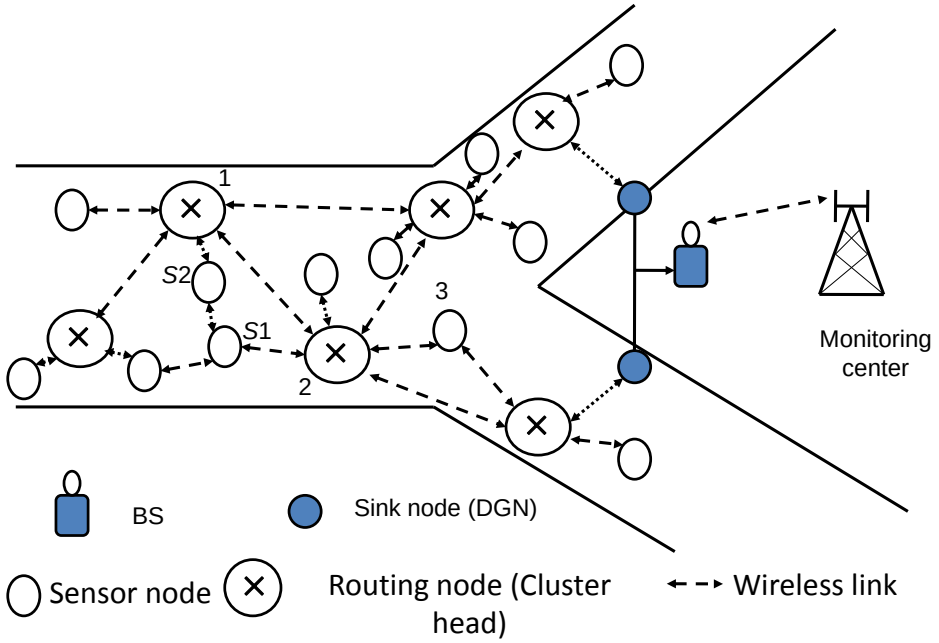

Figure 3.1 – Multi-WSN connection architecture for underground mines.

with router 1 through sensor node S2, and router 1 transmits the information of S1 to the monitoring center (MC) through the BS. If the noise of the wireless link between nodes S1 and S2 becomes high and the EM link is disconnected, then S1 may establish an EM connection with the other sensor nodes using router 1 or it may connect with router 2. Router 2 may transmit the data of node S1 directly to a nearby BS or via router 1 or router 3 depending on the distance and noise level of the EM link. In this way, every sensor nodes can communicate with multiple sensor nodes directly or via another routing node. If any primary link (i.e., link with nearest neighbors) is broken, communication can still go on by switching to another sensor node or routing node to ensure robustness of WSN communication.

The sensor nodes are grouped into a cluster [82], where each node consists of a single antenna, and each cluster is connected with a particular data gathering node (DGN) equipped with multiple antennas. The routing node (DGN in this case) consists of M_r DGN receiving antennas. We start with the equivalent representation of Fig. 3.1 by an L-user cluster set, where each cluster consists of M_t data collecting nodes (DCN) equipped with a single antenna.

Each cluster sends data to the FC through DGN nodes equipped with M_r antenna, where each cluster is connected with each DGN terminal through virtual MIMO links. For long distances between cluster and FC, multi-cluster relays can be implemented. The DGN relays signal using either wire connected link (i.e., optical fiber) or using M-quadrature amplitude modulation (M-QAM) to the FC via time-division multiple access (TDMA). The high-end DGN node is less energy constraint in this work. Each node in any cluster first broadcast its information to all other local nodes at different time slots, and they encode all the symbols received from other nodes according to an Alamouti diversity code so that they will transmit sequences in an Alamouti MIMO system [83]. Every cluster-to-cluster link

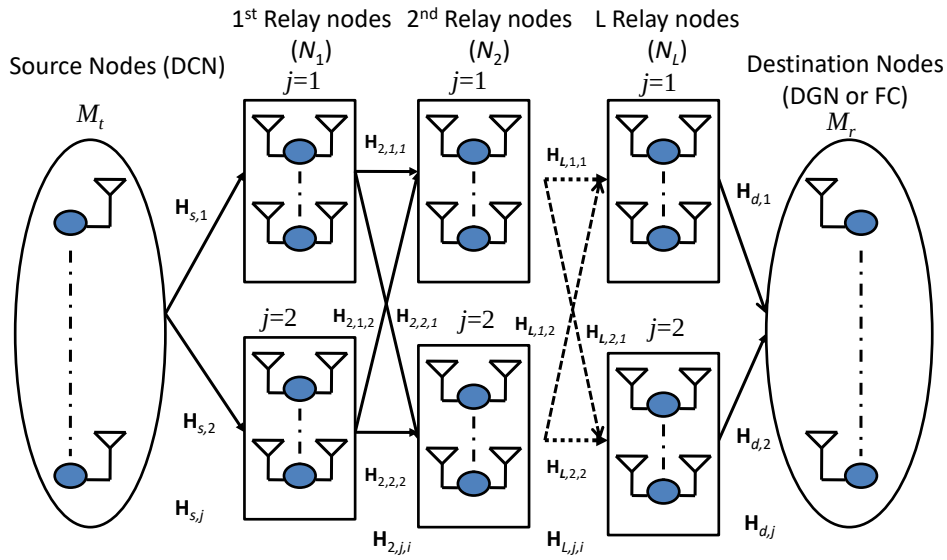

Figure 3.2 – Multi-hop cooperative WSN communication architecture, each node in any relay operated cooperatively under a router to form cluster based cooperative network.

is defined as a cooperative distributed MIMO channel. Transmit diversity is exploited within every cluster-to-cluster hop through a time-division, decode-and-forward, relaying scheme based on two consecutive time slots: the first time slot is known as intracluster slot and is used for data sharing among local cluster nodes, and the second slot is known as the intercluster slot, and is used for data transmission between clusters through a MIMO channel. A TDMA based MAC is used for a group of nodes in a particular cluster by a DGN receiver to connect with it, and the gateway (DGN in this case) will treat the signal from the cluster (remains active) as the desired signal and the signals from other inactive clusters as interference [73]. According to [39], most of the communication takes place through the air, and we consider all the channels in the above network as Rayleigh fading channels.

3.2 Signal Analysis and Problem Statement

We start with the equivalent representation of Fig. 3.1 by considering L relays as in Fig. 3.2 with two parallel terminals each equipped (for notational simplicity) with $N_l, l \in [1, \cdots, L]$ sensor nodes having a single antenna in each. Similarly, the source and destination have M_t and M_r nodes, respectively, each with a single antenna. We consider the non-regenerative AF relay protocol in which the received signal is received and then forwarded to the next relay terminal or final destination. Let us assume that all channel matrices are independent and identically distributed complex Gaussian, i.e., $\mathbf{H}_{s,j} \sim \mathcal{CN}(0, \sigma_s^2 \mathbf{I}), j \in [1,2]$ denote the $N_1 \times M_t$ channel matrices between the source nodes and j-th terminal in the first relay nodes and $\mathcal{CN}(0,1)$ denotes the complex Gaussian distribution with mean 0 and variance 1, $\mathbf{H}_{l,j,i} \sim \mathcal{CN}(0, \sigma_l^2 \mathbf{I}), i \in [1,2]$ denote the $N_l \times N_{l-1}$ channel matrices between the j-th terminal in the l-th relay and the i-th terminal of the previous $(l-1)$-th relay nodes, and $\mathbf{H}_{d,j} \sim \mathcal{CN}(0, \sigma_d^2 \mathbf{I})$ denote the $M_r \times N_L$ channel matrices between the destination nodes and the j-th

terminal of L-th relay as given by

$$\mathbf{H}_{s,j} = \begin{bmatrix} \mathbf{h}_{s,j,1} \\ \vdots \\ \mathbf{h}_{s,j,N_1} \end{bmatrix}, \quad \mathbf{H}_{l,j,i} = \begin{bmatrix} \mathbf{h}_{l,j,1} \\ \vdots \\ \mathbf{h}_{l,j,N_l} \end{bmatrix}, \quad \mathbf{H}_{d,j} = \begin{bmatrix} \mathbf{h}_{d,j,1} \\ \vdots \\ \mathbf{h}_{d,j,M_r} \end{bmatrix}$$

where $\mathbf{h}_{s,j,r} = [h_{s,j,1}, \cdots, h_{s,j,M_t}]$, $r \in [1, \cdots, N_1]$, $\mathbf{h}_{d,j,r} = [h_{d,j,1}, \cdots, h_{d,j,N_L}]$, $r \in [1, \cdots, M_r]$, and $\mathbf{h}_{l,j,r} = [h_{l,j,1}, \cdots, h_{l,j,N_{l-1}}]$, $r \in [1, \cdots, N_l]$.

Let us consider that the signal from the source nodes to the destination nodes are transmitted through the following phases using AF relaying as:
Phase 1: Received signal at j-th terminal of 1st relay, $j \in [1,2]$

$$\mathbf{r}_{j,1} = \mathbf{H}_{s,j}\mathbf{F}_s\mathbf{s} + \mathbf{n}_{s,j} \tag{3.1}$$

Phase l: $\{l = 2,3,4,\cdots,L\}$

$$\mathbf{r}_{j,l} = \mathbf{H}_{l,j,1}\mathbf{F}_{1,l-1}\mathbf{r}_{1,l-1} + \mathbf{H}_{l,j,2}\mathbf{F}_{2,l-1}\mathbf{r}_{2,l-1} + \mathbf{n}_{j,l} \tag{3.2}$$

Finally, at the destination, the received signal is given with $l = L$ by

$$\mathbf{r}_d = \mathbf{H}_{d,1}\mathbf{F}_{1,L}\mathbf{r}_{1,L} + \mathbf{H}_{d,2}\mathbf{F}_{2,L}\mathbf{r}_{2,L} + \mathbf{n}_d \tag{3.3}$$

where $\mathbf{n}_{s,j}$, $\mathbf{n}_{j,l}$, and $\mathbf{n}_d$ are zero-mean complex additive white Gaussian noise (AWGN) vectors of the corresponding links, $\mathbf{F}_s \in \mathbb{C}^{M_t \times N_b}$ is the precoder matrix at the source nodes, and $\mathbf{F}_{j,l-1} \in \mathbb{C}^{N_{l-1} \times N_b}$ is the precoder matrix at the j-th terminal of the $(l-1)$-th relay nodes. The precoder matrix $\mathbf{F}_s$ generates the transmitted signal $\mathbf{x}$ by the multiplication $\mathbf{x} = \mathbf{F}_s\mathbf{s}$ where $\mathbf{s} \in \mathbb{C}^{N_b \times 1}$ is the source signal vector. At the destination nodes, the equalizer matrix estimates the desire signal $\mathbf{s}$ by the matrix vector multiplication $\hat{\mathbf{s}}_d = \mathbf{W}_d\mathbf{r}_d$ where $\mathbf{r}_d$ is the received signal at the destination nodes from the L-th relay nodes and $\mathbf{W}_d \in \mathbb{C}^{N_b \times M_r}$ is the MMSE receiver matrix. Each node in any relay terminal has access to its local measurement and received signal from its immediate neighbors. The optimization problem of the above system can be given subject to local and global power constraints under perfect channel knowledge as

$$U(\mathbf{W}_d, \mathbf{F}_s, \mathbf{F}_{i,l}) \triangleq \arg \min_{\mathbf{W}_d, (\mathbf{F}_s, (\mathbf{F}_{i,l})_{l=1}^{L})} \mathrm{E}[||\mathbf{s} - \hat{\mathbf{s}}_d||^2] \tag{3.4}$$

$$\text{subject to: } \mathrm{tr}\left\{\mathbf{F}_s\mathbf{F}_s^H\right\} \leq P_s$$

$$\mathrm{tr}\left\{\mathbf{F}_{i,l}\mathbf{F}_{i,l}^H(\mathbf{H}_{l,j,i}\mathbf{F}_{i,l-1}\mathbf{F}_{i,l-1}^H\mathbf{H}_{l,j,i}^H + \mathbf{I}_{N_l})\right\} \leq P_{i,l}$$

$$P_s + \sum_{i,l} P_{i,l} \leq P$$

where P_s is the source power constraint, $P_{i,l}$ is the limited power constraint in the i-th terminal of the l-th relay, and P is the total power constraint. The cost function at the destination node depends on

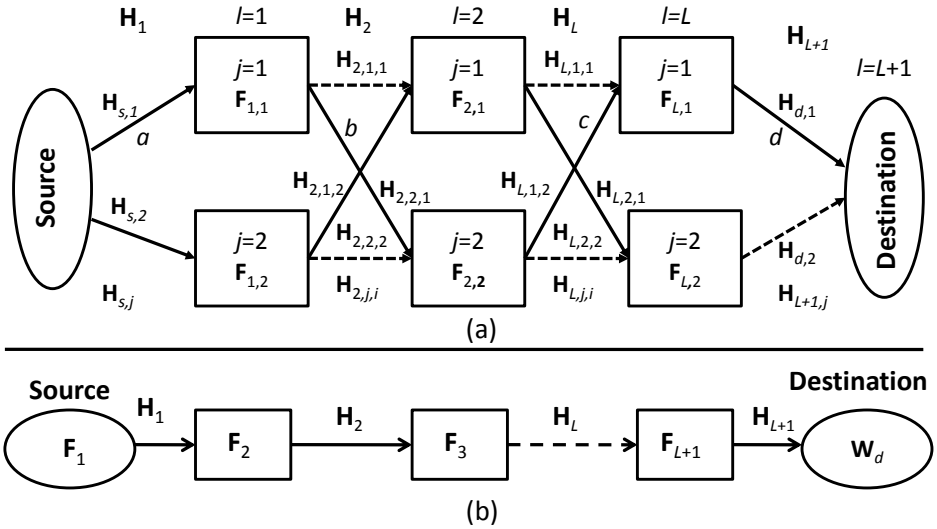

Figure 3.3 – Block diagram of single-way parallel multi-hop MIMO with selection relaying, a) best relaying path; b) equivalent signal transmission.

the joint strategy of the precoder matrices, i.e., $\mathbf{F}_s$ and $\mathbf{F}_{i,l}$, and the receiver detection matrix $\mathbf{W}_d$ that can be expressed as

$$\mathrm{E}[\| \mathbf{s} - \mathbf{W}_d^H \mathbf{r}_d \|^2] = \mathrm{E}[\| \mathbf{s} - \hat{\mathbf{s}}_d \|^2] \triangleq U(\mathbf{W}_d, \mathbf{F}_s, \mathbf{F}_{i,l}) \tag{3.5}$$

The receiver design problem in (3.4) is non-convex in the joint optimization perspective but convex with respect to each $\mathbf{F}_{i,l}$ and $\mathbf{W}_{i,l}$ of individual relays, and is difficult to solve [84]. A non-convex optimization problem is any problem where the objective or any of the constraints are non-convex, and a convex optimization problem is a problem where all of the constraints are convex functions. Unfortunately, due to the non-convex MSE problem formulation for the matrix value of the optimum precoder and the MMSE receiver solution, it is hard to carry out this solution in our case. Channel diagonalizing [28] simplifies the MIMO receiver to a simple scalar form, and thereafter the design problem can be formulated for the optimum solution by using powerful convex optimization tools. In this work, we will represent the nonconvex problem in a convex form with scalar variables that can be solved optimally using powerful nonconvex to convex transformation using majorization theory (see [28] for a complete reference on majorization theory), and then solved it by using the water-filling algorithm.

3.3 Optimization and Design Algorithms: Perfect CSI Case

The multiantenna parallel relay network as in Fig. 3.2 consists of M_t source nodes and M_r destination nodes equipped with a single antenna, and L parallel half-duplex relays equipped with $N_l, l \in [1, \cdots, L]$ relay nodes, each having a single antenna. We assume that due to the high path-loss, signals from the source node are transmitted to the destination through L relay nodes, i.e., no direct link between transmitter and receiver. The MMSE detector matrix at the receiver leads to minimizing the MSE

between the actually transmitted symbol and the output of its detector [85]. For half-duplex AF relaying, all relays attempt to receive the incoming signal in phase 1 and forwards to next relay in phase 2. Since AF relaying retransmits the signal in each relay phase, reliable communication should be guaranteed with QoS requirements as discussed in [20]. For perfect regeneration of the source symbol $\mathbf{s}$ at the destination terminal, there should be $M_t \leq \min\{N_1, \cdots, N_L\}$ antennas which is also true for classical multi-hop MIMO channels [18]. The noise and fading of each stage propagate to the destination but it can be made small using filtering in each stage so that it is negligible in the outage calculation. The input-output relationship at each stage of source-relay-destination is presented in (3.1) to (3.3) using the non-regenerative AF protocol. We use selection relaying that forwards only the signal from the path having the highest channel gain or instantaneous SNR.

3.3.1 Simplification Technique by Best Relaying

The minimization of the objective function in (3.4) now depends mainly on all the relay precoder matrices at the power constraint, and a centralized processing is required to compute the water-filling power allocation in each relay which may lead to high computational complexity. To overcome this difficulty, we use the decomposition of the MSE matrix at the destination node into a sum of MSE matrices at all relay nodes, similar to [18] in which the relay precoder matrix and MMSE matrix optimization is carried out locally. The solution of such a complex problem can be found by diagonal relaying as in Fig. 3.3. The first attempt at the source node involves sending source signal $\mathbf{s}$ to both terminals in the first relay. In the second stage, each terminal sends the estimated signal $\hat{\mathbf{s}}_{j,1}$ to the next relay according to the AF protocol. In this way, in the last stage, the destination estimates the target signal $\hat{\mathbf{s}}_d$ by solving (3.3). Each relay terminal decode the received signal in the first time slot and after regeneration, it is reencoded and forwarded in the second time slot. We represent the block diagonal precoder matrix timing for the l-th relay as:

$$\begin{array}{cccc} t_1 & t_2 & t_3 & t_4 \\ \end{array}$$
$$\begin{bmatrix} \mathbf{F}_{l,1}^{(1)} & \mathbf{0} & \mathbf{0} & \mathbf{0} \\ \mathbf{0} & \mathbf{F}_{l,1}^{(2)} & \mathbf{0} & \mathbf{0} \\ \mathbf{0} & \mathbf{0} & \mathbf{F}_{l,2}^{(1)} & \mathbf{0} \\ \mathbf{0} & \mathbf{0} & \mathbf{0} & \mathbf{F}_{l,2}^{(2)} \end{bmatrix}$$

At time t_1, the 1-st terminal of the $(l+1)$-th relay receives a signal only from the 1-st terminal of the l-th relay, and at time t_2, the 2-nd terminal of the $(l+1)$-th relay receives a signal from the 1-st terminal of the l-th relay. Similarly, at times t_3 and t_4, the first and second terminals of the $(l+1)$-th relay receive information from the second terminal of the l-th relay. The received signal for the $l+1$-th relay can be written as

$$\begin{bmatrix} \mathbf{r}_{1,l+1}^{(1)} \\ \mathbf{r}_{2,l+1}^{(1)} \\ \mathbf{r}_{1,l+1}^{(2)} \\ \mathbf{r}_{2,l+1}^{(2)} \end{bmatrix} = \begin{bmatrix} \mathbf{H}_{l+1,1,1} & \mathbf{0} & \mathbf{0} & \mathbf{0} \\ \mathbf{0} & \mathbf{H}_{l+1,2,1} & \mathbf{0} & \mathbf{0} \\ \mathbf{0} & \mathbf{0} & \mathbf{H}_{l+1,1,2} & \mathbf{0} \\ \mathbf{0} & \mathbf{0} & \mathbf{0} & \mathbf{H}_{l+1,2,2} \end{bmatrix} \begin{bmatrix} \mathbf{F}_{l,1}^{(1)} & \mathbf{0} & \mathbf{0} & \mathbf{0} \\ \mathbf{0} & \mathbf{F}_{l,1}^{(2)} & \mathbf{0} & \mathbf{0} \\ \mathbf{0} & \mathbf{0} & \mathbf{F}_{l,2}^{(1)} & \mathbf{0} \\ \mathbf{0} & \mathbf{0} & \mathbf{0} & \mathbf{F}_{l,2}^{(2)} \end{bmatrix} \begin{bmatrix} \mathbf{r}_{1,l} \\ \mathbf{r}_{1,l} \\ \mathbf{r}_{2,l} \\ \mathbf{r}_{2,l} \end{bmatrix} + \begin{bmatrix} \mathbf{n}_{1,l+1}^{(1)} \\ \mathbf{n}_{1,l+1}^{(2)} \\ \mathbf{n}_{2,l+1}^{(1)} \\ \mathbf{n}_{2,l+1}^{(2)} \end{bmatrix} \tag{3.6}$$

where $\mathbf{F}_{l,j}^{(i)}, i \in [1,2]$ is the relay amplifiter and its optimal design will be given in the next section. We use the best-relay selection scheme [27], so that the relay terminal forwards the signal corresponding to the channel having higher channel gain compared to the rest of the channels. The selection relaying makes decision to find the best path having the highest SNR compared to other possible link between the source-relay and relay-destination link pairs. The relay in the best path is known as best relay which can perfectly forward the decoded messages to the destination [86]. The works in [87], [88] provided details on optimal selection relay power implementations and showed that it improved the system performance. But the procedure for finding the set of optimum relay in our case becomes very complex for a large number of relay terminals. Using best-relaying, the j-th terminal of relay $l+1$ selects $\mathbf{r}_{j,l+1}^{(1)}$, i.e., $\mathbf{r}_{j,l+1} = \mathbf{r}_{j,l+1}^{(1)}$ if $||\mathbf{H}_{l+1,j,1}||_F \geq ||\mathbf{H}_{l+1,j,2}||_F$ else $\mathbf{r}_{j,l+1} = \mathbf{r}_{j,l+1}^{(2)}$, where $||.||_F$ is the Frobenious norm. We will simplify the parallel multi-relay network by invoking the technique described in [86]. Let path $l = 1$ represents the source to first relay terminal, and $l = 2, \cdots, L$ represent the relay-to-relay links, and $l = L+1$ represent the last relay to destination link. The best relay maximizes the mutual information at each relay terminal by finding the best channel from the two previous relay terminals. For example, at the destination node in Fig. 3.3(a), path d will be selected when $||\mathbf{H}_{d,1}||_F \geq ||\mathbf{H}_{d,2}||_F$. Similarly, in one case, we identify the link $a-b-c-d$ as the best path for the equivalent link. We use reactive relaying [86], where the set of relay in the best path is referred as active and the set of other relays is referred as inactive. The inactive relays may remain switched off for the power saving mode.

Our main idea is to decompose the error optimization problem in (3.4) in a joint nested minimization as [89]

$$\min_{\mathbf{F}_1,(\mathbf{F}_l)_{l=2}^{L+1}} \left[\min_{R_{\text{best}}} U_d \left(\mathbf{F}_1, (\mathbf{F}_l)_{l=2}^{L+1}, R_{\text{best}} \right) \right] \tag{3.7}$$

$$\text{subject to: } R_{\text{best}} > 0$$

$$\text{tr}\left\{ \mathbf{F}_1 \mathbf{F}_1^H \right\} \leq P_1$$

$$\text{tr}\left\{ \mathbf{F}_l (\mathbf{H}_l \mathbf{F}_{l-1} \mathbf{F}_{l-1}^H \mathbf{H}_l^H) \mathbf{F}_l^H \right\} \leq P_l, l = 2, \cdots, L+1$$

$$P_1 + \sum_l P_l \leq P_T$$

where $P_t = P/2$. We will solve (3.7) for the parallel relay network in two steps. In the first step, we will find the best path R_{best} that gives the best SNR at the destination which alternatively minimizes the sum of MSE errors. In the second step, we jointly design the non-iterative source precoder, the relay precoders and the destination MMSE filter for the equivalent series source-relay-destination link at local and global power constraint with perfect channel knowledge at all nodes. In this work, we will find the set of optimum relays by searching the best path, R_{best}, which corresponds to the path that gives the maximum value of the square root of the mean of the gain of all possible pairs of channel links. We will find the best path from all the possible hidden combinations by a recursive search method.

The received signal at the l-th relay for the equivalent representation in Fig. 3.3(b) using (3.6) is given by

$$\mathbf{r}_2 = \mathbf{H}_1\mathbf{F}_1\mathbf{s} + \mathbf{n}_1,\ \mathbf{r}_l = \mathbf{H}_{l-1}\mathbf{F}_{l-1}\mathbf{r}_{l-1} + \bar{\mathbf{n}}_l,\ l = 3, \cdots, L+1 \tag{3.8}$$

where $\bar{\mathbf{n}}_l$ is the $N_l \times 1$ noise vector respectively, given by for $l = 3, \cdots, L+1$

$$\bar{\mathbf{n}}_l = \sum_{j=2}^{l-1} \left(\bigotimes_{i=l-1}^{j} (\mathbf{H}_i\mathbf{F}_i)\mathbf{n}_{j-1} \right) + \mathbf{n}_{l-1} \tag{3.9}$$

with $\bar{\mathbf{n}}_1 = \mathbf{n}_1$, where $\bigotimes_{l=L+1}^{1} \mathbf{X}_l$ denotes $\mathbf{X}_{L+1} \times \cdots \times \mathbf{X}_1$. The received signal at the l-th relay can be broadly expressed as

$$\mathbf{r}_l = \mathbf{A}_{l-1}\mathbf{s} + \bar{\mathbf{n}}_l, l = 3, \cdots, L+1 \tag{3.10}$$

where $\mathbf{A}_l$ is the $N_{l+1} \times N_b$ equivalent channel matrix given by

$$\mathbf{A}_l = \mathbf{H}_l\mathbf{F}_l \cdots \mathbf{H}_1\mathbf{F}_1 = \bigotimes_{i=l}^{1} \mathbf{H}_i\mathbf{F}_i, l = 2, \cdots, L \tag{3.11}$$

The covariance matrix of $\bar{\mathbf{n}}_l$, $\mathbf{C}_l = \mathrm{E}[\bar{\mathbf{n}}_l\bar{\mathbf{n}}_l^H], l = 2, \cdots, L+1$ is given by using (3.9)

$$\mathbf{C}_1 = \mathbf{I}_{N_2}$$

$$\mathbf{C}_l = \sum_{j=2}^{l} \left(\bigotimes_{i=l}^{j} (\mathbf{H}_i\mathbf{F}_i) \bigotimes_{i=j}^{l} (\mathbf{F}_i^H\mathbf{H}_i^H) \right) + \mathbf{I}_{N_{l+1}}, l = 2, \cdots, L+1 \tag{3.12}$$

with $\mathbf{I}_{N_{L+2}} = \mathbf{I}_{M_r}$. If the MSE matrix at the destination node is equal to the sum of MSE matrices at all relay nodes, then we can write the MSE matrix $\mathbf{E}_d$ for the MMSE receiver matrix $\mathbf{W}_d$ as [18]

$$\mathbf{E}_d \left\{\mathbf{F}_l\right\}_{l=1}^{L+1} = \left[\mathbf{I}_{N_b} + \mathbf{A}_{L+1}^H \mathbf{C}_{L+1}^{-1} \mathbf{A}_{L+1} \right]^{-1} \tag{3.13}$$

Using (3.11) and (3.12) in (3.13), we have

$$\mathbf{E}_d \left\{\mathbf{F}_l\right\}_{l=1}^{L+1} = \left[\mathbf{I}_{N_b} + \bigotimes_{i=1}^{L+1} (\mathbf{F}_i^H\mathbf{H}_i^H) \left(\sum_{j=2}^{L+1} (\bigotimes_{i=L+1}^{j} (\mathbf{H}_i\mathbf{F}_i) \bigotimes_{i=j}^{L+1} (\mathbf{F}_i^H\mathbf{H}_i^H)) + \mathbf{I}_{N_l} \right)^{-1} \bigotimes_{i=L+1}^{1} (\mathbf{H}_i\mathbf{F}_i) \right]^{-1} \tag{3.14}$$

where $\mathbf{A}_{L+1}$ is the global channel at destination and can be obtained from (3.11), and $\mathbf{C}_{L+1}$ is the covariance matrix of $\bar{\mathbf{n}}_{L+1}$ defined as

$$\mathbf{C}_{L+1} = \sum_{j=2}^{L+1} \left(\bigotimes_{i=L+1}^{j} (\mathbf{H}_i \mathbf{F}_i) \bigotimes_{i=j}^{L+1} (\mathbf{F}_i^H \mathbf{H}_i^H) \right) + \mathbf{I}_{M_r} \tag{3.15}$$

By introducing $N_b \times N_l$ matrices $\mathbf{W}_l$ and $N_l \times N_b$ matrices $\mathbf{B}_l$, we express the optimal relay amplifying filter as [90]

$$\mathbf{F}_1 = \mathbf{B}_1, \mathbf{F}_l = \mathbf{B}_l \mathbf{W}_l, l = 2, \cdots, L+1 \tag{3.16}$$

where $\mathbf{W}_l$ and $\mathbf{B}_l$ stand for the l-th relay receiver and precoder filters. The error matrix in (3.14) can be decomposed into $L+1$ individual matrices as

$$\mathbf{E}_d \{\mathbf{B}_{L+1}\} = \left(\mathbf{I}_{N_b} + \mathbf{H}_1 \mathbf{B}_1 \mathbf{B}_1^H \mathbf{H}_1^H \right)^{-1} + \sum_{l=2}^{L+1} \left(\mathbf{R}_{l-1}^{-1} + \mathbf{H}_l \mathbf{B}_l \mathbf{B}_l^H \mathbf{H}_l^H \right)^{-1} \tag{3.17}$$

Proof: See Appendix B

We will optimize the first term of (3.17) in the first step corresponding to the source precoder using the general precoder design as described in [66], and we will minimize the sum of the MSE terms in the second term through designing the relay precoder $\mathbf{B}_l$ for the rest of the relay terminals.

Each of the possible MIMO links from source to destination of the network in Fig. 3.1 provides an individual MSE error matrix as given in (3.17). The goal of the simplification is to find the optimum path that gives the minimum MSE error compared to all other possible paths. We will start by considering any random multi-hop MIMO link.

Taking eigenvalue decomposition (EVD) of $\mathbf{H}_l \mathbf{H}_l^H$ as $\mathbf{H}_l = \mathbf{U}_l \Sigma_l \mathbf{U}_l^H$, where $\mathbf{U}_l \in \mathcal{C}^{N_l \times N_l}$ represents a unitary matrix and Σ_l is a $K \times K$ diagonal matrix of elements $\lambda_{l,1} \geq, \cdots, \geq \lambda_{l,K}$, $K = N_b = \min\{N_l, N_{l-1}\}$. Then, in the same manner as in [19], we can write the optimal structure of $\mathbf{B}_1$ and $\mathbf{B}_l$ for the Schor-convex optimization as

$$\mathbf{B}_1 = \mathbf{U}_{1,1} \Lambda_1 \mathbf{U}_0, \mathbf{B}_l = \mathbf{U}_{l,1} \Lambda_l \mathbf{V}_{l,1}^H, l = 2, \cdots, L+1 \tag{3.18}$$

where $\mathbf{U}_0$ is an $N_b \times N_b$ unitary rotation matrix and $\mathbf{U}_{l,1}$ contains the first N_b columns of $\mathbf{U}_l$. The matrix $\mathbf{V}_{l,1} \in \mathcal{C}^{N_l \times N_b}$ contains the first N_b columns of $\mathbf{V}_l, l = 2, \cdots, L+1$, where $\mathbf{V}_l$ is a unitary matrix taken from the EVD of $\mathbf{W}_l \mathbf{H}_l \mathbf{B}_{l-1} = \mathbf{V}_l \Lambda_{w,l} \mathbf{V}_l^H$. For white noise $\bar{\mathbf{n}}_{L+1}$, the $k, k = 1, \cdots, N_b$-th diagonal element of matrix $\mathbf{E}_d \{\mathbf{F}_l\}_{l=1}^{L+1}$ can be expressed with unique power allocation of $\mathbf{B}_l = \mathrm{diag}\{\sigma, \cdots, \sigma\}, \forall l$ by substituting (3.18) back into (3.17)

$$\left[\mathbf{E}_d \{\Lambda_l\}_{l=1}^{L+1} \right]_{k,k} = \frac{1}{1 + \lambda_{1,k}^2 \sigma^2} + \frac{1}{1 + \lambda_{2,k}^2 \sigma^2} + \cdots + \frac{1}{1 + \lambda_{L+1,k}^2 \sigma^2}, k = 1, \cdots, N_b \tag{3.19}$$

We are also interested by the average MSE at destination that can be expressed as

$$\bar{\mathbf{E}}_d \{\Lambda_l\}_{l=1}^{L+1} = \frac{1}{N_b} \sum_{k=1}^{N_b} \sum_{l=1}^{L+1} \frac{1}{1 + \lambda_{l,k}^2 \sigma^2} \tag{3.20}$$

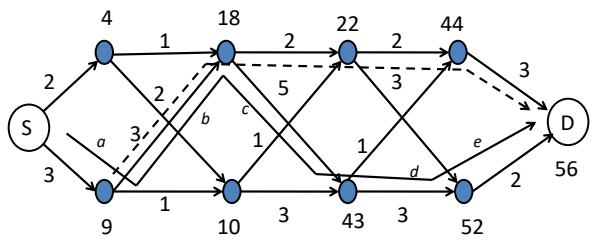

Figure 3.4 – Recursive determination of best path.

From the numerical computation we found that the k-th diagonal element of the error matrix $\left[\mathbf{E}_d\left\{\Lambda_l\right\}_{l=1}^{L+1}\right]_{k,k}$ in (3.19) decreases with the increasing value of the channel gain $\lambda_{l,k}^2, \forall l$. Hence, we can minimize (3.19) by maximizing the sum term $\sum_{l=1}^{L+1}\lambda_{l,k}^2, \forall l$, and this path gives the maximum SNR gain of the corresponding sub-channel at destination. We can apply (3.19) to find the optimum sub-channel that gives the highest SNR among a set of possible sub-channels from source to destination or the average MSE minimization in (3.20) can be used to find the optimum MIMO channel that gives the highest channel gain at destination over all possible MIMO links. This concept is used in the well known Viterbi algorithm for finding the most likely sequence of hidden states [91]. For example, in Fig. 3.4, we assume channel gains for a 4-relay network where source-relay, relay-relay, and relay-destination links are considered as SISO links. For both terminals of the first relay, we have the square value of the corresponding channel gains. Each terminal of the 2nd relay considers only the maximum of the sum of the square of the corresponding pair of channel gains from source to first relay and first relay to second relay, respectively. The highest sum values can be used to find the optimum path for each terminal of the 3rd relay, and continuing this process, we can find the optimum path for each terminal of the 4-th relay. From the destination, we will find the sum of the square of its channel gain with the gain of the associated terminal in the last relay. With the given typical channel gain values, we find the path $a-b-c-d-e$ that gives the maximum sum value of 56 is the best path R_{best}.

Now, we attempt to apply the above approximation to find the best path R_{best} from source to destination of our proposed system as in Fig. 3.3(a). Let us define SVD of $\mathbf{H}_{s,j}=\mathbf{U}_{s,j}\Sigma_{s,j}\mathbf{V}_{s,j}^H$, $\mathbf{H}_{l,j,i}=\mathbf{U}_{l,j,i}\Sigma_{l,j,i}\mathbf{V}_{l,j,i}^H$, and $\mathbf{H}_{d,j}=\mathbf{U}_{d,j}\Sigma_{d,j}\mathbf{V}_{d,j}^H$. The diagonal elements of $\Sigma_{s,j}=\text{diag}\left\{\lambda_{s,j,1},\cdots,\lambda_{s,j,K}\right\}$, $\Sigma_{l,j,i}=\text{diag}\left\{\lambda_{l,j,i,1},\cdots,\lambda_{l,j,i,K}\right\}$, and $\Sigma_{d,j}=\text{diag}\left\{\lambda_{d,j,1},\cdots,\lambda_{d,j,K}\right\}$ are in decreasing order, where $K=\min\left\{M_t,N_l,M_r\right\}, \forall l$. Usually, the last diagonal element of $\Sigma_{s,j}$, $\Sigma_{l,j,i}$, and $\Sigma_{d,j}$ shows a very small gain, and it has a very high error probability. To account for this effect, we will take the square root of the mean of the square of the diagonal elements of each matrix to represent the overall channel status. We find the best path R_{best} for the network through the following optimization

$$R_{\text{best}}=\arg\max_{j\in[1,2]}\gamma_{d,j} \tag{3.21}$$

where $\gamma_{d,j}$ is the mean of the sum of the square of the j-th channel gain at destination. The optimum set of equivalent channel matrices that solves (3.21) can be found by applying the algorithm shown in Algorithm 1.

Algorithm 1 Step for finding best path

set $\gamma_{1,j} = \sqrt{\frac{1}{K}(\sum_{k=1}^{K} \lambda_{s,j,k}^2)}, j \in [1,2]$

for $l = 2 : L$ **do**

$$\gamma_{l,j}, j \in [1,2] = \begin{cases} \sqrt{\frac{1}{K}(\sum_{k=1}^{K} \lambda_{l,j,1,k}^2)} + \gamma_{l-1,1}, & \text{if } (\sqrt{\frac{1}{K}(\sum_{k=1}^{K} \lambda_{l,j,1,k}^2)} + \gamma_{l-1,1}) \geq (\sqrt{\frac{1}{K}(\sum_{k=1}^{K} \lambda_{l,j,2,k}^2)} + \gamma_{l-1,2}) \\ \sqrt{\frac{1}{K}(\sum_{k=1}^{K} \lambda_{l,j,2,k}^2)} + \gamma_{l-1,2}, & \text{otherwise} \end{cases}$$

end for

set $\gamma_{d,j} = \sqrt{\frac{1}{K}(\sum_{k=1}^{K} \lambda_{d,j,k}^2)} + \gamma_{L,j}, j \in [1,2]$

set

$$\mathbf{H}_{L+1} = \mathbf{H}_{d,j}, \text{where } j = \begin{cases} 1, & \text{if } (\sqrt{\frac{1}{K}(\sum_{k=1}^{K} \lambda_{d,1,k}^2)} + \gamma_{L,1}) \geq (\sqrt{\frac{1}{K}(\sum_{k=1}^{K} \lambda_{d,2,k}^2)} + \gamma_{L,2}) \\ 2, & \text{otherwise} \end{cases}$$

set $l = L$

while $l \geq 2$ **do**

$$\mathbf{H}_{l} = \mathbf{H}_{l,j,i}, \text{where } i = \begin{cases} 1, & \text{if } (\sqrt{\frac{1}{K}(\sum_{k=1}^{K} \lambda_{l,j,1,k}^2)} + \gamma_{l-1,1}) \geq (\sqrt{\frac{1}{K}(\sum_{k=1}^{K} \lambda_{l,j,2,k}^2)} + \gamma_{l-1,2}) \\ 2, & \text{otherwise} \end{cases}$$

$l = l - 1$

$j = i$

end while

$$\mathbf{H}_1 = \mathbf{H}_{s,j}$$

In proactive relaying, the set of relay terminals gives the optimal path, which is termed the active set, and the set of inactive terminals will be disconnected from the network. The active source-relay-destination series link can be represented by the set of channel matrices $\mathbf{H}_l, l = 1, \cdots, L$ as shown in Fig. 3.3(b) using proactive relaying.

3.3.2 Optimum Precoder Design

We can compute the l-th relay local receiver matrix $\mathbf{W}_l$ for $l = 2, \cdots, L+1$ as [18]

$$\mathbf{W}_l = (\mathbf{H}_{l-1}^H \mathbf{F}_{l-1}^H \mathbf{H}_{l-1} \mathbf{F}_{l-1} + \mathbf{C}_{l-1})^{-1} \mathbf{H}_{l-1} \mathbf{F}_{l-1} \tag{3.22}$$

The desired signal from the source can be estimated more accurately using a Wiener filter, so we consider a Wiener filter in each relay stage. We employ the Wiener filter $\mathbf{W}_d \in \mathcal{C}^{M_r \times N_L}$ at the destination

$$\mathbf{W}_d = (\mathbf{H}_{L+1}^H \mathbf{F}_{L+1}^H \mathbf{H}_{L+1} \mathbf{F}_{L+1} + \mathbf{C}_{L+1})^{-1} \mathbf{H}_{L+1} \mathbf{F}_{L+1} \tag{3.23}$$

We will consider three approaches. In the first approach, we count the propagation of fading and noise effect from all previous nodes by defining the matrix $\mathbf{R}_l$. In the second approach, we consider that the

matrix $\mathbf{R}_l$ approaches the identity matrix $\mathbf{I}_{N_b}$. In the final approach, we will transmit the input signal through a pair of strong sub-channels and the weak sub-channels will be fed zero power.

Approach 1

The matrix $\mathbf{R}_l = \mathbf{A}_l^H \mathbf{D}_l^{-1} \mathbf{A}_l$ where $\mathbf{D}_l = \mathbf{A}_l \mathbf{A}_l^H + \mathbf{C}_l$, requires the solution of the relay filter $\mathbf{F}_l$ of all previous steps. The relay filter $\mathbf{F}_l$ is the joint expression of two matrices $\mathbf{B}_l$ and $\mathbf{W}_l$, i.e., $\mathbf{F}_l = \mathbf{B}_l \mathbf{W}_l$. We will find the solution for $\mathbf{B}_l, \forall l$ in this section. We can compute $\mathbf{W}_l$ for a given source precoder $\mathbf{F}_1$ and previous relay precoders $\mathbf{F}_{l-1}$ which requires the recursive operation as given in Algorithm 2. The

Algorithm 2 Step for finding $\mathbf{W}_l$

```
solve W_2 for a given F_1 using (3.22)
for l = 2 : L do
    compute B_l
    find W_{l+1} for a given W_l and B_l
end for
```

transmission power consumed by the l-th relay node is $\mathrm{tr}(\mathrm{E}[\bar{\mathbf{r}}_l \bar{\mathbf{r}}_l^H]), l = 2, \cdots, L+1$, where $\bar{\mathbf{r}}_l = \mathbf{B}_l \mathbf{r}_l$, and using (3.8) we have

$$\mathrm{tr}(\mathrm{E}[\bar{\mathbf{r}}_l \bar{\mathbf{r}}_l^H]) = \mathrm{tr}(\mathbf{B}_l \mathbf{D}_l \mathbf{B}_l^H) \tag{3.24}$$

Our design is based on (3.17) where the MSE at destination is the sum of MSEs of individual nodes and the error optimization problem can be summarized as

$$\min_{\{\mathbf{B}_l\}_{l=1}^{L+1}} \mathrm{tr}\Big(\mathbf{E}_d\{\mathbf{B}_l\}\Big) \tag{3.25}$$

$$\text{subject to: } \mathrm{tr}(\mathbf{F}_1 \mathbf{F}_1^H) \le P_1$$

$$\mathrm{tr}(\mathbf{B}_l \mathbf{D}_l \mathbf{B}_l^H) \le P_l, l = 2, \cdots, L+1$$

$$P_1 + \sum_{l=2}^{L+1} P_l \le P$$

Using lemma 2 and lemma 4 as given in appendix A, we can express $\mathbf{R}_l$ as

$$\mathbf{R}_l = [\mathbf{I}_{N_b} + \mathbf{G}_l^{-1}]^{-1} = \mathbf{G}_l - \mathbf{G}_l(\mathbf{I}_{N_b} + \mathbf{G}_l)^{-1}\mathbf{G}_l \tag{3.26}$$

where $\mathbf{G}_l = \mathbf{A}_l^H \mathbf{C}_l^{-1} \mathbf{A}_l$. Now, we write the EVD in the right side of (3.26) as $\mathbf{R}_l = \mathbf{U}_l \Xi_l \mathbf{U}_l^H$ where $\mathbf{U}_l \in \mathcal{C}^{N_b \times N_b}$ is a unitary matrix, and $\Xi_l = \mathrm{diag}\{\xi_{l,1}, \cdots, \xi_{l,K}\}$. Substituting the EVD of $\mathbf{H}_l$, $\mathbf{B}_l$, and $\mathbf{R}_l$ into (3.25), we have

$$\min_{\{\sigma_{l,i}\}_{l=1}^{L+1}} \sum_{i=1}^{N_b} \frac{1}{\xi_{l,i}^{-1} + \lambda_{l,i}^2 \sigma_{l,i}^2} \tag{3.27}$$

$$\text{subject to: } \sum_{l=1}^{L+1} \sum_{i=1}^{N_b} |\sigma_{l,i}|^2 = P \tag{3.28}$$

The problem (3.27)-(3.28) has a water-filling solution given by

$$\sigma_{l,i}^2 = \frac{1}{\lambda_{l,i}^2}\left(\sqrt{\frac{\lambda_{l,i}^2}{\mu_l \xi_{l,i}^2}} - \frac{1}{\xi_{l,i}^2}\right)^+, l = 2, \cdots, L+1 \tag{3.29}$$

where the μ_l's are the waterlevels.

Proof: See Appendix C

We can find $\sigma_{1,i}^2$ for $\mathbf{B}_1$ by putting $\xi_{1,i} = 1$ in (3.29). The procedure of optimizing source and relay precoding matrices is described in Algorithm 3. A similar transceiver design has been implemented in

Algorithm 3 Procedure for optimizing the source and relay precoder matrices

1: solve the best relay selection problem in Algorithm 1 to obtain series optimum MIMO channel matrices $\mathbf{H}_1, \mathbf{H}_2, \cdots, \mathbf{H}_{L+1}$.
2: design source precoder $\mathbf{F}_1 = \mathbf{B}_1$ using (3.18) with $\xi_{1,i} = 1$ in (3.29)
3: **for** $l = 2 : L+1$ **do**
4: find the EVD of $\mathbf{R}_l$ using (3.26)
5: find matrices $\mathbf{B}_l$ from (3.18) using (3.29)
6: compute matrices $\mathbf{W}_l$ for a given $\mathbf{F}_{l-1}$ using Algorithm 2
7: find $\mathbf{F}_l = \mathbf{B}_l \mathbf{W}_l$
8: **end for**

[18] for multi-hop MIMO AF relaying but it requires the EVD computation of the $\mathbf{A}_l^H \mathbf{D}_l^{-1} \mathbf{A}_l$ matrix which is very difficult. On the other hand, our design algorithm consists of the EVD computation of $\mathbf{A}_l^H \mathbf{C}_l^{-1} \mathbf{A}_l$ in (3.26) which is very simple to implement.

Approach 2

We consider the high SNR region where $\mathbf{R}_l$ approaches the identity matrix $\mathbf{I}_{N_b}$. In this case, each relay precoder matrix $\mathbf{B}_l$ can be determined independently of all previous hops [18], [90].

$$\min_{\mathbf{W}_d, \{\mathbf{F}_l\}_{l=1}^{L+1}} \operatorname{tr}\left(\mathbf{E}_d\left\{\mathbf{F}_l\right\}\right) \tag{3.30}$$

$$\text{subject to: } \operatorname{tr}(\mathbf{B}_1 \mathbf{B}_1^H) \leq P_1$$

$$\operatorname{tr}\left\{\mathbf{B}_l(\mathbf{H}_l \mathbf{B}_{l-1} \mathbf{B}_{l-1}^H \mathbf{H}_l^H)\mathbf{B}_l^H\right\} \leq P_l, l = 2, \cdots, L+1$$

$$\sum_{l=1}^{L+1} P_l \leq P$$

where P_1 and P_l denote the power available at the source node and l-th relay node for transmission. The design attempts only to Schur-convex $\mathbf{E}_d$, i.e., the objective functions are increasing in each argument. In this case, the error optimization problem can be expressed using (3.25) as

$$\min_{\{\mathbf{F}_l\}_{l=1}^{L+1}} \operatorname{tr}\left([\mathbf{I}_{N_b} + \mathbf{H}_l^H \mathbf{B}_l^H \mathbf{B}_l \mathbf{H}_l]^{-1}\right) \tag{3.31}$$

$$\text{subject to: } \mathrm{tr}(\mathbf{B}_1\mathbf{B}_1^H) \leq P_1$$

$$\mathrm{tr}\left\{\mathbf{B}_l(\mathbf{H}_l\mathbf{B}_{l-1}\mathbf{B}_{l-1}^H\mathbf{H}_l^H)\mathbf{B}_l^H\right\} \leq P_l, l = 2, \cdots, L+1$$

$$\sum_{l=1}^{L+1} P_l \leq P$$

Substituting (3.18) into (3.31), the matrix variable optimization problem is converted to the convex form with system scalar variables. Our goal is to find the solution of $\mathbf{B}_l$ by putting the diagonal elements of $\Lambda_l = \mathrm{diag}\left\{\sigma_{l,1}, \cdots, \sigma_{l,K}\right\}, \forall l$ in (3.18). We can write similar to (3.29)

$$\min_{\{\sigma_{l,i}\}_{l=1}^{L+1}} \sum_{i=1}^{N_b} \frac{1}{1+\lambda_{l,i}^2\sigma_{l,i}^2} \tag{3.32}$$

$$\text{subject to: } \sum_{l=1}^{L+1}\sum_{i=1}^{N_b} |\sigma_{l,i}|^2 = P \tag{3.33}$$

The problem (3.32)-(3.33) has a water-filling solution similar to (3.29)

$$\sigma_{l,i}^2 = \frac{1}{\lambda_{l,i}^2}\left(\sqrt{\frac{\lambda_{l,i}^2}{\mu_l}} - 1\right)^+, l = 1, \cdots, L+1 \tag{3.34}$$

Compared to the problem for approach 1, the precoder design in (3.34) is very simple due to scalar variables and has a smaller computational complexity because it does not need to compute the EVD of $\mathbf{R}_l$. We can further simplify the computation for both approaches by considering $\mathbf{U}_l = \mathbf{V}_l^H = \mathbf{I}_{N_b}$. The transceiver design for this approach can be obtained using Algorithm 3 with $\mathbf{R}_l = \mathbf{I}_{N_b}$.

Approach 3

Note that in order to achieve the optimal performance in terms of mutual information, the strong subchannels $\lambda_{l,i}$ of all hops are paired according to their actual gain magnitude, i.e., the source signal is transmitted over the strong m-th subchannel in the first hop are forwarded by the m-th subchannel of all relays if $\lambda_{l,m} \geq \lambda_{th}$, where λ_{th} is the threshold level while the weak subchannels $\lambda_{l,m} \leq \lambda_{th}$ in all hops should be paired together [92]. For the Schur-convex objective function, we will transmit the source signal through the N substreams $\lambda_{l,m}, m = 1, \cdots, N$ associated to strong nonzero channel eigenvalues, i.e., $\lambda_{l,m} \geq \lambda_{th}$ whereas the remainder $N_0 = N_b - N$ subchannels are assigned zero power $\sigma_{l,n}^2 = 0, n = 1, \cdots, N_0$ [93] and the strong sub-channels satisfy $\sum_{l=1}^{L+1}\sum_{i=1}^{N} |\sigma_{l,i}|^2 = P$. In this case, the source symbol $\mathbf{s} \in \mathbb{C}^{N\times 1}$ is received perfectly at the receiver if $N \leq \min\left\{M_t, N_1, \cdots, N_L, M_r\right\}$.

Chapter 4

Performance Results

4.1 Introduction

We will consider the following transceiver design algorithms:

— Relay diversity ordering selection (RDS): The algorithm of traditional selection relaying works with the aid of a local decision making technique where the incoming signals in any relay (or local receiving node) from the previous two relays are selected using the selection diversity scheme to forward the maximum instantaneous SNR signal to the next terminal. The protocol for best relay selection in this case is based on the instantaneous channel conditions [94], specially used in slow fading environment, or based on relay ordering [95]. With the traditional selection relaying scheme, each relay terminal of the l-th relay (Fig. 3.3(a)) forwards the signal from either the 1st or the 2nd terminal of the previous $(l-1)$-th relay based on the local gain of the corresponding channel i.e., the j-th terminal of the l-th relay accepts the signal from the $\mathbf{H}_{l-1,j,1}$ channel if $||\mathbf{H}_{l-1,j,1}||_F^2 \geq ||\mathbf{H}_{l-1,j,2}||_F^2$ else from the $\mathbf{H}_{l-1,j,2}$ channel. Each terminal in all relays forwards the signal based on the local decision instead of looking for the overall global channel condition. The final decision is also taken based on the SNR of the last relay node, i.e., the destination selects $\mathbf{H}_{d,1}$ if $||\mathbf{H}_{d,1}||_F \geq ||\mathbf{H}_{d,2}||_F$ where $||.||_F$ is the Frobenius norm. This scheme only works on the basis of local channel information. As a result the solution is not optimal but it is very simple to implement.

— Best relay selection (BRS): This design is developed according to the simplification in Algorithm 1, where each relay terminal decides the best path based on global channel knowledge. In this scheme, any terminal will select the channel having the maximum value of the gain. Communication is performed only by the set of nodes having the best SNR gain in the simplified form as shown in Fig. 3.3(b). The rest of the nodes will remain inactive. Using this solution, we can save power from the inactive relay as it works depending on proactive relaying.

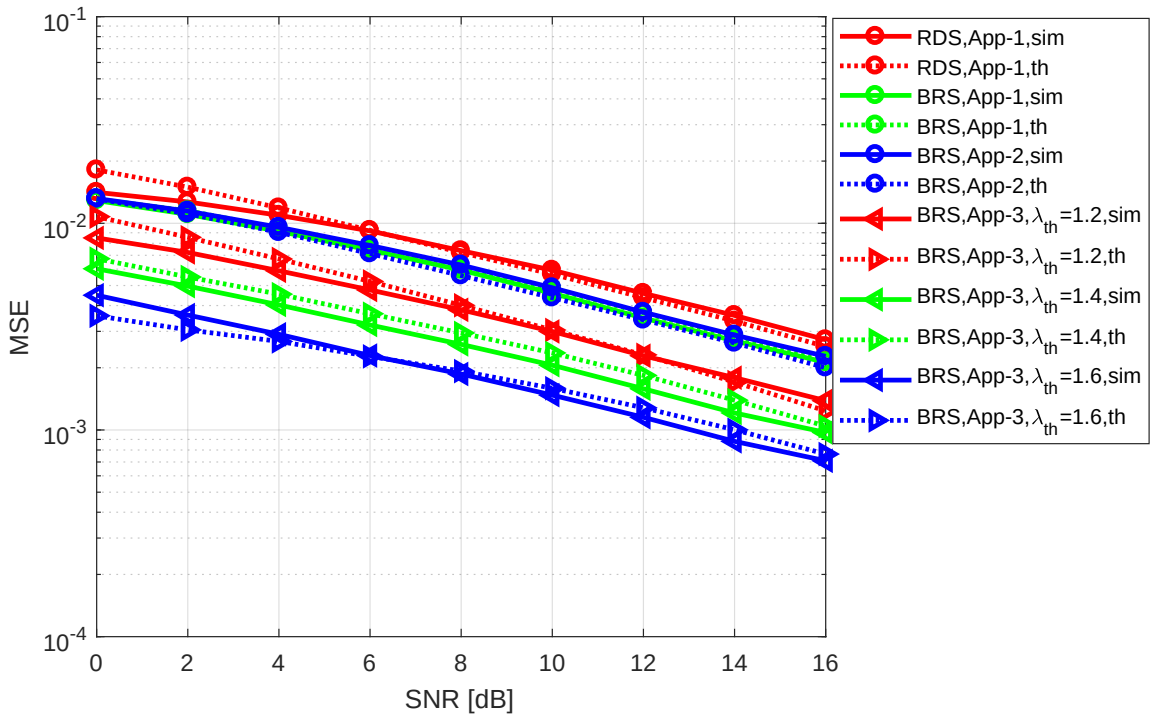

Figure 4.1 – MSE versus SNR with equal number of source-relay-destination antennas.

4.2 Error Performance with Fixed Number of Relays

4.2.1 Equal number of antennas

We demonstrate the error performance of the proposed solutions in the case of perfect CSI knowledge of each channel at each transmitter and receiver. In all simulations, we use the actual channel parameters based on [5] where measurements have been performed in the CANMET mine, Val-d'Or, Québec, Canada, in order to produce accurate study of channel propagation. The results show the path-loss exponent ν in the range between 1.4 and 1.8 for the mine gallery at the 70 m level. We observe the MSE and BER performances for all simulations with 4 nodes for all source-relay-destination terminals, i.e., $M_t = M_r = 4$, $N_l = 4, \forall l$, and simulation results are averaged for 10^5 independent realizations of channel matrices $\mathbf{H}_{s,j}$, $\mathbf{H}_{l,j,i}$, and $\mathbf{H}_{d,j}$, where the elements of the channel matrices are given by (2.14) and the channels are constant within a frame. Simulations are done by transmitting frames consisting of 45 packets, and each packet contains 4 symbols. We use 16-QAM modulation to transmit 180 symbols in the frame from source to destination using a 5 relay AF MIMO system. We have carried out Matlab simulations to evaluate MSE and BER performances based on channel measurements in [5] in the millimeter-wave (mmW) carrier frequency of $f = 60$ GHz with a 2.1 GHz bandwidth for source to destination distance set to $d = 30$ m and width of the gallery set to $w = 2.5$ m.

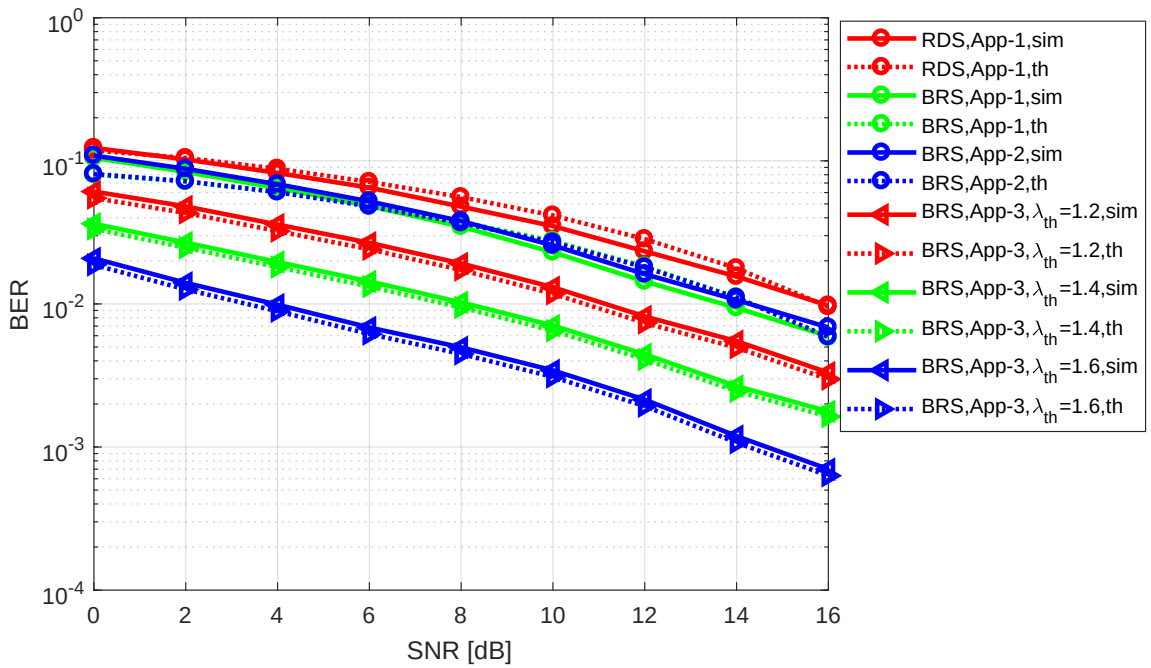

Figure 4.2 – BER performance comparison with equal number of source-relay-destination antennas.

For the multi-hop topology, the MSE optimization problem is much more challenging than the existing works with a simpler network architecture, and is a complicated function of the source, relay, and receiver matrices. The QoS performance of a digital communication system is given usually in BER, but the above optimization theory has been driven in terms of MSE. We can easily give the optimization in terms of BER by designing a linear receiver such that it minimizes each MSE, maximizes each subchannel SNR, and alternatively minimizes each BER [93], i.e.,

$$\text{BER} \approx aQ(\sqrt{b\text{SNR}})/k; k = \log_2(M) \tag{4.1}$$

where a and b are constant depending on the constellation size, M, Q is the Q-function given by $Q(x) = (1/\sqrt{2\pi})\int_x^\infty e^{-y^2/2}dy$, and the i-th signal-to-interference-plus-noise ratio (SINR) is related to the i-th MSE by $\text{SINR}_i = (1/\text{MSE}_i) - 1$. Here, (4.2) relates the BER of the channel for the signal SNR and we can use it to compute the theoretical BER of the channel. Therefore, the MSE optimization is the equivalent of the optimization in terms of BER. The simulated and theoretical MSE performance for the above design cases with path-loss exponent $\nu = 1.5$ to 1.8 and a 5 relay system with source to destination distance $d = 30$ m are plotted in Fig. 4.1 with individual node power constraint of 10 W. The theoretical MSE is calculated using (3.17). The distance for each direct path of Fig. 3.2 is d_1 and for each diagonal path is $\sqrt{d_1^2 + w^2}$, where $d_1 = d/(L+1)$ and w is the width of the gallery. The simulated and theoretical BERs obtained by all algorithms for the above system are illustrated in Fig. 4.2 versus SNR. The theoretical BER is calculated using (3.17) and (4.2). We use approach 1 for RDS

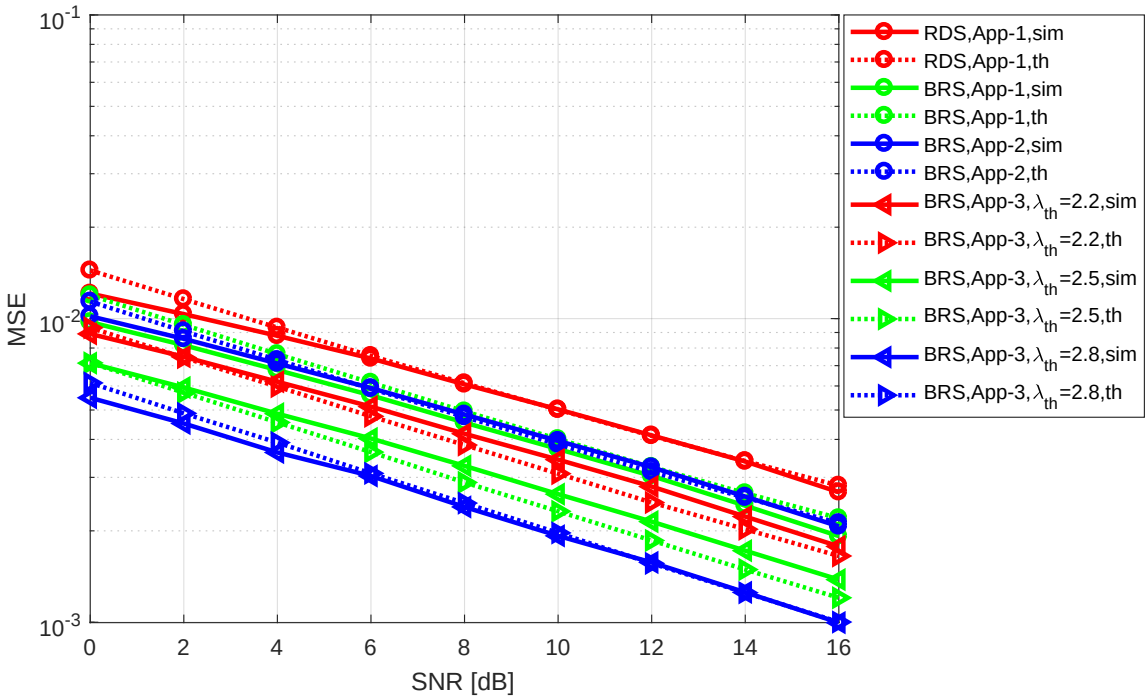

Figure 4.3 – MSE versus SNR with unequal number of source-relay-destination antennas.

and it provides worst MSE and BER performances than for the BRS. The BRS with approach 1 is the best solution while the BRS with approach 2 is sub-optimal. It is also observed that the BRS with approach 1 approaches the BRS with approach 2 in the MSE and BER performance curves at high SNRs and this is because in this region, the noise covariance matrix $\mathbf{R}_l$ is approximated by the identity matrix $\mathbf{I}_{N_b}$ [18], [90]. Moreover, the BRS with approach 3 for threshold $\lambda_{th} = 1.2$, $\lambda_{th} = 1.4$, and $\lambda_{th} = 1.6$ shows both MSE and BER performance improvements. It can be noted that by increasing the threshold value λ_{th}, the transceiver uses only the strong sub-channels and bypasses the weak sub-channel, i.e., less sub-channels are used. Therefore, the data rate of approach 3 decreases with increasing value of the threshold λ_{th}.

4.2.2 Unequal number of antennas

In this example, a 5 relay system is simulated with $M_t = 4$, $N_1 = 3$, $N_2 = 4$, $N_3 = 5$, $N_4 = 3$, $N_5 = 4$, and $M_r = 4$ for individual source and relay terminal transmission power constraint $P_1 = 2.5M_t$ W, and $P_l = 2.5N_l$ W for $l = 1, \cdots, 5$ with source-destination distance $d = 30$ m. The simulated and theoretical MSE and BER comparisons of the four algorithms are plotted in Fig. 4.3 and Fig. 4.4, respectively. Unlike in Fig. 4.1 and Fig. 4.2, it can be seen in Fig. 4.3 and Fig. 4.4 that there are MSE and BER performances improvements over the equal number of antennas relay system. It is also observed that the gap of the performance curve between BRS with approach 1 and approach 2 is higher.

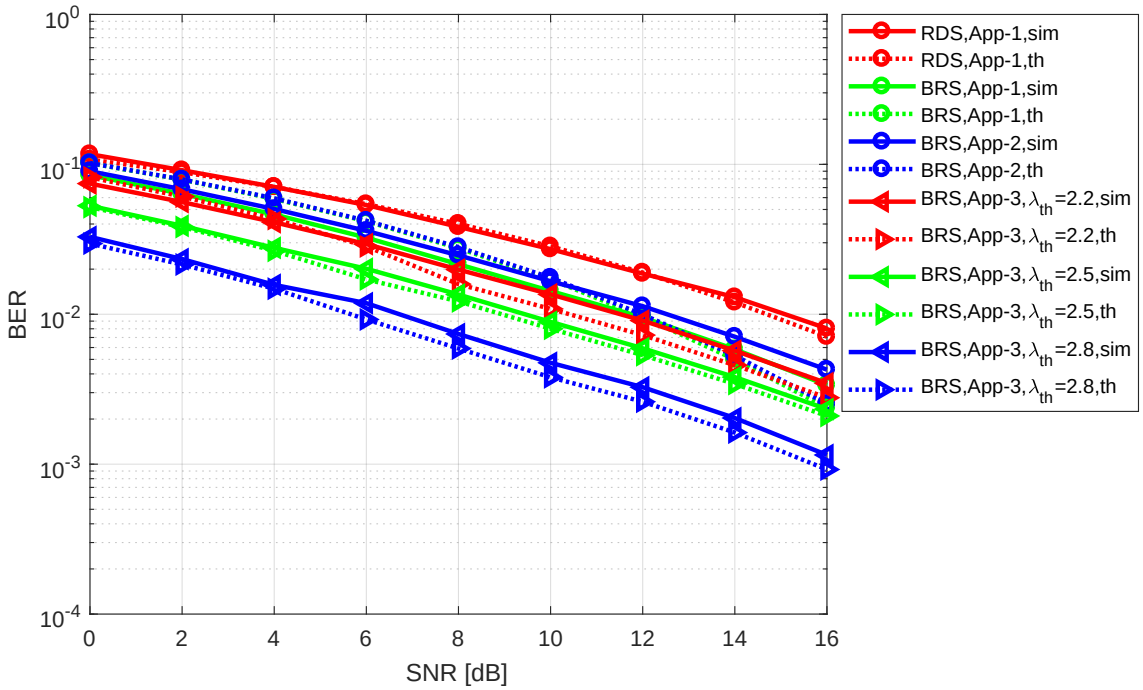

Figure 4.4 – BER versus SNR with unequal number of source-relay-destination antennas.

Table 4.1 – MSE, BER, and data rate comparison of approach 3 for equal number of antennas.

λ_{th}	MSE	BER	Data rate (Gb/s)
1.2	0.0035	0.0206	14
1.4	0.0026	0.0105	6.8
1.6	0.0015	0.0043	2.6

4.3 Error Performance and Data Rate

The data rate with the above two design cases for the system are plotted in Fig. 4.5 where the data rate is calculated by

$$\text{Data rate} = \frac{k \times N_b}{T_s} \text{ b/s} \tag{4.2}$$

where T_s is the symbol duration. It can be shown from the curve that the unequal number of antennas system provides less transmission rate than the first example. The reason is that the system in the second example has $N_b = 3$ which is less than $N_b = 4$ of the first example, i.e., the second example uses less sub-channels for transmission than the first example. The BRS with approach 1 and approach 2 have a constant transmission rate with the threshold value for both equal and unequal numbers of antennas. Similarly, like the first example, the BRS with approach 3 for threshold $\lambda_{th} = 2.2$, $\lambda_{th} = 2.5$, and $\lambda_{th} = 2.8$ shows both MSE and BER performance improvements. On the other hand, the BRS with approach 3 decreases the data rate with the increasing value of the threshold λ_{th}. In both examples, we notice that in approach 3, the increasing value of threshold λ_{th} increases the error performance but

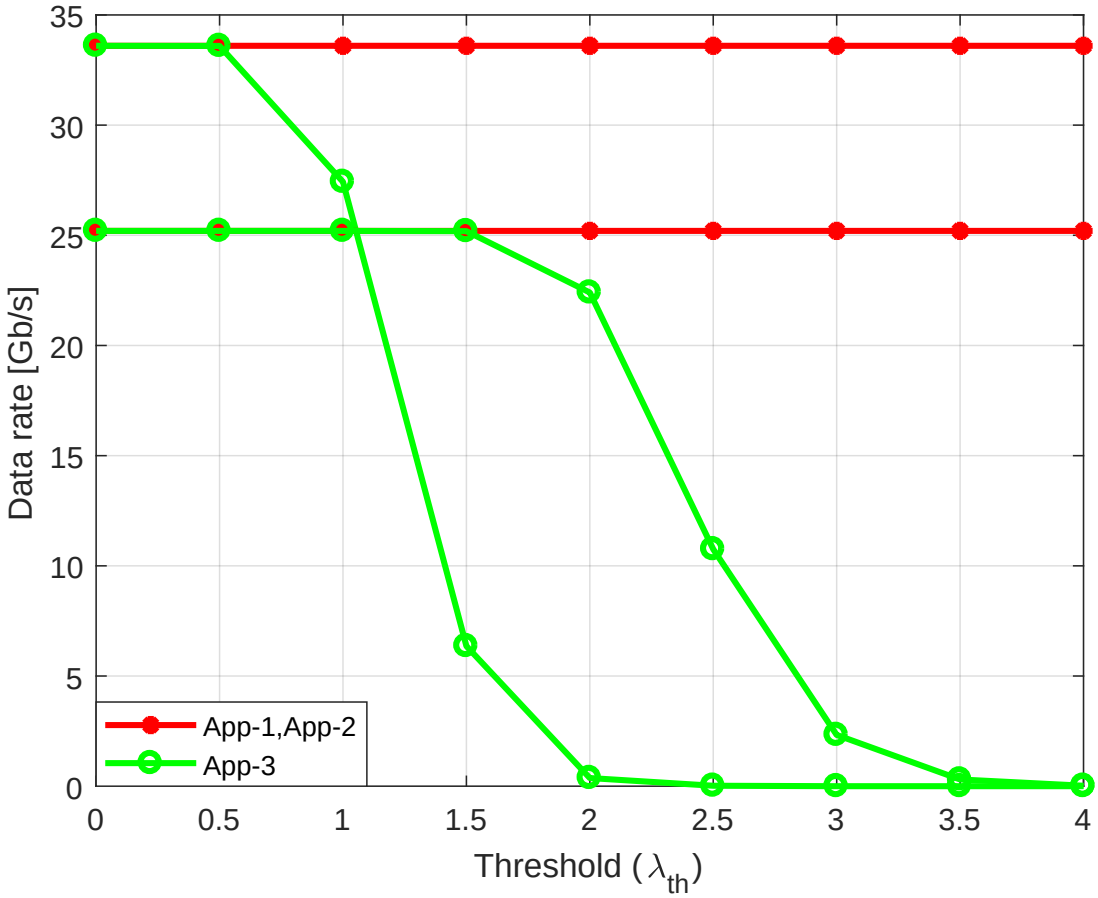

Figure 4.5 – Data rate for BRS with approach 1, approach 2, and approach 3 with equal number and unequal number of source-relay-destination antennas.

decreases the data rate. For example, in Fig. 4.5, a threshold value λ_{th} beyond 2 and 3.5 for equal number of antennas and unequal number of antennas provide zero data rate. We summarized the MSE and BER performances of approach 3 against the date rate for the first example at SNR = 8 dB in Table 4.1. From the table, we can see that increasing the value of threshold λ_{th} increases the MSE and BER performances but decreases the data rate and we find a similar result for the second example. So, there is a tradeoff between the error performance improvement and the transmission rate of the system.

4.4 Error Performance with Varying Number of Relays

Equation (3.17) states that the error performance decreases with the increasing number of relaying terminals. We verified this by evaluating the theoretical and simulated MSE and BER of the above system for different number of relay terminals with 4 antennas at the source, all relays and destination

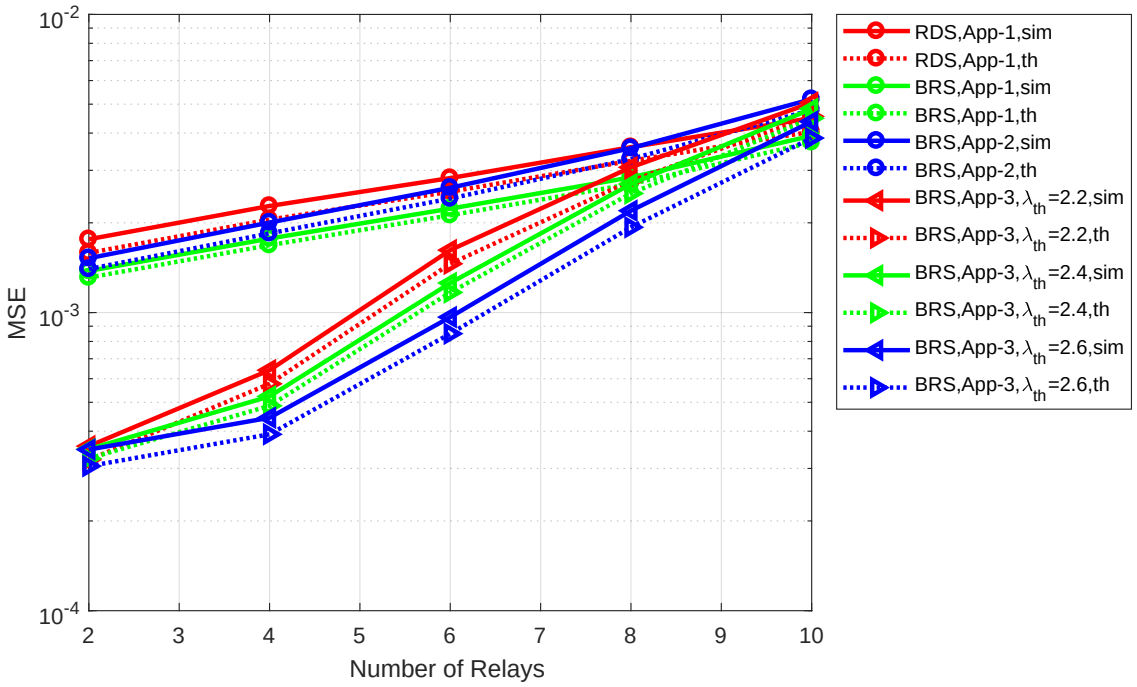

Figure 4.6 – MSE versus different number of relays at SNR = 15 dB.

Table 4.2 – Number of operations required to execute EVD of $\mathbf{R}_l$ for $M_t = M_r = N = 4$, and $L = 5$.

	Approach 1	Approach 2
Computational complexity	$L(10N^3+1) = 3205$	$L(3N^3) = 960$
Processing time (ms)	8.1	3.2

have the same total distance, and the results are plotted in Fig. 4.6 and Fig. 4.7, respectively. In this case, we used threshold values $\lambda_{th} = 2.2$, $\lambda_{th} = 2.4$, and $\lambda_{th} = 2.6$ for the BRS with approach 3. It can be noted that a higher number of relays (for example, number of relays beyond 9) provides both MSE and BER performances similar to approach 2. This is because, in this region, all sub-channels are strong and participate in the transmission. In all the simulation results, it is shown that approach 3 provides the best MSE and BER performances while approach 1 outperforms approach 2. From the last two simulations, it can be recommended that designers should try to use as small a number of relays as possible, which basically depends on the operational range of each sensor node.

4.5 Complexity Analysis

The EVD computation of the noise covariance matrix $\mathbf{R}_l$ in (3.26) in each relaying stage of approach 1 includes extra mathematical manipulations which increases the computational complexity in the water-filling solution. The number of computations and the processing time of water-filling calculations for approach 1 and approach 2 with equal number of antennas for 5 relays is summarized in

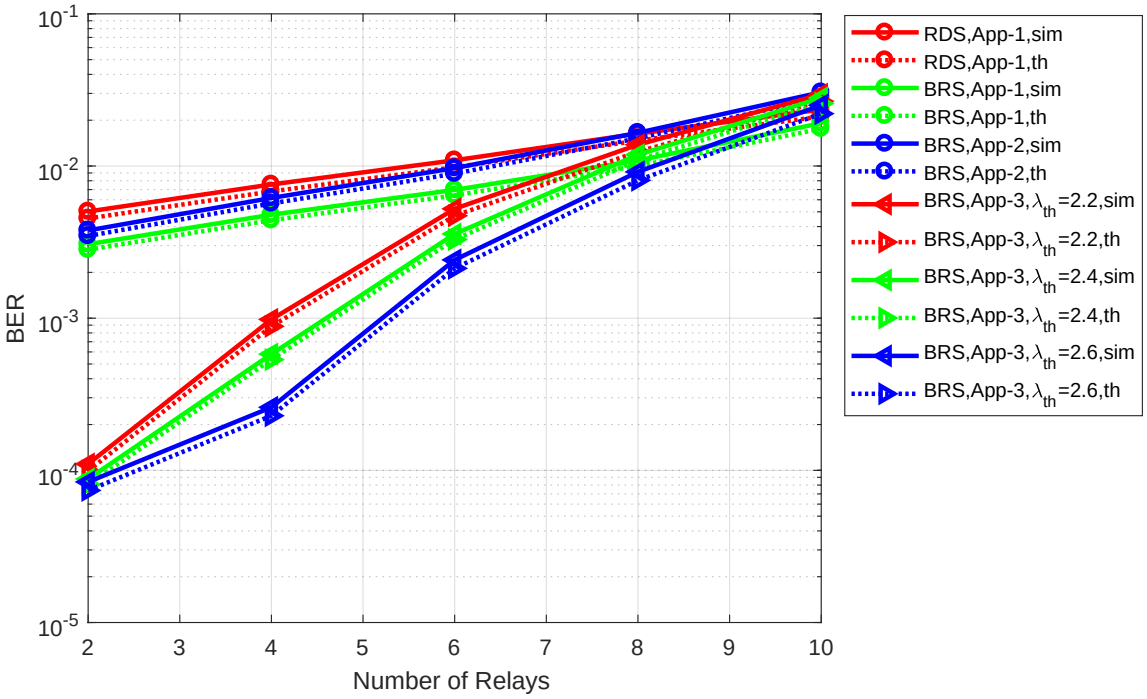

Figure 4.7 – BER versus different number of relays at SNR = 15 dB.

Table 4.2, and the processing time is evaluated on a processor running at 1.8 GHz. We can see that the extra cost function in approach 1 may decrease the transmission rate. Similarly, this approach includes extra computational cost for any number of antennas systems.

Chapter 5

Conclusion

In this chapter, we summarize the main contributions of the thesis and point out some possible future research areas. This thesis attempted to exploit the hidden complexity for the design of relay amplifier matrices for parallel multi-hop AF relay and then find the optimization formulation. The design contained two steps. In the first step, we simplified the parallel relay network into a series multi-hop networks as discussed in the BRS approach in Chapter 4, and in the second step, we considered the optimal power allocation under an equality power constraint of each relay terminal as discussed in approach 1, approach 2, and approach 3 in Chapter 4. A comparative analysis of the optimum power allocations for equal numbers of transmitter and receiver antennas MIMO systems has been presented using the known channel statistics at both transmitter and receiver. We used only the SVD decomposition for the optimum solution of the power allocation problem. In an actual case, a WSN contains hundreds or thousands of sensor nodes distributed randomly in a large area. From one time instant to the next, the number of active nodes and inactive nodes may vary. For this reason, we also carried out network simulations using a varying number of antennas at each relay terminal. In all simulations, we have considered each relay terminal having a transmission power of 10 W and a source-to-destination distance of 30 m. This algorithm will be a very efficient technique to deploy WSNs in highly fading environments like underground mines. Here, the solution is provided with AF relaying and it is the simplified technique now being used in the majority of works in the literature.

In a virtual antenna array, a set of cooperative relays forwards the received information toward the next relay or the destination using the selection distributed algorithm. The algorithm selects the most probable path having the highest SNR to forward the information toward the destination. The traditional relay selection is based on instantaneous channel gains. For wireless communication with a small number of hops, the algorithm can be easily applied, but for a large number of hops, it is really difficult to select the best channel gain path. In this work, we have established a recursive search algorithm to find the best path from source-to-destination. Simulation results show that this path provides the highest MSE and BER performances in comparison to the traditional best path selection method. By exploiting the best path between the source and destination, we have proposed the design of source and relay amplifying matrices for a parallel multi-hop AF MIMO relay system with known CSI at all

nodes. The proposed algorithm provides the optimum solution for finding the equivalent path, and we prove the theoretical analysis by simulations. Although we model two parallel relays, this analysis can be extended to any number of parallel layers. One of the interesting results from the simulation analysis is that the optimum best path searching method (BRS) in multihop parallel relaying provides excellent performance over conventional selection relaying (RDS). We can use BRS in a proactive mode to save power of all inactive relay that will increase the overall network lifetime.

The power allocation problem for cooperative systems is carried out depending on the objective function at individual node power constraint or total power constraint or with both individual and total power constraints. The objective function drive the way of optimum power allocation assuming individual or total power constraints. In this work, we considered the MSE minimization at the destination subject to only the total power constraint for known CSI. We considered that the MSE at the destination is the sum of individual node MSEs. The optimization considered that the Fusion Center (FC) has the knowledge of forward and backward CSI information. The FC controls the power allocation of each relay node using a feedback channel. The algorithm of power optimization can also be done using an individual node power constraint only for analytical simplicity. We designed the source precoder and relay amplifier matrices using three techniques. In approach 1, the actual noise covariance matrix $\mathbf{R}_l$ has been used to provide the optimal solution. A sub-optimal power allocation has been implemented based on the assumption that the noise covariance matrix $\mathbf{R}_l$ approaches an identity matrix for design simplicity. We compared the computational complexity and required execution time of the two algorithms. It can be concluded that approach 1 gives the best solution but requires more mathematical computations. In approach 3, we sent a signal only through the strong sub-channels. As a result, both MSE and BER performances are increased but the data rate decreases. Finally, we recommended to choose the power allocation solution depending on the channel condition where the relay will be deployed.

We have carried out the analysis for perfect CSI knowledge at all possible links. For a large scale complex network, it is really difficult to send the exact CSI to the FC. On the other hand, the environment introduces time-varying fading characteristics. Under these conditions, we need to model all possible links with imperfect CSI. For the imperfect CSI case, the optimal path finding can be done with a statistical average. The power allocation algorithm for the precoder can be implemented using a robust transceiver designing scheme. So, a difficulty arises for the design in the case of imperfect CSI knowledge at all terminals. In the future, the design can be carried out in the case of imperfect CSI at all terminals.

Appendix A

Convex optimization

Convex optimization methods are ubiquitous and have been widely used in the design and analysis of many problems in communication and signal processing applications. Here, we provide convex mathematical tools useful to analyze some challenging resource allocation problems of WSNs in multi-hop communication networks.

In mathematics, optimization is the selection of a best element from a set of available alternatives. An optimization problem with arbitrary equality and inequality constraints is given by [41]

$$\min_{\mathbf{x}} f_0(\mathbf{x}) \tag{A.1}$$

$$\text{subject to: } f_i(\mathbf{x}) \leq 0,\ i \in [1:m]$$

$$A\mathbf{x} = \mathbf{b}$$

where $\mathbf{x} \in \mathcal{R}^n$ are convex if the functions f_i are convex, f_0 is the cost or objective function, and $f_1, \cdots, f_m$ are m inequality constraint functions. The set of the following points in the problem can be denoted by

$$\mathcal{D} = \{\mathbf{x} : f_i(\mathbf{x}) \leq 0, i \in [1:m], A\mathbf{x} = \mathbf{b}\}$$

and is feasible if $\mathcal{D} \neq \emptyset$, where $\emptyset$ represents an empty set, and infeasible otherwise [41]. The optimal value or minimal value of the problem is denoted by $p^* = \inf\{f_0(\mathbf{x}) : \mathbf{x} \in \mathcal{D}\}$, and is achieved at an optimal solution $\mathbf{x}^*$, i.e., $p^* = f_0(\mathbf{x}^*)$. The main way to reformulate a problem in convex form is to devise a convex problem equivalent to the original nonconvex one by changing a series of variables [89]. Taking the Lagrangian of (A.1), we have

$$L(\mathbf{x}, \lambda, \nu) = f_0(\mathbf{x}) + \sum_{i=1}^{m} \lambda_i f_i(\mathbf{x}) + \nu^T (A\mathbf{x} - \mathbf{b})$$

The optimization variable $\mathbf{x}$ is called the primal variable and Lagrange multipliers λ and ν are called the dual variables. The dual objective $\phi(\lambda, \nu)$ is defined as the minimum value of the Lagrangian over $\mathbf{x}$ which leads to the dual problem

$$\phi(\lambda, \nu) = \min_{\mathbf{x}} L(\mathbf{x}, \lambda, \nu)$$

The solution of the primal optimal point $\mathbf{x}^*$ and the dual optimal point (λ^*, ν^*) are linked together through the following Karush-Kuhn-Tucker (KKT) condition

$$\nabla_{\mathbf{x}} f_0(\mathbf{x}^*) + \sum_{i=1}^{m} \lambda_i^* \nabla_{\mathbf{x}} f_i(\mathbf{x}^*) + (\nu^*)^T \nabla_{\mathbf{x}} (A\mathbf{x}^* - \mathbf{b}) = 0 \tag{A.2}$$

The KKT condition in (A.2) is sufficient for the solution of both primal and dual problems.

Appendix B

Proof of (3.17)

We will carry out the work for multi-hop MIMO relaying by invoking the following useful matrix inversion lemma [96]. For matrices $\mathbf{A}$, $\mathbf{B}$, $\mathbf{C}$, and $\mathbf{D}$ with appropriate dimensions, the following identity holds.

Lemma 1: $(\mathbf{I}+\mathbf{AB})^{-1} = \mathbf{I}-\mathbf{A}(\mathbf{I}+\mathbf{BA})^{-1}\mathbf{B}$

Lemma 2: $(\mathbf{A}+\mathbf{BCD})^{-1} = \mathbf{A}^{-1}-\mathbf{A}^{-1}\mathbf{B}(\mathbf{DA}^{-1}\mathbf{B}+\mathbf{C}^{-1})^{-1}\mathbf{DA}^{-1}$

Lemma 3: $(\mathbf{I}+\mathbf{A}^H\mathbf{BA})^{-1} = \mathbf{I}-\mathbf{A}^H(\mathbf{AA}^H+\mathbf{B}^{-1})^{-1}\mathbf{A}$, using lemma 2

Lemma 4: $(\mathbf{A}^{-1}+\mathbf{B})^{-1} = \mathbf{A}-\mathbf{A}(\mathbf{A}+\mathbf{B}^{-1})^{-1}\mathbf{A}$, using lemma 2

The MSE matrix in (3.13) can be organized using lemma 3

$$\mathbf{E}_d = \mathbf{I}_{N_b} - \mathbf{A}_{L+1}^H(\mathbf{A}_{L+1}\mathbf{A}_{L+1}^H+\mathbf{C}_{L+1})^{-1}\mathbf{A}_{L+1} \tag{B.1}$$

Using (3.11) and (3.15), the second term of (B.1) can be written as

$$\begin{aligned}
\mathbf{A}_{L+1}\mathbf{A}_{L+1}^H+\mathbf{C}_{L+1} &= \bigotimes_{i=L+1}^{1}(\mathbf{H}_i\mathbf{F}_i)\bigotimes_{i=1}^{L+1}(\mathbf{F}_i^H\mathbf{H}_i^H)+\sum_{j=2}^{L+1}\left(\bigotimes_{i=L+1}^{j}(\mathbf{H}_i\mathbf{F}_i)\bigotimes_{i=j}^{L+1}(\mathbf{F}_i^H\mathbf{H}_i^H)\right)+\mathbf{I}_{M_r}\\
&= \sum_{j=1}^{L+1}\left(\bigotimes_{i=L+1}^{j}(\mathbf{H}_i\mathbf{F}_i)\bigotimes_{i=j}^{L+1}(\mathbf{F}_i^H\mathbf{H}_i^H)\right)+\mathbf{I}_{M_r}\\
&= \mathbf{H}_{L+1}\mathbf{F}_{L+1}(\mathbf{A}_L\mathbf{A}_L^H+\mathbf{C}_L)\mathbf{F}_{L+1}^H\mathbf{H}_{L+1}^H+\mathbf{I}_{M_r}\\
&= \mathbf{H}_{L+1}\mathbf{F}_{L+1}\mathbf{D}_L\mathbf{F}_{L+1}^H\mathbf{H}_{L+1}^H+\mathbf{I}_{M_r}
\end{aligned}$$

where $\mathbf{D}_L = (\mathbf{A}_L\mathbf{A}_L^H+\mathbf{C}_L)$. We assume $\mathbf{F}_l = \mathbf{B}_l\mathbf{W}_l = \mathbf{B}_l(\mathbf{A}_{l-1}^H\mathbf{A}_{l-1}+\mathbf{C}_{l-1})^{-1}\mathbf{A}_{l-1} = \mathbf{B}_l\mathbf{D}_{l-1}^{-1}\mathbf{A}_{l-1}, l = 2,\cdots,L+1$, and putting it in the second term of (B.1) with $\mathbf{A}_{L+1} = \mathbf{A}_L\mathbf{H}_{L+1}\mathbf{F}_{L+1}$

$$\mathbf{E}_d = \mathbf{I}_{N_b} - \mathbf{A}_L^H\mathbf{B}_{L+1}^H\mathbf{D}_L^{-1}\mathbf{A}_L^H\mathbf{H}_{L+1}^H(\mathbf{H}_{L+1}\mathbf{B}_{L+1}\mathbf{A}_L\mathbf{D}_L^{-1}\mathbf{B}_{L+1}^H\mathbf{H}_{L+1}^H\mathbf{A}_L^H+\mathbf{I}_{N_b})^{-1}\mathbf{H}_{L+1}\mathbf{B}_{L+1}\mathbf{D}_L^{-1}\mathbf{A}_L\mathbf{A}_L \tag{B.2}$$

Using lemma $\mathbf{A}^H(\mathbf{ABA}^H+\mathbf{I})\mathbf{A}=\mathbf{B}^{-1}-(\mathbf{BA}^H\mathbf{AB}+\mathbf{B})^{-1}$ [18] in (B.2)

$$\begin{aligned}
\mathbf{E}_d &= \mathbf{I}_{N_b}-\mathbf{A}_L^H\mathbf{D}_L^{-1}\mathbf{A}_L+\mathbf{A}_L^H\mathbf{D}_L^{-1}\left(\mathbf{D}_L^{-1}\mathbf{B}_{L+1}^H\mathbf{H}_{L+1}^H\mathbf{A}_L^H\mathbf{H}_{L+1}\mathbf{B}_{L+1}\mathbf{A}_L\mathbf{D}_L^{-1}+\mathbf{D}_L^{-1}\right)^{-1}\mathbf{D}_L^{-1}\mathbf{A}_L \\
&= \mathbf{I}_{N_b}-\mathbf{A}_L^H(\mathbf{A}_L^H\mathbf{A}_L+\mathbf{C}_L)^{-1}\mathbf{A}_L+\mathbf{A}_L^H\left(\mathbf{B}_{L+1}^H\mathbf{H}_{L+1}^H\mathbf{A}_L^H\mathbf{D}_L^{-1}\mathbf{H}_{L+1}\mathbf{B}_{L+1}\mathbf{A}_L+\mathbf{I}_{N_b}\right)^{-1}\mathbf{D}_L^{-1}\mathbf{A}_L \\
&= (\mathbf{I}_{N_b}+\mathbf{A}_L^H\mathbf{C}_L^{-1}\mathbf{A}_L)^{-1}+\mathbf{A}_L^H\mathbf{D}_L^{-1}\mathbf{A}_L\left(\mathbf{A}_L^H\mathbf{D}_L^{-1}\mathbf{A}_L\mathbf{B}_{L+1}^H\mathbf{H}_{L+1}^H\mathbf{H}_{L+1}\mathbf{B}_{L+1}+\mathbf{I}_{N_b}\right)^{-1}, \text{using lemma 3} \\
&= (\mathbf{I}_{N_b}+\mathbf{A}_L^H\mathbf{C}_L^{-1}\mathbf{A}_L)^{-1}+\mathbf{A}_L^H\mathbf{D}_L^{-1}\mathbf{A}_L-\mathbf{A}_L^H\mathbf{D}_L^{-1}\mathbf{A}_L(\mathbf{H}_{L+1}\mathbf{B}_{L+1}\mathbf{B}_{L+1}^H\mathbf{H}_{L+1}^H) \\
&\quad \left(\mathbf{A}_L^H\mathbf{D}_L^{-1}\mathbf{A}_L(\mathbf{H}_{L+1}\mathbf{B}_{L+1}\mathbf{B}_{L+1}^H\mathbf{H}_{L+1}^H)+\mathbf{I}_{N_b}\right)^{-1}\mathbf{A}_L^H\mathbf{D}_L^{-1}\mathbf{A}_L, \text{using lemma 1} \\
&= (\mathbf{I}_{N_b}+\mathbf{A}_L^H\mathbf{C}_L^{-1}\mathbf{A}_L)^{-1}+[(\mathbf{A}_L^H\mathbf{D}_L^{-1}\mathbf{A}_L)^{-1}+\mathbf{H}_{L+1}\mathbf{B}_{L+1}\mathbf{B}_{L+1}^H\mathbf{H}_{L+1}^H]^{-1}, \text{using lemma 4}
\end{aligned} \tag{B.3}$$

It is worth noting that $\mathbf{R}_L=\mathbf{A}_L^H\mathbf{D}_L^{-1}\mathbf{A}_L$ stands for the covariance matrix of the $(L+1)$-th relay signal, and in the high SNR region, it rapidly approaches the identity matrix $\mathbf{I}_{N_b}$ [90]. Now, from (B.3), we have

$$\begin{aligned}
\mathbf{E}_d &= (\mathbf{I}_{N_b}+\mathbf{A}_L^H\mathbf{C}_L^{-1}\mathbf{A}_L)^{-1}+\left[\mathbf{H}_{L+1}\mathbf{B}_{L+1}\mathbf{B}_{L+1}^H\mathbf{H}_{L+1}^H+\mathbf{R}_L^{-1}\right]^{-1} \\
&= \mathbf{E}_L+[\mathbf{R}_L^{-1}+\mathbf{H}_{L+1}\mathbf{B}_{L+1}\mathbf{B}_{L+1}^H\mathbf{H}_{L+1}^H]^{-1}
\end{aligned} \tag{B.4}$$

From (B.4), we can express $\mathbf{E}_L$

$$\mathbf{E}_L=\mathbf{E}_{L-1}+[\mathbf{R}_{L-1}^{-1}+\mathbf{H}_L\mathbf{B}_L\mathbf{B}_L^H\mathbf{H}_L^H]^{-1} \tag{B.5}$$

Again, $\mathbf{E}_1=(\mathbf{I}_{N_b}+\mathbf{A}_1^H\mathbf{C}_1^{-1}\mathbf{A}_1)^{-1}=(\mathbf{I}_{N_b}+\mathbf{H}_1\mathbf{B}_1\mathbf{B}_1^H\mathbf{H}_1^H)^{-1}$. We have, finally

$$\mathbf{E}_d=\mathbf{E}_1+\sum_{l=2}^{L+1}\mathbf{E}_l=(\mathbf{I}_{N_b}+\mathbf{H}_1\mathbf{B}_1\mathbf{B}_1^H\mathbf{H}_1^H)^{-1}+\sum_{l=2}^{L+1}(\mathbf{R}_{l-1}^{-1}+\mathbf{H}_l\mathbf{B}_l\mathbf{B}_l^H\mathbf{H}_l^H)^{-1} \tag{B.6}$$

Appendix C

Proof of (3.27)

Taking the Lagrangian function of (3.27)

$$\mathcal{L}(\mu_l, \{\sigma_{l,i}\}_{i=1}^{N_b}) = \sum_{i=1}^{N_b} \frac{1}{\xi_{l,i}^{-2} + \lambda_{l,i}^2 \sigma_{l,i}^2} + \mu_l \left(\sum_{i=1}^{N_b} \sigma_{l,i}^2 - P \right) \tag{C.1}$$

Taking the Karush-Kuhn-Tucker (KKT) condition of (C.1) with respect to $\sigma_{l,i}$ gives

$$|\sigma_{l,i}^2| = \frac{1}{\xi_{l,i}^2 \lambda_{l,i}^2} \left[\left(\frac{\xi_{l,i}^4 \lambda_{l,i}^2}{\mu_l} \right)^{1/2} - 1 \right] = \frac{1}{\lambda_{l,i}^2} \left(\sqrt{\frac{\lambda_{l,i}^2}{\mu_l}} - \frac{1}{\xi_{l,i}^2} \right)^+ \tag{C.2}$$

Bibliography

[1] J. Cecilio and P. Furtado, *Wireless Sensors in Heterogeneous Network Systems*. Computer Communications and Networks, Springer International Publishing, 2014.

[2] P. Misra, S. Kanhere, and S. Jha, "Safety Assurance and Rescue Communication System in High-stress Environments: A Ming Case Study," *IEEE Communication Magazine*, vol. 48, no. 4, pp. 66–73, April 2010.

[3] K. Sohrabi, J. Gao, V. Ailawadhi, and G. J. Pottie, "Protocols for Self-Organization of a Wireless Sensor Network," *IEEE Personal Communications*, vol. 7, no. 5, pp. 16–27, Oct. 2000.

[4] P. K. Biswas and S. Phoha, "Self-organizing sensor networks for integrated target surveillance," *IEEE Trans. On Parallel and Distributed Systems*, vol. 55, no. 8, pp. 1033–1047, Aug. 2006.

[5] M. El Khaled, P. Fortier, and M. L. Ammari, "A Performance Study of Line-of-Sight Millimeter Wave Underground Mine Channel," *IEEE Antennas and Wireless Prop. Lett.*, vol. 13, pp. 1148–1158, June 2014.

[6] W. Farjow, K. Raahemifar, and X. Fernando, "Novel Wireless Channels characterization model for underground mines," *Applied Mathematical Modeling, ELSEVIER*, vol. 39, no. 19, pp. 5997–6007, Oct. 2015.

[7] I. F. Akyildiz, "Wireless Sensor Networks in Challenged Environments such as Underwater and Underground," *14 Proc. of the 17th ACM int. conf. on Modeling, Analysis and Simulation of Wireless and Mobile Systems*, 2014.

[8] J. C. F. Li, S. Dey, and J. Evans, "Maximal Lifetime Power and Rate Allocation for Wireless Sensor Systems With Data Distortion Constraints," *IEEE Trans. On Signal Processing*, vol. 56, no. 5, pp. 2076–2090, May 2008.

[9] K. Asaduzzaman and Y. Hyung, "Energy efficient cooperative LEACH protocol for wireless sensor networks," *Journal of Commun., and Networks*, vol. 12, no. 4, pp. 358–365, Aug. 2010.

[10] Z. Wang, V. Aggarwal, and X. Wang, "Iterative Dynamic Water-Filling for Fading Multiple-Access Channels With Energy Harvesting," *IEEE Journal on Selected Areas on Comm.*, vol. 33, no. 3, pp. 382–395, March 2015.

[11] T. Wang, A. Cano, G. B. Giannakis, and J. N. Laneman, "High-Performance Cooperative Demodulation With Decode-and-Forward Relays," *IEEE Trans. on Communications*, vol. 55, no. 7, pp. 1427–1438, July 2007.

[12] I. F. Akyildiz, Weilian Su, Y. Sankarasubramaniam, and E. Cayirci, "A survey on sensor networks," *IEEE Communications Magazine*, vol. 40, no. 8, pp. 102–114, Aug 2002.

[13] M. O. Hasna and M. S. Alouini, "Optimal power allocation for relayed transmissions over Rayleigh-fading channels," *IEEE Trans. On Wireless Commun.*, vol. 3, no. 6, pp. 1999–2004, Nov 2004.

[14] T. Wang, R. C. de Lamare, and A. Schmeink, "Alternating Optimization Algorithms for Power Adjustment and Receive Filter Design in Multihop Wireless Sensor Networks," *IEEE Trans. On Vehicular Technology*, vol. 64, no. 1, pp. 173–184, Jan. 2015.

[15] S. J. Boyer, D. D. Falconer, and H. Yanikomeroglu, "Multihop Diversity in Wireless Relaying Channels," *IEEE Trans. Commun.*, vol. 52, no. 10, pp. 1820–1830, Oct. 2004.

[16] U. Niesen, D. Shaah, and G. W. Wornell, "Adaptive alternating minimization algorithms," *IEEE Trans. On Information Theory*, vol. 55, no. 3, pp. 1423–1429, Mar. 2009.

[17] M. H. Chaudhary and L. Vandendorpe, "Adaptive Power Allocation in Wireless Sensor Networks with Spatially Correlated Data and Analog Modulation: Perfect and Imperfect CSI," *EURASIP Jouranl on Wireless Communication and Networking*, vol. 2010, no. 2010, Springer 2010.

[18] Y. Rong, "Simplified Algorithms for Optimizing Multiuser Multi-Hop MIMO Relay Systems," *IEEE Trans. Commun.*, vol. 59, no. 10, pp. 2896–2904, Oct. 2011.

[19] H. B. Kong, H. M. Shin, and T. Oh and I. Lee, "Joint MMSE Transceiver Designs for MIMO AF Relaying Systems with Direct Link," *IEEE Trans. On Wireless Commu.*, vol. 16, no. 6, pp. 3547–3560, Nov. 2017.

[20] J. Y. Ryu and W. Choi, "Balanced Linear Precoding in Decode-and-Forward Based MIMO Relay Communications," *IEEE Trans. On Wireless Commu.*, vol. 10, no. 7, pp. 2390–2400, July 2011.

[21] Z. He, X. Zhang, Y. Bi, W. Jiang, and Y. Rong, "Optimal Source and Relay Design for Multiuser MIMO AF Relay Communication Systems With Direct Links and Imperfect Channel Information," *IEEE Trans. On Wireless Commu.*, vol. 15, no. 3, pp. 2025–2038, Mar. 2016.

[22] Z. He, W. Jiang, and Y. Rong, "Robust Design for Amplify-and-Forward MIMO Relay Systems With Direct Link and Imperfect Channel Information," *IEEE Trans. On Wireless Commu.*, vol. 14, no. 1, pp. 353–363, Jan. 2015.

[23] B. Schein and R. Gallager, "The Gaussian parallel relay network," *IEEE International Symposium on Information Theory*, 25–30 June 2000.

[24] S. O. Gharan, A. Bayesteh, and A. K. Khandani, "Asymptotic Analysis of Amplify and Forward Relaying in a Parallel MIMO Relay Network," *IEEE Trans. On Information Theory*, vol. 57, no. 4, pp. 2070–2082, April 2011.

[25] ——, "Diversity-Multiplexing Tradeoff in Multiantenna Multirelay Networks: Improvements and Some Optimality Results," *IEEE Trans. On Information Theory*, vol. 59, no. 6, pp. 3892–3914, June 2013.

[26] S. Lin, W. W. L. Ho, Y. c. Liang, "Block diagonal geometric mean decomposition (BD-GMD) for MIMO broadcast channels," *IEEE Trans. on Communications*, vol. 7, no. 7, pp. 2778–2789, July 2008.

[27] S. S. Ikki, M. H. Ahmed, "Performance analysis of adaptive decode-and-forward cooperative diversity networks with best-relay selection," *IEEE Trans. on Communications*, vol. 58, no. 1, pp. 68–72, Jan. 2010.

[28] D. P. Palomar, M. A. Lagunas, J. M. Cioffi, "Optimum linear joint transmit-receive processing for MIMO channels with QoS constraints," *IEEE Trans. On Signal Processing*, vol. 52, no. 5, pp. 1179–1197, May 2004.

[29] A. B. Gershman and N. D. Sidiropoulos, *Space-Time processing for MIMO communications*. John Wiley and Sons, 2005.

[30] Y. S. Cho, J. Kim, W. Y. Yang, and C. G. Kang, *MIMO-OFDM Wireless Communications With Matlab*. John Wiley and Sons, Singapore, 2010.

[31] S. Alamouti, "A simple transmit diversity technique for wireless communications," *IEEE J. Select. Areas Commun.*, vol. 16, pp. 1451—-1458, Oct. 1998.

[32] J. N. Laneman, G. W. Wornell, and D. N. C. Tse, "An efficient protocol for realizing cooperative diversity in wireless networks," *Proceedings of 2001 IEEE International Symposium on Information Theory*, June 2001.

[33] J. N. Laneman and G. W. Wornell, "Distributed space-time-coded protocols for exploiting cooperative diversity in wireless networks," *IEEE Trans. On Information Theory*, vol. 49, no. 10, pp. 2415–2425, Oct. 2003.

[34] M. Naeem, M. Patwary, and M. Abdel-Maguid, "Universal and Dynamic Clustering Scheme for Energy Constrained Cooperative Wireless Sensor Networks," *IEEE Access*, no. 99, pp. 1–1, 2017.

[35] J. N. Laneman, D. N. C. Tse, and G. W. Wornell, "Cooperative diversity in wireless networks: Efficient protocols and outage behavior," *IEEE Trans. On Information Theory*, vol. 50, no. 12, pp. 3062–3080, Dec. 2004.

[36] I. F. Akyildiz, and E. P. Stuntebeck, "Wireless underground sensor networks: Research challenges," *Ad Hoc Networks, ELSEVIER*, vol. 4(2006), pp. 669–686, 2006.

[37] W. Farjow, K. Raahemifar, and X. Fernando, "Novel Wireless Channels characterization model for underground mines," *Applied Mathematical Modeling*, vol. 39, no. 19, pp. 5997–6007, Oct. 2015.

[38] J. R. A. Solares, L. Sboui, Z. Rezki, and M.-S. Alouini, "Power Minimization of a Wireless Sensor Node under Different Rate Constraints," *IEEE Trans. Signal Process.*, vol. 64, no. 13, pp. 3458–3469, July 2016.

[39] I. F. Akyildiz, Z. Sunm and M. C. Vuran, "Signal Propagation techniques for Wireless Underground Communication Networks," *Physical Communication*, vol. 2(2009), pp. 167–183, 2009.

[40] Z. Yi, and II-Min Kim, "Relay Ordering in a Multi-Hop Cooperative Diversity Network," *IEEE Trans. on Communications*, vol. 57, no. 9, pp. 2590–2596, Sep 2009.

[41] A. EI Gamal and Y.-H. Kim, *Network Information Theory*. Cambridge University Press, 2011.

[42] John M. Cioffi, "Chapter 4," *Notes for Course EE479 taught at Stanford University during Fall 2005*.

[43] Q. Qi, A. Minturn, and Y. Yang, "An Efficient Water-filling Algorithm in OFDM-based Cognitive Radio," *Int. Conf. On Systems and Informatics*, pp. 2069–2073, 2012.

[44] M. S. Stankovic, K. H. Johansson, and D. M. Stipanovic, "Distributed Seeking of Nash Equilibria With Applications to Mobile Sensor Networks," *IEEE Trans. On Automatic Control*, vol. 57, no. 4, pp. 904–919, April 2012.

[45] D. N. Nguyen, and M. Krunz, "A Cooperative MIMO Framework for Wireless Sensor Networks," *ACM Trans. On Sensor Networks*, vol. 10, no. 3, pp. 43.1–43.28, 2014.

[46] S. Cui, A. J. Goldsmith, and A. Bahai, "Energy-Efficiency of MIMO and Cooperative MIMO Techniques in Sensor Networks," *IEEE Journal on Selec. Areas in Comm.*, vol. 22, no. 6, pp. 1089–1098, 2004.

[47] T. Cover and J. Thomas, *Elements of Information Theory*. Wiley, New York, NY, USA, 2006.

[48] J. Campello de Souza, *Discrete Bit Loading for Multicarrier Modulation Systems*. PhD. Dissertation, Stanford University, 1999.

[49] M. R. Akhondi, A. Talevski, S. Carlsen, and S. Petersen, "Applications of Wireless Sensor Networks in the Oil, Gas and Resources Industries," *24th IEEE int conf. On Advanced Information Networking and Applications*, 20–23 April 2010.

[50] Y. Yang, S. Zhang, and P. Q. Wang, "Long distance wireless sensor networks applied in coal mine," *Procedia Earth Planet.Sci.*, vol. 2011, no. 1, pp. 1461–1467, 2011.

[51] L. R.-Garcia, P. Barreiro, and J. I. Robla, "Performance of ZigBee-Based Wireless Sensor Nodes for Real-time Monitoring of Fruit Logistics," *J. Food Eng.*, vol. 2011, no. 87, pp. 405–415, 2011.

[52] F. Tian and X. Xu, "Design of Wireless Sensor Networks Node in Coalmine," *2009 second int. conf. on Intelligent Computation Tech. and Auto.*, vol. 4, pp. 1–5, 10-11 Oct. 2009.

[53] A. Qandour, D. Habibi, and I. Ahmad, "Applied Application of Sensor Networks in Underground Mines," *9th IEEE int. cont. On Networking, Sensing and Control 2012(ICNSC-2012)*, pp. 11–14, 11–14 April 2012.

[54] Y. Zhang, W. Yang, D. Han, and Y.-II. Kim, "An Integrated Environment Monitoring System for Underground Coal Mines-Wireless Sensor Network Subsystem with Multi-Parameter Monitoring," *Sensors*, vol. 2014, no. 14, pp. 13 149–13 170, 2014.

[55] X. Zhang, H. V. Poor, and M. Chiang, "Optimal Power Allocation for Distributed Detection over MIMO channels in Wireless Sensor Networks," *IEEE Trans. On Signal Processing*, vol. 56, no. 9, pp. 4124–4140, 2008.

[56] D. Liu, K. Zhang, and J. Ding, "Energy-efficient transmission scheme for mobile data gathering in wireless sensor networks," *IEEE commu.,*, vol. 10, no. 3, pp. 114–123, DOI: 10.1109/CC.2013.6488839 2013.

[57] J. Ding, D. Liu, X. Wang, and H. Wu, "An Energy-Efficient Virtual MIMO Transmission Scheme for Cluster-based Wireless Sensor Networks," *Proceedings of 12th IEEE International Conference on Communication Technology (ICCT)*, vol. 3, pp. 809–813, DOI: 10.1109/ICCT.2010.5688684 2010.

[58] A. Chaibrassou and A. Mouhsen, "A Multi-Channel Cooperative MIMO Routing Protocol for Clustered WSNs," *Proceedings of 2nd int conf., on electrical and information tech., (ICEIT)*, pp. 231–236, DOI: 10.1109/EITech.2016.7519595 2016.

[59] J.-S. Kim, S.-H. Moon, S.-R. Lee, and I. Lee, "A New Channel Quantization Strategy for MIMO Interference Alignment with Limited Feedback," *IEEE Trans. On Wireless Commu.*, vol. 11, no. 1, pp. 358–366, Jan. 2012.

[60] M Z. Shakir and T. S. Durrani, "MIMO Identical Eigenmode Transmission System (IETS)-A channel decomposition Perspective," *15th European Signal Processing Conference (EUSIPCO 2007)*, Sept. 3-7 2007.

[61] J. N. Laneman, D. N. C. Tse, and G. W. Wornell, "Cooperative Diversity in Wireless Networks: Efficient Protocols and Outage Behavior," *IEEE Trans. On Information Theory*, vol. 50, no. 12, pp. 3062–3080, Dec. 2004.

[62] M. H. Chaudhary and L. Vandendorpe, "Adaptive Power Allocation in Wireless Sensor Networks with Spatially Correlated Data and Analog Modulation: Perfect and Imperfect CSI," *EURASIP Jouranl on Wireless Communication and Networking, Springer*, doi:10.1155/2010/817961 2010.

[63] D. Guo, S. Shamai, and S. Verdu, "Mutual Information and Minimum Mean-Square Error in Gaussian Channels," *IEEE Trans. On Information Theory*, vol. 51, no. 4, pp. 1261–1282, April 2005.

[64] K. Venkat and T. Weissman, "Pointwise Relations between Information and Estimation in Gaussian Noise," *IEEE Trans. On Information Theory*, vol. 58, no. 10, pp. 6264–6281, Oct. 2012.

[65] D. Zhang, G. Wei, J. Zhu, and Z. Tian, "On the Bounds of Feedback Rates for Pilot-Assisted MIMO Systems," *IEEE Trans. On Vehicular Technology*, vol. 56, no. 4, pp. 1727–1736, July 2007.

[66] Yi Jiang, Jian Li, and W. W. Hager, "Uniform channel decomposition for MIMO communications," *IEEE Transactions on Signal Processing*, vol. 53, no. 11, pp. 4283–4294, Nov. 2005.

[67] Kevin L. Mills, "A brief Survey of Self-organization in wireless sensor networks," *Wirel. Comun. Mob.Comput., Wiley InterScience*, vol. 7, no. 7, pp. 823–834, 2007.

[68] R. H. Gohary and H. Yanikomeroglu, "Convergence of Iterative Water-filling with Quantized Feedback: A sufficient Condition," *IEEE Trans. On Signal Processing*, vol. 60, no. 5, pp. 2688–2693, May 2012.

[69] P. Misra, S. Kanhere, D. Ostry, and S. Jha, "Safety Assurance and Rescue Communication Systems in High-Stress Environments: A Mining Case Study," *IEEE Comm. Magazine*, vol. 48, no. 4, pp. 66–73, April 2010.

[70] C. Feature, "Wireless Sensor Network Challenges and Solutions," *Microwave Journal*, pp. 22–34, Aug. 2012.

[71] C. Lin, G. Wu, and P. Pirozmand, "GTRF: A Game Theory Approach for Regulating Node Behavior in Real-Time Wireless Sensor Networks," *Sensors*, pp. 12 932–12 958, 2015.

[72] A. H. Sayed, *Adaptation, Learning, and Optimization Over Networks*. Now Publishers Inc., 2004.

[73] K. Akkaya and M. Younis, "A survey on routing protocols for wireless sensor networks," *Ad Hoc Networks*, vol. 3, no. 2005, pp. 325–349, 2005.

[74] M. A. Alsheikh, S. Lin, D. Niyato, and H.-P. Tan, "Machine Learning in Wireless Sensor Networks: Algorithms, Strategies, and Applications," *IEEE Communications Surveys and Tutorials*, vol. 16, no. 4, pp. 1996–2018, April 2014.

[75] S. Dulman, T. Nieberg, J. Wu, and P. Havinga, "Trade-off between Traffic overhead and Reliability in Multipath Routing for Wireless Sensor Networks," *WCNC Workshop*, pp. 1996–2018, Mar. 2003.

[76] W. Ye, J. Heidemann, and D. Estrin, "An Energy-Efficient MAC Protocol for Wireless Sensor Networks," *Proceedings of IEEE*, vol. 3, pp. 1567–1576, 2002.

[77] L. Sboui, Z. Rezki, and M.-S. Alouini, "Energy-Efficient Power Allocation for Underlay Cognitive Radio Systems," *IEEE Trans. On Cognitive Communications and Networking*, vol. 1, no. 3, pp. 273–283, Sep. 2015.

[78] R. M. Corless, G. H. Gonnet, D. E. Hare, D. J. Jeffrey, and D. E. Knuth, "On the Lambert W function," *Adv. comput. Math*, vol. 5, no. 1, pp. 329–359, 1996.

[79] X. Kang, R. Zhang, Y.-C. Liang, and H. K. Garg, "Optimal Power Allocation Strategies for Fading Cognitive Radio Channels with Primary User Outage Constraint," *IEEE Journal on Selected Areas in Communications*, vol. 29, no. 2, pp. 374–383, Feb. 2011.

[80] Z. Chen, J. Yuan, and B. Vucetic, "Analysis of Transmit Antenna Selection/Maximal-Ratio Combining in Rayleigh Fading Channels," *IEEE Trans. On Vehicular Technology*, vol. 54, no. 4, pp. 1312–1321, July 2005.

[81] C. Huang, R. Zhang, and S. Chi, "Optimal Power Allocation for Wireless Sensor Networks with Outage Constraint," *IEEE Wireless Communication Letters*, vol. 3, no. 2, pp. 209–212, April 2014.

[82] A. D. Coso, U. Spagnolini, and C. Ibars, "Cooperative Distributed MIMO Channel in Wireless Sensor Networks," *IEEE Journal on Selected Areas in Communications*, vol. 25, no. 2, pp. 402–414, Feb. 2007.

[83] S. Cui, A. J. Goldsmith, and A. Bahai, "Energy-Efficiency of MIMO and Cooperative MIMO Techniques in Sensor Networks," *IEEE Journal On Selected Areas on Communications*, vol. 22, no. 6, pp. 1089–1098, Aug. 2004.

[84] J. Rubio, A. Pascual-Iserte, D. P. Palomar, and A. Goldsmith, "Joint Optimization of Power and Data Transfer in Multiuser MIMO Systems," *IEEE Trans. On Signal Processing*, vol. 65, no. 1, pp. 212–227, January 2017.

[85] N. Kim, Y. Lee, and H. Park, "Performance Analysis of MIMO System with Linear MMSE Receiver," *IEEE Trans. On Wireless Commu.*, vol. 7, no. 11, pp. 4474–4478, Nov. 2008.

[86] O. Amin, R. Mesleh, S. S. Ikki, M. H. Ahmed, and O. A. Dobre, "Performance Analysis of Multiple-Relay Cooperative Systems With Signal Space Diversity," *IEEE Trans. On Vehicular Technology*, vol. 64, no. 8, pp. 3414–3425, Aug. 2015.

[87] H. Cui, M. Ma, L. Song, and B. Jiao, "Relay Selection for Two-Way Full Duplex Relay Networks With Amplify-and-Forward Protocol," *IEEE Trans. On Wireless Communications*, vol. 13, no. 7, pp. 3768–3777, July 2014.

[88] I. Krikidis, H. A. Suraweera, P. J. Smith, and C. Yuen, "Full-Duplex Relay Selection for Amplify-and-Forward Cooperative Networks," *IEEE Trans. On Wireless Communications*, vol. 11, no. 12, pp. 4381–4393, Dec. 2012.

[89] S. Boyd, and L. Vandenbergue, *Convex Optimization*. Cambridge University Press, 2004.

[90] C. Song, K. J. Lee, and I. Lee, "MMSE Based Transceiver Designs in Closed-Loop Non-Regenerative MIMO Relaying Systems," *IEEE Trans. On Wireless Communications*, vol. 9, no. 7, pp. 2310–2319, July 2010.

[91] G. D. Forney, "The Viterbi algorithm," *Proceedings of the IEEE*, vol. 61, no. 3, pp. 268–278, March 1973.

[92] Y. Rong and Y. Hua, "Optimality of diagonalization of multi-hop MIMO relays," *IEEE Trans. On Wireless Communications*, vol. 8, no. 12, pp. 6068–6077, Dec. 2009.

[93] D. P. Palomar, J. M. Cioffi, and M. A. Lagunas, "Joint Tx-Rx beamforming design for multicarrier MIMO channels: a unified framework for convex optimization," *IEEE Trans. On Signal Processing*, vol. 51, no. 9, pp. 2381–2401, Sep. 2003.

[94] A. Bletsas, A. Khisti, D. P. Reed, and A. Lippman, "A simple Cooperative diversity method based on network path selection," *IEEE Journal on Selected Areas in Communications*, vol. 24, no. 3, pp. 659–672, March 2006.

[95] Y. Jing and H. Jafarkhani, "Single and multiple relay selection schemes and their achievable diversity orders," *IEEE Trans. On Wireless Communications*, vol. 8, no. 3, pp. 1414–1423, March 2009.

[96] A. D. Poularikas, *The Handbook of Formulas and Tables for Signal Processing*. CRC Press, 1999.